

AD-758 515

AN ENVIRONMENTAL HEAT TRANSFER STUDY OF
A ROCKET MOTOR STORAGE CONTAINER SYSTEM

Allen H. Wirzburger

Naval Postgraduate School
Monterey, California

December 1972

DISTRIBUTED BY:

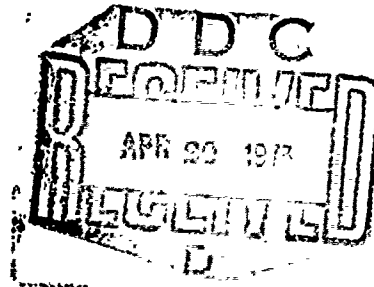
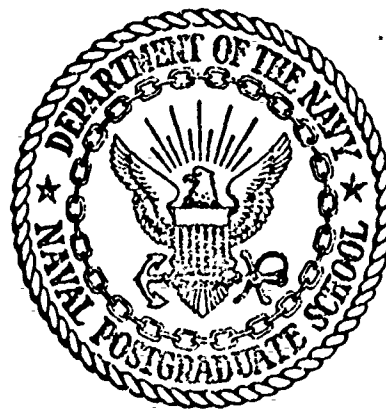


National Technical Information Service
U. S. DEPARTMENT OF COMMERCE
5285 Port Royal Road, Springfield Va. 22151

AD 758515

NAVAL POSTGRADUATE SCHOOL

Monterey, California



THESIS

AN ENVIRONMENTAL HEAT TRANSFER STUDY
OF
A ROCKET MOTOR STORAGE CONTAINER SYSTEM

by

Allen Henry Wirzburger

Thesis Advisor:

T. E. Cooper

December 1972

Reproduced by
NATIONAL TECHNICAL
INFORMATION SERVICE
U.S. Department of Commerce
Springfield VA 22151

Approved for public release; distribution unlimited.

168

Security Classification

DOCUMENT CONTROL DATA - R & D

(Security classification of title, body of abstract and indexing annotation must be entered when the overall report is classified)

1. ORIGINATING ACTIVITY (Corporate author)	2a. REPORT SECURITY CLASSIFICATION Unclassified
Naval Postgraduate School Monterey, California 93940	2b. GROUP

3. REPORT TITLE

An Environmental Heat Transfer Study of a Rocket Motor
Storage Container System

4. DESCRIPTIVE NOTES (Type of report and, inclusive dates)

Master's Thesis: December 1972

5. AUTHOR(S) (First name, middle initial, last name)

Allen H. Wirzburger

6. REPORT DATE December 1972	7a. TOTAL NO. OF PAGES 168	7b. NO. OF REFS 16
8a. CONTRACT OR GRANT NO.	9a. ORIGINATOR'S REPORT NUMBER(S)	
9. PROJECT NO. c. d.	9b. OTHER REPORT NO(S) (Any other numbers that may be assigned this report)	
10. DISTRIBUTION STATEMENT		
Approved for public release; distribution unlimited.		
11. SUPPLEMENTARY NOTES	12. SPONSORING MILITARY ACTIVITY Naval Postgraduate School Mcnterey, California 93940	

13. ABSTRACT

The heat transfer characteristics of a rocket motor storage container system have been investigated using analytical and experimental techniques. Analytically, both closed form and numerical solutions have been developed. These solutions may be used to determine maximum temperatures and temperature gradients within the rocket motor. Comparison between theoretical and experimental values of temperature are within the estimated experimental uncertainties of $\pm 3^{\circ}\text{F}$. It is proposed that the theoretical solutions can be used to thermally optimize container design.

A secondary investigation was carried out to determine the feasibility of using cholesteric liquid crystals, a temperature sensitive material, to thermally map the surface of the container. The crystals appear to remain stable under desert type conditions and produce brilliantly colored displays of the temperature field.

DD FORM 1 NOV 1973 (PAGE 1)

S/N 0101-807-6811

Security Classification

14. KEY WORDS	LINK A		LINK B		LINK C	
	ROLE	WT	ROLE	WT	ROLE	WT
heat transfer						
conduction						
radiation						
convection						
concentric cylinders						
TRUMP						
liquid crystals						
dump storage						
environmental effects						

DD FORM 1 NOV 66 1473 (BACK)

S/N 0101-807-6621

An Environmental Heat Transfer Study
of
A Rocket Motor Storage Container System

by

Allen Henry Wirzburger
Lieutenant, United States Navy
S.B., Massachusetts Institute of Technology, 1964

Submitted in partial fulfillment of the
requirements for the degree of

MASTER OF SCIENCE IN MECHANICAL ENGINEERING

from the
NAVAL POSTGRADUATE SCHOOL
December 1972
COLOR ILLUSTRATIONS REPRODUCED
IN BLACK AND WHITE

Author

Allen H. Wirzburger

Approved by:

Thomas E. Cooper

Thesis Advisor

Robert G. New
Chairman, Department of Mechanical Engineering

Milton H. Clawson
Academic Dean

TABLE OF CONTENTS

I.	INTRODUCTION -----	11
II.	BACKGROUND -----	14
III.	EXPERIMENTAL PROCEDURE -----	17
IV.	THEORETICAL ANALYSIS -----	28
	A. ONE DIMENSIONAL ANALYTICAL MODEL -----	28
	B. TRUMP MODEL -----	36
V.	RESULTS -----	43
	A. ANALYTICAL MODEL -----	43
	B. TRUMP MODEL -----	47
	1. One Dimensional -----	47
	2. Two Dimensional -----	52
	C. GENERAL -----	55
	D. LIQUID CRYSTALS -----	58
VI.	CONCLUSIONS -----	62
VII.	RECOMMENDATIONS -----	64
	APPENDIX A: INTRODUCTION TO LIQUID CRYSTALS -----	66
	APPENDIX B: ANALYTICAL SOLUTION -----	72
	APPENDIX C: TRUMP SOLUTION -----	99
	APPENDIX D: EXPERIMENTAL DATA -----	151
	APPENDIX E: UNCERTAINTY ANALYSIS -----	161
	LIST OF REFERENCES -----	164
	INITIAL DISTRIBUTION LIST -----	166
	FORM DD 1473 -----	167

LIST OF TABLES

I. Calibration of Liquid Crystals -----	25
II. Thermal Properties of Materials -----	100
III. Matrix Form of Energy Balance Equations -----	110
IV. Radiosities at Nodes -----	111
V. Change in Parameters Due to Changes in Thermal Properties -----	161

LIST OF ILLUSTRATIONS

Figure

1.	Simulated Storage Dump at China Lake -----	15
2.	Thermocouple Locations on Experimental System -----	18
3.	Top View of Rocket Motor Storage Container System -----	19
4.	Stevenson Shelter -----	20
5.	Rocket Motor Mounted in Storage Container -----	22
6.	Experimental System at Dump Storage Site -----	26
7.	Comparison of Sinusoidal Temperature Variation to Bulk Temperature -----	29
8.	Variation in Time Delay with Change in Biot Modulus -----	33
9.	Variation in Relative Amplitude with Change in Biot Modulus -----	34
10.	Analytical Prediction of Temperature Variation with Time -----	38
11.	Comparison of Bulk Temperature to Two TRUMP Approximations -----	39
12.	Comparison of Analytical and Experimental Temperatures at Surface of Rocket Motor -----	44
13.	Comparison of Analytical and Experimental Temperatures at Center of Rocket Motor -----	45
14.	Comparison of 1-D TRUMP and Experimental Temperatures at Surface of Rocket Motor -----	48
15.	Comparison of 1-D TRUMP and Experimental Temperatures at Center of Rocket Motor -----	49
16.	Comparison of Temperatures from Four TRUMP Variations at Surface of Rocket Motor -----	50
17.	Comparison of Temperatures from Four TRUMP Variations at Center of Rocket Motor -----	51

18.	Comparison of 2-D TRUMP and Experimental Temperatures at Surface of Rocket Motor -----	53
19.	Comparison of 2-D TRUMP and Experimental Temperatures at Center of Rocket Motor -----	54
20.	Temperature Distribution at Surface of Storage Container at Maximum Bulk Temperature -----	56
21.	Temperature Distribution at Surface of the Rocket Motor at Maximum Bulk Temperature -----	57
22.	Thermal Mapping with Liquid Crystals -----	59
23.	Liquid Crystals Feasible Under Hostile Environment -----	60
24.	Molecular Structure of Cholesteric Ester -----	67
25.	Light Reflection from Liquid Crystals -----	67
26.	Analytical Model of Experimental System -----	73
27.	Location of Nodes for One Dimensional TRUMP Model -----	101
28.	Location of Nodes for Two Dimensional TRUMP Model -----	104
29.	Graphical Construction for Crossed-Strings Method -----	105
30.	Radiation Network -----	108
31.	Equivalent Radiation Network -----	112
32.	Thermocouple Locations for Experimental Data -----	152

TABLE OF SYMBOLS

a	$= \sqrt{\frac{\omega r_o^2}{a}}$ = conduction parameter
A_n	= area of surface n $\frac{\text{sq in}}{\text{in}}$
B	$= \frac{1}{T}$ = volume coefficient of expansion $\frac{1}{\alpha R}$
c	= specific heat $\frac{\text{BTU}}{\text{lbm} \cdot ^\circ\text{F}}$
D_n	$= D_n' + D_n''$ = length of minimum length line, n in.
D_n'	= length of tangential segment of minimum length line, n in.
D_n''	= length of radial segment of minimum length line, n in.
E	$= \frac{\epsilon}{1-\epsilon}$ = emissivity parameter
F_{m-n}	= view factor, fraction of isotropic radiation from A_m intercepted directly by A_n
\mathcal{F}_{m-n}	= radiation exchange factor, fraction of radiation passing from A_m to A_n directly and indirectly
g	= acceleration of gravity $\frac{\text{ft}}{\text{sec}^2}$
h_{CON}	= convection heat transfer coefficient $\frac{\text{BTU}}{\text{hr-ft}^2 \cdot ^\circ\text{F}}$
h_{RAD}	= radiation heat transfer coefficient $\frac{\text{BTU}}{\text{hr-ft}^2 \cdot ^\circ\text{F}}$
\bar{h}	$= h_{CON} + h_{RAD}$ = effective heat transfer coefficient $\frac{\text{BTU}}{\text{hr-ft}^2 \cdot ^\circ\text{F}}$
i	$= \sqrt{-1}$
J_n	= radiosity of node n $\frac{\text{BTU}}{\text{hr-ft}^2}$
k	= thermal conductivity $\frac{\text{BTU}}{\text{hr ft} \cdot ^\circ\text{F}}$

- k_c = effective thermal conductivity $\frac{\text{BTU}}{\text{hr ft}^{\circ}\text{F}}$
 r_n = radial distance from center of rocket motor to point n in
 r_o = inner radius of rocket motor in
 s_n = length of surface n in
 t = time min
 T = temperature of position r at time t $^{\circ}\text{R}$
 T_{∞} = storage container temperature $^{\circ}\text{R}$
 T_M = maximum temperature of storage container $^{\circ}\text{R}$
 T_A = average temperature of storage container $^{\circ}\text{R}$
 Z = $\sqrt{\frac{iwr_o^2}{\alpha}} \xi$ = dimensionless distance parameter
 α = thermal diffusivity $\frac{\text{ft}^2}{\text{hr}}$
 β = $\frac{hr_o}{k}$ = Biot modulus
 δ = width of air gap in
 ϵ = emissivity
 ξ = $\frac{r}{r_o}$ = dimensionless distance
 θ = $\frac{T - T_A}{T_M - T_A}$ = dimensionless temperature
 θ^* = dimensionless temperature for supplementary problem
 θ_a = construction angle for crossed-strings method radians
 θ_r = relative amplitude of maximum temperature at point of interest to the maximum temperature of the storage container
 μ = dynamic viscosity $\frac{\text{lbf}}{\text{ft-hr}}$

- ρ = density $\frac{\text{lbm}}{\text{ft}^3}$
 σ = Stefan-Boltzman constant $0.171 \times 10^{-8} \frac{\text{BTU}}{\text{hr ft}^2 \text{R}^4}$
 τ = $\tau(t)$ = solution of ψ ;
 = $e^{im\omega t}$ for large values of time
 ϕ = $\phi(r)$ = solution of ψ
 ψ = complex temperature = $\theta^*(r,t) + i\theta(r,t)$
 ω = frequency of sinusoidal variation $\frac{2\pi}{24 \text{ hours}}$
 ω_T = resulting uncertainty in calculated temperature ${}^\circ\text{R}$
 ω_C = uncertainty in calculated temperature due to variation in volumetric heat capacity ${}^\circ\text{R}$
 ω_K = uncertainty in calculated temperature due to variation in conductivity ${}^\circ\text{R}$
 ω_ϵ = uncertainty in calculated temperature due to variation in emissivity ${}^\circ\text{R}$

 $Gr = \frac{\rho^2 g B(\Delta T) \delta^3}{\mu^2} = \text{Grashof Number}$
 $Pr = \frac{c\mu}{k} = \text{Prandtl Number}$

Bessel Functions

I_0 , J_0 , K_0 , BER , BEi

$$X_R = BER_0(a) + \frac{a}{\sqrt{2\beta}} BER_1(a) + \frac{a}{\sqrt{2\beta}} BEi_1(a)$$

$$X_i = BEi_0(a) + \frac{a}{\sqrt{2\beta}} BEi_1(a) - \frac{a}{\sqrt{2\beta}} BER_1(a)$$

$$\delta^* = \tan^{-1} \frac{BEi_0(a\xi)X_R - BER_0(a\xi)X_i}{BER_0(a\xi)X_R + BEi_0(a\xi)X_i} = \text{time delay radians}$$

ACKNOWLEDGEMENTS

I wish to express my sincere appreciation to my advisor, Professor Thomas E. Cooper, for his invaluable assistance in the preparation of this thesis. A special thanks is also due Mr. Howard C. Schafer of the Naval Weapons Center, China Lake for the use of his facilities for the experimental part of this thesis.

I would also like to express my thanks to the Naval Post-graduate School Computer Facility Staff for their guidance in the computer work.

I. INTRODUCTION

The purpose of this investigation was to develop a heat transfer model that will allow prediction of the temperature distribution in a container stored rocket motor placed in a hostile thermal environment such as the desert. It is proposed that such a model would be a useful tool for thermally optimizing future container designs. As extreme variations in the rocket motor temperature may lead to large thermal stresses in the propellant which could result in fracture, or otherwise degrade the performance of the motor, a major objective of this study was to design a model that could reliably predict the thermal gradient in the motor. The predictions would be based on the surface temperature distribution, the thermal properties and the geometrical details of the system. The model may also be used to predict a critical temperature range over which the propellant must be chemically stable when in a storage situation. The upper limit of this temperature range is referred to as the design temperature of the system. As the design temperature for most weapon development projects is derived from dump storage conditions, a dump storage situation was used to obtain the experimental data for this project.

Several approaches were taken to predict the rocket motor temperature distribution from a knowledge of only the surface temperature distribution of the storage container and the thermal properties and geometrical details of the

experimental model. The experimental model used in this test was a once-fired Navy antisubmarine rocket (ASROC) motor, filled with dry desert blow sand to simulate the propellant, and placed in its storage container. This container system was placed in a dump storage site at the Naval Weapons Center, China Lake, California to simulate a desert environment.

The method of complex temperatures [Ref. 1] was used to develop an analytical prediction of the transient temperature field that exists in a container stored rocket motor. The analytical model assumes that heat is transferred only in the radial direction and that the container surface temperature variation is sinusoidal with time. Comparison between theory and experiment is within experimental uncertainty when temperature is interpreted as "bulk" temperature. The analytical model is especially useful for studying geometrical and thermal physical property effects on rocket motor temperature. Such parameter studies have been carried out and the results are presented in a form that will be useful from a container design point of view.

TRUMP [Refs. 2 and 3], a computer program for transient and steady-state temperature distributions in multidimensional systems, was used to obtain detailed information about the thermal state of the rocket motor. TRUMP allows actual container surface temperature distributions to be used as well as sinusoidal variations. In addition, both one dimensional (radial) and two dimensional (radial and circumferential)

heat transfer were modeled with TRUMP, using both the sinusoidal and actual temperature distributions. The actual temperature distributions were obtained from the experimental data of the motor container system.

Comparisons between the experimental values and those predicted by the models were in good agreement, with those predicted by TRUMP using the actual temperature distribution as the boundary condition being the closest. However, the sinusoidal variations used in both the analytical model and the TRUMP model are also suitable for design purposes.

Another aspect of this project was to obtain the storage container surface temperature distribution using cholesteric liquid crystals, a material that undergoes brilliant changes in color over known, well defined temperature ranges. Color slides and movies were taken of the liquid crystals demonstrating the feasibility of using them for on site temperature measurements.

II. BACKGROUND

In 1959 the Naval Weapons Center, China Lake recognized the need for a concerted attack on the problem of thermal criteria assignment for new weapon systems. In 1963 a task force was established to study the complete environmental criteria determination problem. The key to this problem seemed to be the thermal area in the storage and transportation events of any item. It was realized that transportation was a short term situation compared to the storage situation. Therefore, the major portion of the life of an item must be in storage. There are three types of storage; covered, igloo and dump. The dump storage situation leads to the more extreme thermal exposure situations which then leads to the design temperature.

As data was not available for the dump storage situation, instrumented storage dumps were created at representative places on a worldwide basis so that statistical data could be derived on a variety of ordnance. The first site was at China Lake, California, in the middle of the Mojave Desert. This site now has the capability to return about 250 channels of information on a continuous time-temperature basis (Figure 1). Other arctic and tropical sites were set up to study extreme conditions.

The dump storage situation was reproduced to study the extreme situation. The ordnance was exposed singly, directly situated on the ground, with the long axis aligned in the

Figure 1. Simulated Storage Site at China Lake.



north-south direction to allow maximum normal exposure of the container surface to the sun's rays. In actual practice, ordnance is usually stacked and oriented in other than a north-south direction, thereby avoiding the extreme situation. Ordnance sitting on the ground receives reflected radiation from the ground, cannot quickly give off heat by conduction to the soil, and is not as apt to be cooled by the prevailing breeze; therefore, extreme temperatures result.

The most important source of heat to the ordnance is the direct radiation from the sun, with reflected radiation of secondary importance. For extreme conditions to occur the wind must be calm (less than 5 knots), the sky clear, and the outside air temperature high. After sunrise, the ordnance skin temperature rises much more rapidly than the ambient air temperature; therefore, the surrounding air cools the ordnance, rather than heats it.

The rocket motors used for the tests were military surplus. Even though the material had served its intended in-fleet purpose, it was still representative of new hardware, when viewed in a thermodynamic context. When inert rocket motors were available, they were used intact; however, in most cases, once-fired hardware was used. Thoroughly dried desert blown sand, being similar in thermal properties to most propellants, was used to backfill empty rocket motors. It was assumed that the thermal response of the sand filled motors was essentially the same as actual propellant filled motors.

III. EXPERIMENTAL PROCEDURE

Although Naval Weapons Center, China Lake had accumulated vast amounts of data in the past, it was decided to implement a rocket motor storage container system especially for this project. This would allow base data to be taken exactly where it was required. It also allowed variations in the system without interfering with one of China Lake's ongoing projects. An ASROC system was chosen for this study. The outer storage container was 75 inches long with an inner diameter of 18 inches and a wall thickness of 1/16 inch. The rocket motor was 57 inches long with an outside diameter of 12 inches and a wall thickness of 1/4 inch. Both the container and motor were made of steel.

The rocket motor storage container system was instrumented with 20 gage copper-constantan insulated thermocouple wire which has an ISA Calibration of $\pm 1\text{-}1/2^{\circ}\text{F}$ over the range -75 to $+200^{\circ}\text{F}$. Twenty-one thermocouples were originally placed on the system with positions indicated in Figures 2 and 3. The ambient air temperature was measured with thermocouple number 19 which was located in a Stevenson shelter about 60 feet away from the system (Figure 4). The thermocouples were mounted intrinsically on the motor and storage container. Two small holes were drilled approximately 1/8 inch apart in the metal and the individual wires were inserted in the holes. The metal was then hammered around the wires until a snug fit was obtained. Bead thermocouples were mounted at the

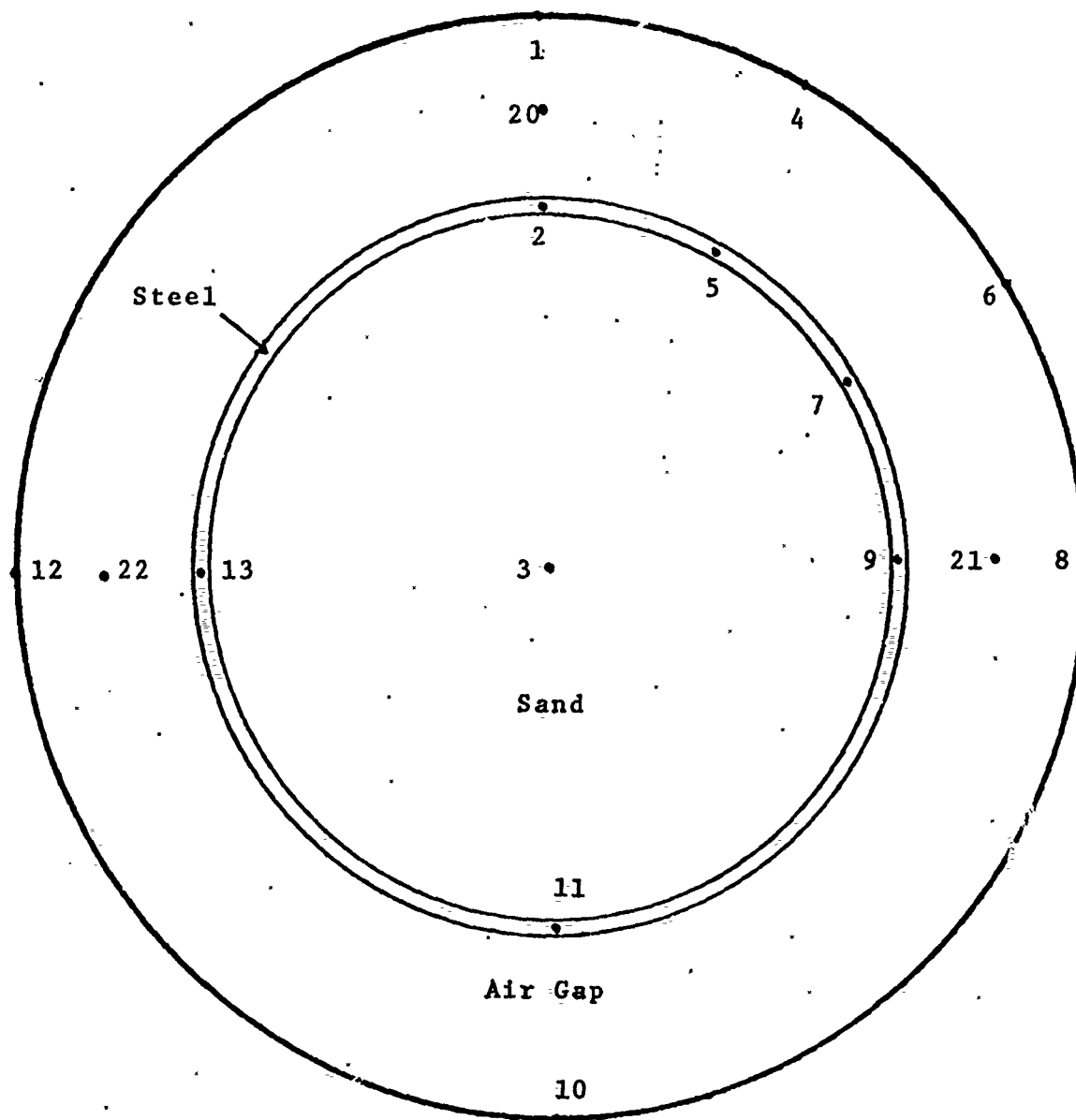


Figure 2. Thermocouple Locations on Experimental System.

Five thermocouples were located under the section painted with the liquid crystals. Their locations corresponding to the ones shown above are: #14= #1, #15= #2, #16= #8, #17= #9, and #18= #3 (See Figure 3).

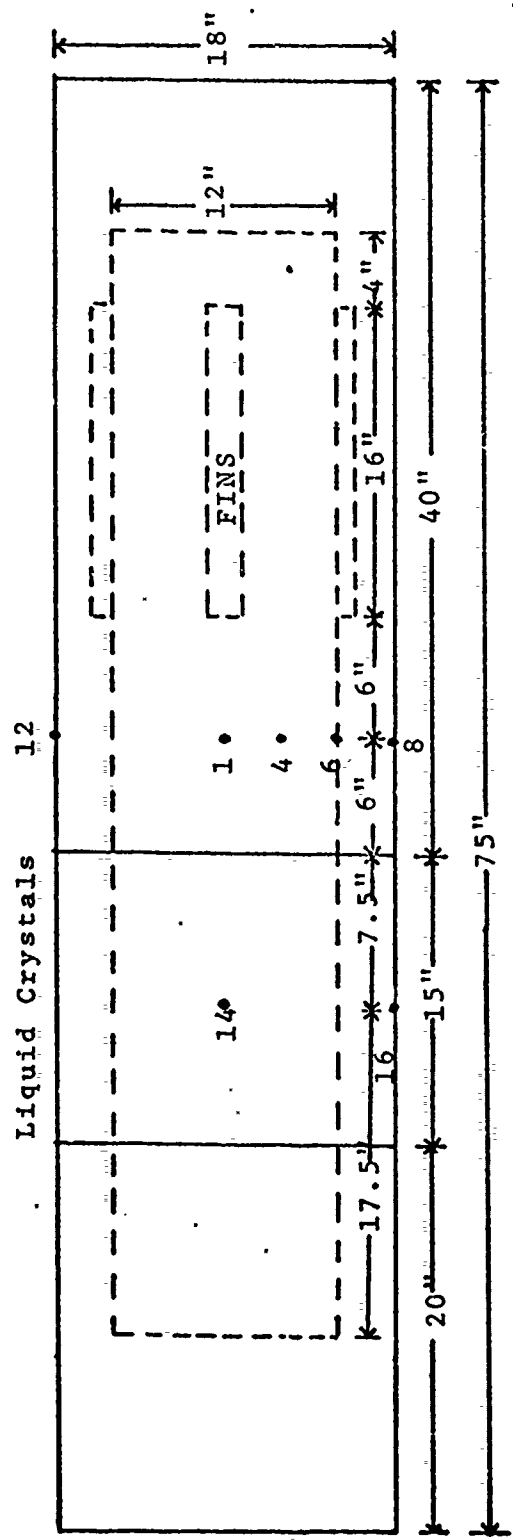


Figure 3. Top view of Rocket Motor Storage Container System.

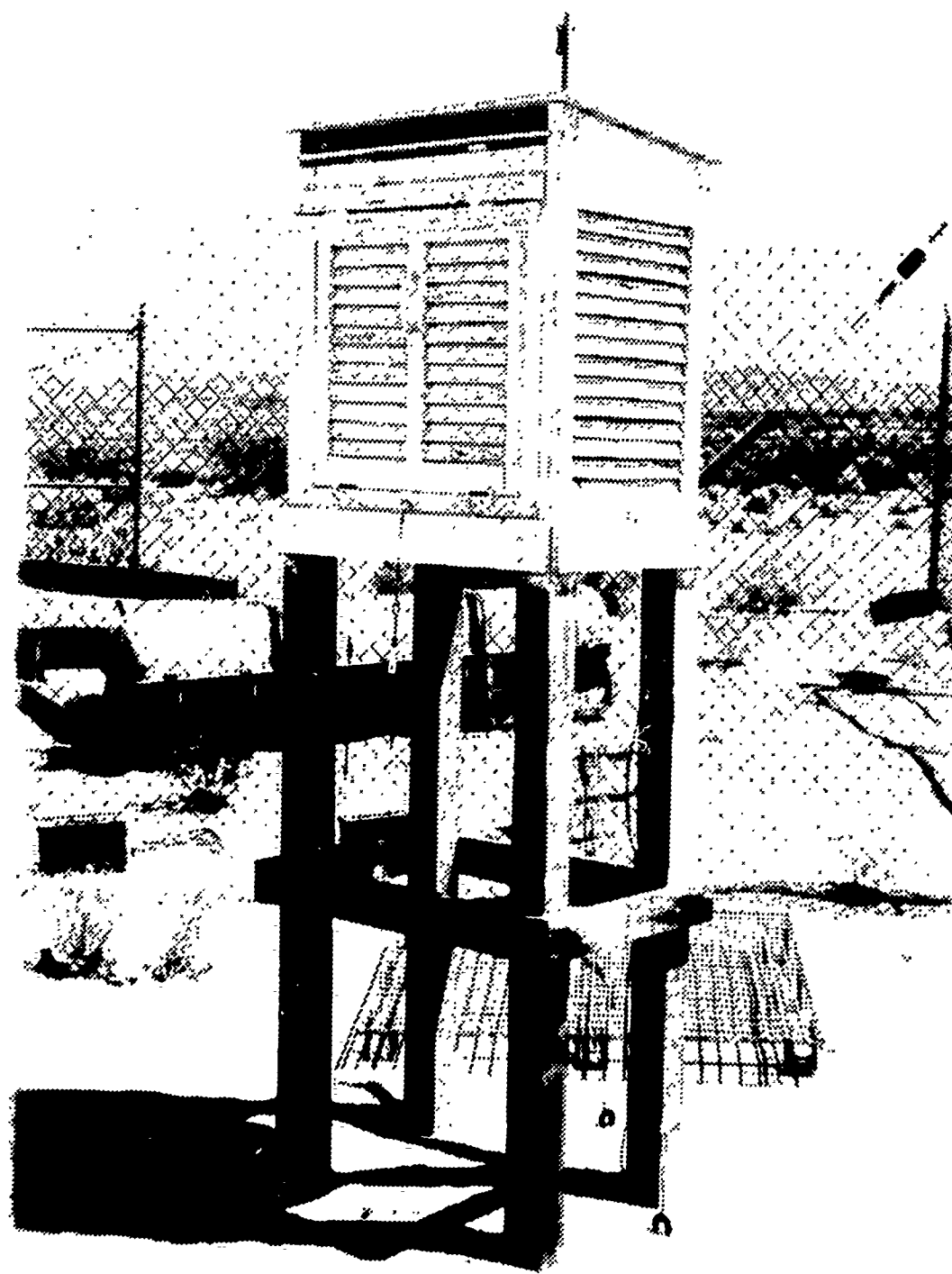


Figure 4. Stevenson Shelter.

center of the motor and in the air gap. The thermocouples located at the center of the motor were supported by small pieces of wood several inches from the head. The use of these supports was necessary to keep the thermocouples in position when the motor was being filled with sand. After all the thermocouples on the rocket motor were in place, the rocket motor was filled with dry desert blown sand. The wires from the two thermocouples located in the center of the motor were led out a hole in the end cap. To avoid settling of the sand after the motor was in place on the site, with a resulting air gap being formed between the sand and the motor skin, the sand was compacted by striking the sides of the motor with small sledge hammers and then adding additional sand through the hole in the end cap. This was continued until the sand was tightly packed. The hole in the end cap was then sealed. The rocket motor was carefully placed in its storage container (Figure 5) which had previously been instrumented with thermocouples. The thermocouples in the air gap were mounted by affixing the lead wire to the rocket motor at the desired position and then putting a 90 degree bend in the wire so that it placed the bead of the thermocouple approximately 1.5 inches into the air gap. Neither the thermocouples in the center of the motor nor those in the air gap could be considered accurately positioned; however, every effort was made to minimize positioning errors. All thermocouple wires were located inside the storage container and were led through a

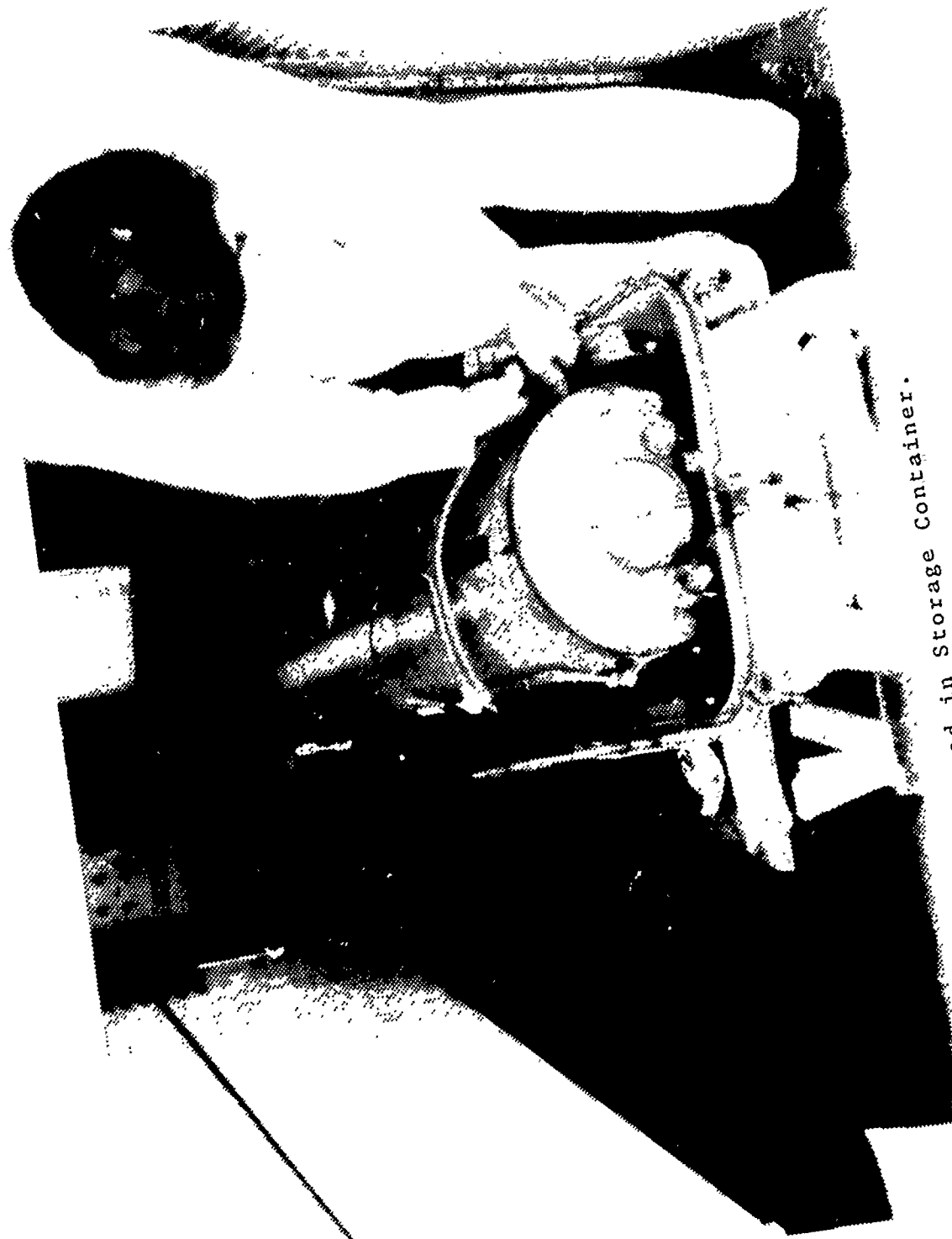


Figure 5. Rocket Motor Mounted in Storage Container.

Reproduced from
best available copy.

hole in one end. This hole was then sealed. The two halves of the storage container were then bolted shut.

The outer surface of the rocket motor and the inner and outer surfaces of the storage container were all painted various shades of haze gray. Weathering had caused the painted surfaces to appear fairly rough. This is typical of the conditions of a storage dump. From the condition of the surfaces, it was estimated that the emissivity was approximately 0.9.

Prior to loading the rocket motor into the storage container, it was decided to apply liquid crystals (See Appendix A) to part of the storage container surface in order to obtain a thermal mapping of the surface temperature at any instant of time. Liquid crystals are temperature sensitive materials that produce immediate thermal images in a pattern of colors which respond rapidly to minute changes in substrate surface temperatures. A second reason for applying the crystals to the container surface was to determine the feasibility of using the crystals under adverse environmental conditions (desert atmosphere). Prior to applying the crystals, a 15 inch strip of the storage container, 20 inches from one end, was sprayed with two coats of Testors Spray Pla Eamel No. 1249, Flat Black as a background for the crystals. A one inch strip of 11 different ranges of crystal, with approximately 1/2 inch of black paint between them, was applied over the black paint. Two coats of each crystal were applied, using a small paint brush. The first coat was allowed to dry completely before the second coat

was applied. After the crystals were dry, two coats of Rez polyurethane (gloss clear plastic coating, interior-exterior 77-5) coating were applied by brush completely covering the crystals and black painted area. The polyurethane coating was applied to protect the crystals from wind blown sand and from the ultraviolet rays of the sun. Ten of the eleven crystals had been previously calibrated [Ref. 4]. Using the constant temperature bath procedure recommended in Ref. 4, R-27 was calibrated and the complete calibration results are shown in Table I.

The rocket motor storage container system was then moved to the China Lake dump storage site. The system was aligned in a north-south direction, well away from the influence of other ordnance (Figure 6). The thermocouple leads were connected through a junction box and underground cable to a Honeywell Electronik 25 Recorder which had been calibrated to read the thermocouple output directly in degrees Fahrenheit to an accuracy of $\pm 1^{\circ}\text{F}$. The recorder was located in an air-conditioned building about 60 feet from the system.

Initial data indicated that the number 7 thermocouple was not responding properly and therefore this data was neglected. Initial color photographs were taken of the liquid crystals and it was immediately apparent that good thermal mappings could be obtained if the crystals were stable under the adverse desert environment. The brilliance of the colors exhibited by the crystals under the bright desert sun was much better than had been expected. The

TABLE I
Calibration of Liquid Crystals

NCR	Desig.	Color Change	Manufacturer's Responses	Calibration Bath 2 Coats Liquid Crystals
			°C	°C
R-27		Red	27.0	25.6+.5
		Green	28.6	28.0+.5
		Blue	30.0	28.7+.5
R-33		Red	33.0	32.7+.5
		Green	34.6	33.3+.5
		Blue	36.0	34.2+.5
R-37		Red	37.0	36.2+.5
		Green	38.6	37.1+.5
		Blue	40.0	38.0+.5
R-41		Red	41.0	40.3+.5
		Green	42.6	41.0+.5
		Blue	44.0	42.0+.5
R-45		Red	45.0	42.8+.5
		Green	46.6	43.6+.5
		Blue	48.0	44.3+.5
R-49		Red	49.0	46.7+.5
		Green	50.6	47.1+.5
		Blue	52.0	48.4+.5
R-53		Red	53.0	50.5+.5
		Green	54.6	52.1+.5
		Blue	56.0	53.3+.5
R-56		Red	56.0	53.8+.5
		Green	57.6	56.0+.5
		Blue	59.0	56.5+.5
R-59		Red	59.0	56.9+.5
		Green	60.6	57.5+.5
		Blue	62.0	58.9+.5
S-62		Red	62.0	60.1+.5
		Green	62.6	60.4+.5
		Blue	63.0	60.9+.5
S-64		Red	64.0	60.9+.5
		Green	64.6	61.4+.5
		Blue	65.0	62.7+.5

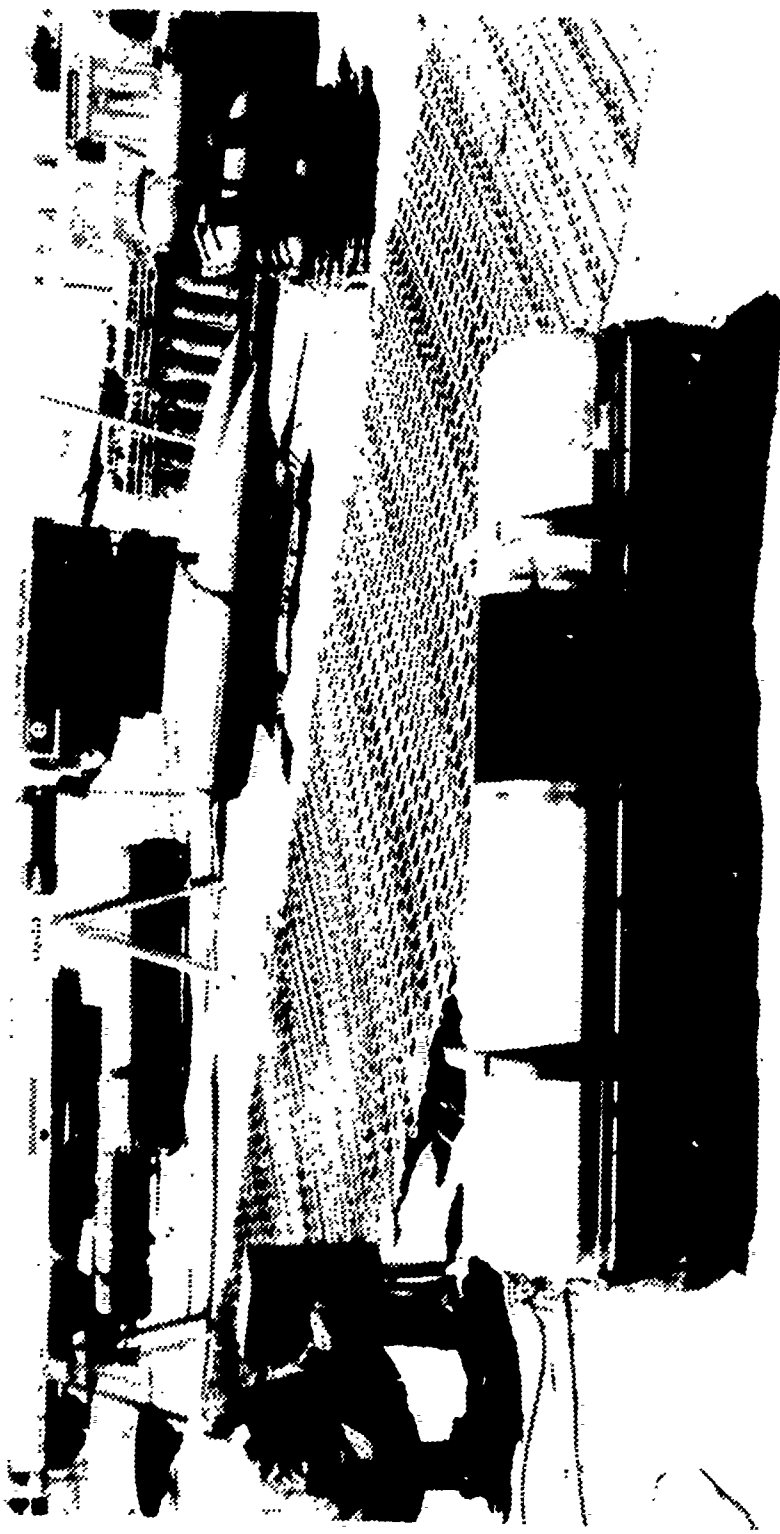


Figure 6. Experimental System at Dump Storage Site.

Reproduced from
best available copy.

system was allowed two weeks to reach a periodic steady state before additional photographic data was obtained.

Extensive photographic data was collected on 27 and 28 July 1972 after two weeks of exposure to the desert environment. Both super 8 mm and 16 mm color movies and 35 mm color slides were taken of the liquid crystals. No colored filters were used on any of the cameras, although standard haze filters were used to take the super 8 mm movies and most of the 35 mm slides.

At this time, a second storage container, this one without a rocket motor inside, was instrumented with intrinsic thermocouples in the same manner as the previous container. As only three data channels remained open on the recorder, only three thermocouples were applied to this new container. The three thermocouples were applied at the 0300, 0900, and 1200 positions at the midpoint of the container. This container was set end to end with the system that was already in place at the site. The purpose of this study was to determine if the inclusion of the rocket motor in the container had a significant effect on the surface temperature of the container. Thermocouple #7 was connected at the 0900 position, #23 at the 1200 position, and #24 at the 0300 position. It was immediately apparent that thermocouple #7 was continuing to give unreliable readings and therefore the data taken on channel #7 was neglected.

IV. THEORETICAL ANALYSIS

A. ONE-DIMENSIONAL ANALYTICAL MODEL

The first step was to try to devise an analytical model that would simulate the actual rocket motor storage container experimental system. The first simplifying assumption was that the storage container temperature could be modeled by a sine wave which had a period of 24 hours. A comparison of the sinusoidal variation to the average (bulk) storage container temperature [obtained by averaging the four thermocouple readings on the surface of the container (1, 8, 10, and 12) as shown in Appendix D] is given in Figure 7.

The method of complex temperature as presented by Arpaci [Ref. 1] was used to find the steady periodic solution of a body experiencing a periodic sinusoidal disturbance. A complete analytical derivation is given in Appendix B. The general heat conduction equation in cylindrical coordinates was the basis for this derivation. It was assumed that there was one dimensional radial heat flow with no conduction in the axial or circumferential directions, that no heat sources existed in the model, that the rocket motor storage container system was infinitely long, and that the sinusoidally varying surface temperature was spatially uniform over the entire container surface. The storage container temperature is assumed to vary as

$$T_{\infty} = (T_M - T_A) \sin \omega t + T_A$$

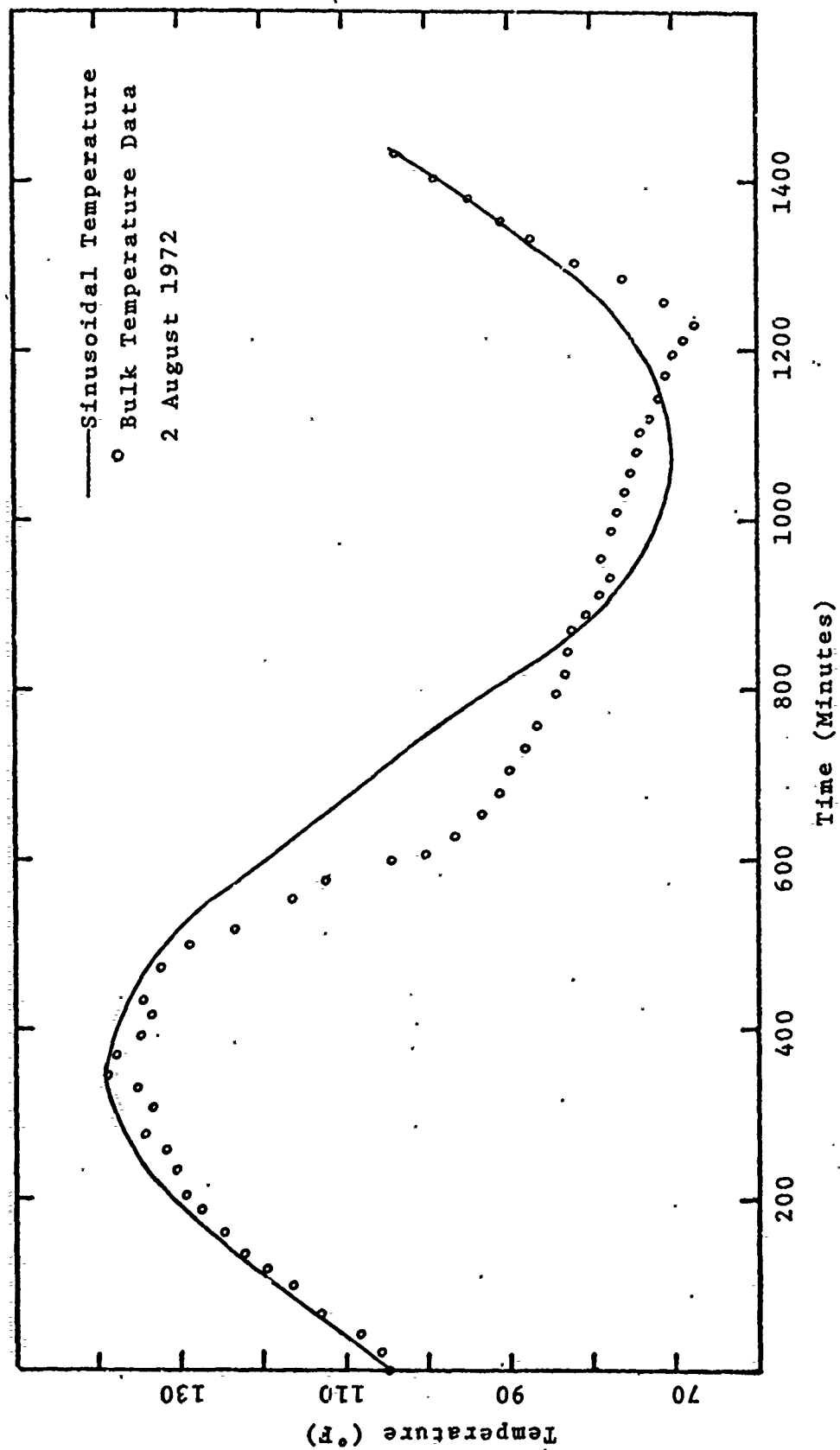


Figure 7. Comparison of Sinusoidal Temperature Variation to Bulk Temperature.

where T_M = maximum bulk temperature of the storage container
 T_A = average bulk temperature of the storage container
 ω = frequency of the sinusoidal variation ($2\pi/24$ hours)
 t = time (hours)

It was assumed that all the thermal properties remained constant over the temperature range of the problem. The effective heat transfer coefficient, \bar{h} , across the air gap between the storage container and the rocket motor combines the heat transfer effects of radiation, convection, and conduction into one coefficient. The radiation coefficient was linearized by assuming constant representative temperatures in the equation

$$h_{RAD} = \mathcal{F}_{1-2}\sigma (T_1 + T_2)(T_1^2 + T_2^2)$$

where σ is the Stefan-Boltzmann constant and \mathcal{F}_{1-2} is the radiation exchange factor. The convection coefficient is the effective conductivity of air, obtained from the Beckmann correlations [Ref. 5], divided by the width of the air gap. In the analytical model, the effective conductivity was assumed to equal the conductivity, thereby treating it as pure conduction and giving the equation

$$\bar{h} = h_{RAD} + h_{CON}$$

An initial condition was not specified in this derivation as the only concern was the steady-state, periodic behavior. The steady-state solution is (Appendix B)

$$\theta(r,t) = \frac{T(r,t) - T_A}{T_M - T_A} = \frac{\sqrt{BER_o^2(a\xi) + BEi_o^2(a\xi)}}{\sqrt{x_R^2 + x_i^2}} \sin(\omega t + \delta^*)$$

$$\theta(r,t) = \theta_r \sin(\omega t + \delta^*)$$

where $T(r,t)$ = the temperature of a point r in the rocket motor at time t

$$a = \sqrt{\frac{\omega r_o^2}{\alpha}} = \text{conduction parameter}$$

$\xi = \frac{r}{r_o}$ = dimensionless distance from the center of the rocket motor

r_o = inner radius of the rocket motor

r = distance from the center of the rocket motor

$\alpha = \frac{k}{\rho c}$ = thermal diffusivity

ρ = density

k = thermal conductivity

c = specific heat

BER = real Bessel Function

BEi = imaginary Bessel Function

$$X_R = BER_0(a) + \frac{a}{\sqrt{2}\beta} BER_1(a) + \frac{a}{\sqrt{2}\beta} BEi_1(a)$$

$$X_i = BEi_0(a) + \frac{a}{\sqrt{2}\beta} BEi_1(a) - \frac{a}{\sqrt{2}\beta} BER_1(a)$$

$\beta = \frac{hr_o}{k}$ = Biot modulus

$$\delta^* = \tan^{-1} \frac{BEi_0(a\xi)X_R - BER_0(a\xi)X_i}{BER_0(a\xi)X_R + BEi_0(a\xi)X_i}$$

Two computer studies were done based on the steady state solution. The first study was a completely dimensionless situation which served as a parameter study of the effects of varying a and β on the temperature and the time lag of the temperature at various positions in the model.

$$a = \sqrt{\frac{\omega r_o^2}{\alpha}} = \text{conduction parameter}$$

and

$$\beta = \frac{hr_o}{k} = \text{Biot modulus}$$

Parameter a was varied from 1.0 to 5.0 and β was varied from 0.1 to 100. These were the only values studied, as

only values within this range are of interest in this type problem. The computer program and its output are given at the end of Appendix B. The output lists the following values:

- 1) a , the conduction parameter
- 2) β , the Biot modulus
- 3) ξ , the non-dimensional distance from the center of the motor
- 4) δ^* , the time delay between the maximum storage container temperature and the maximum temperature reached at the point of interest in the motor
- 5) θ_r , the relative amplitude of the maximum temperature at the point of interest compared to the maximum temperature of the storage container

The time delay is given in radians, where 2π radians equals one complete cycle. A graph of the time delay versus β for a constant value of "a" is given in Figure 8 at three different positions within the motor. A graph of the relative amplitudes of the temperatures versus β for a constant value of "a" is given in Figure 9. It was noted that for a constant value of "a", the time delay decreased as β became larger. As the point of interest approaches the center of the rocket motor, the time delay increases. The relative amplitude of the temperatures also becomes larger as β is increased when the value of "a" is held constant. If β is held constant and "a" is varied, the time delay increases and the relative amplitude decreases as "a" increases.

The second study was obtaining the analytical solution to the particular rocket motor storage container system.

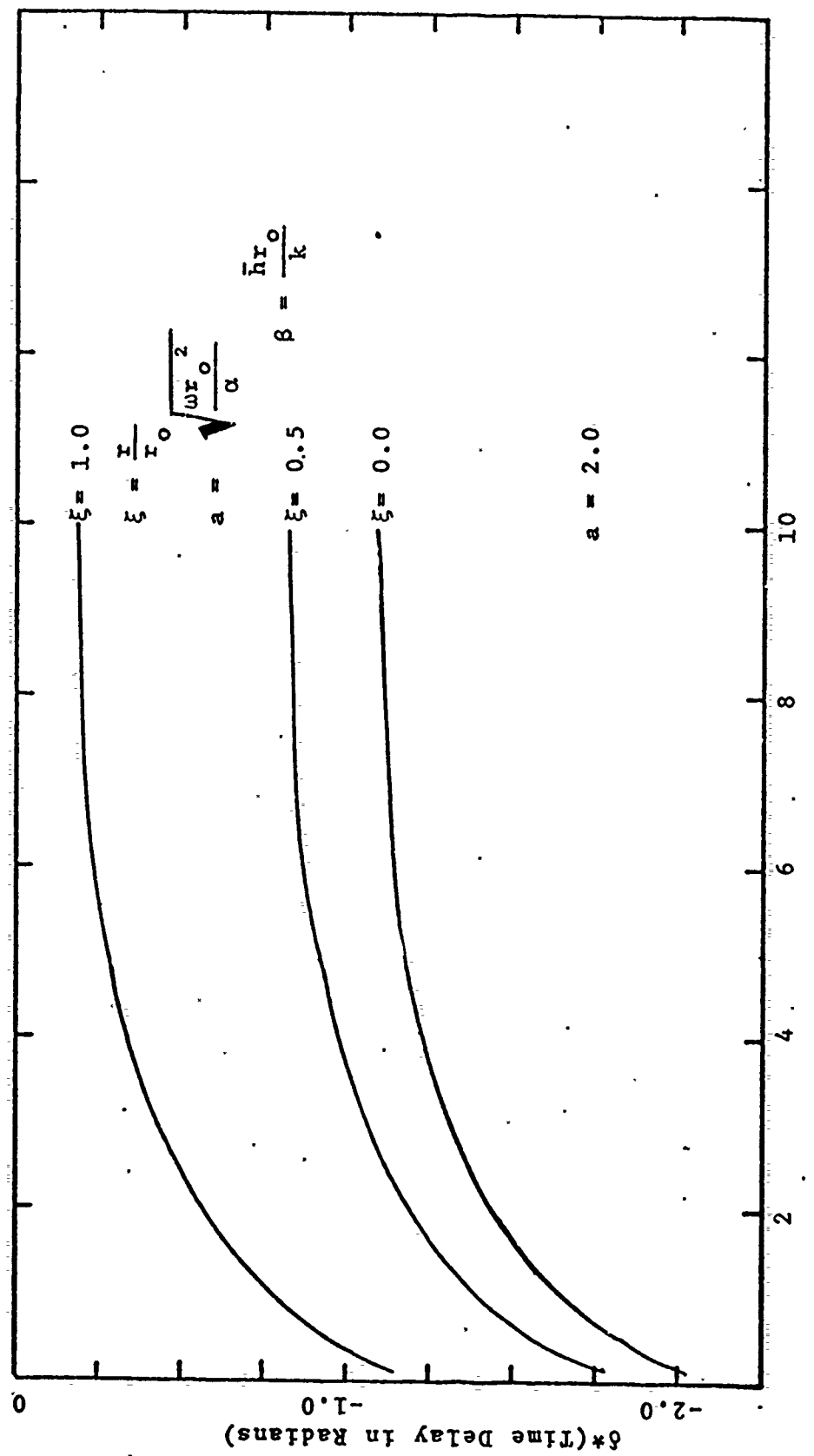


Figure 8. Variation in Time Delay with Change in Biot Modulus

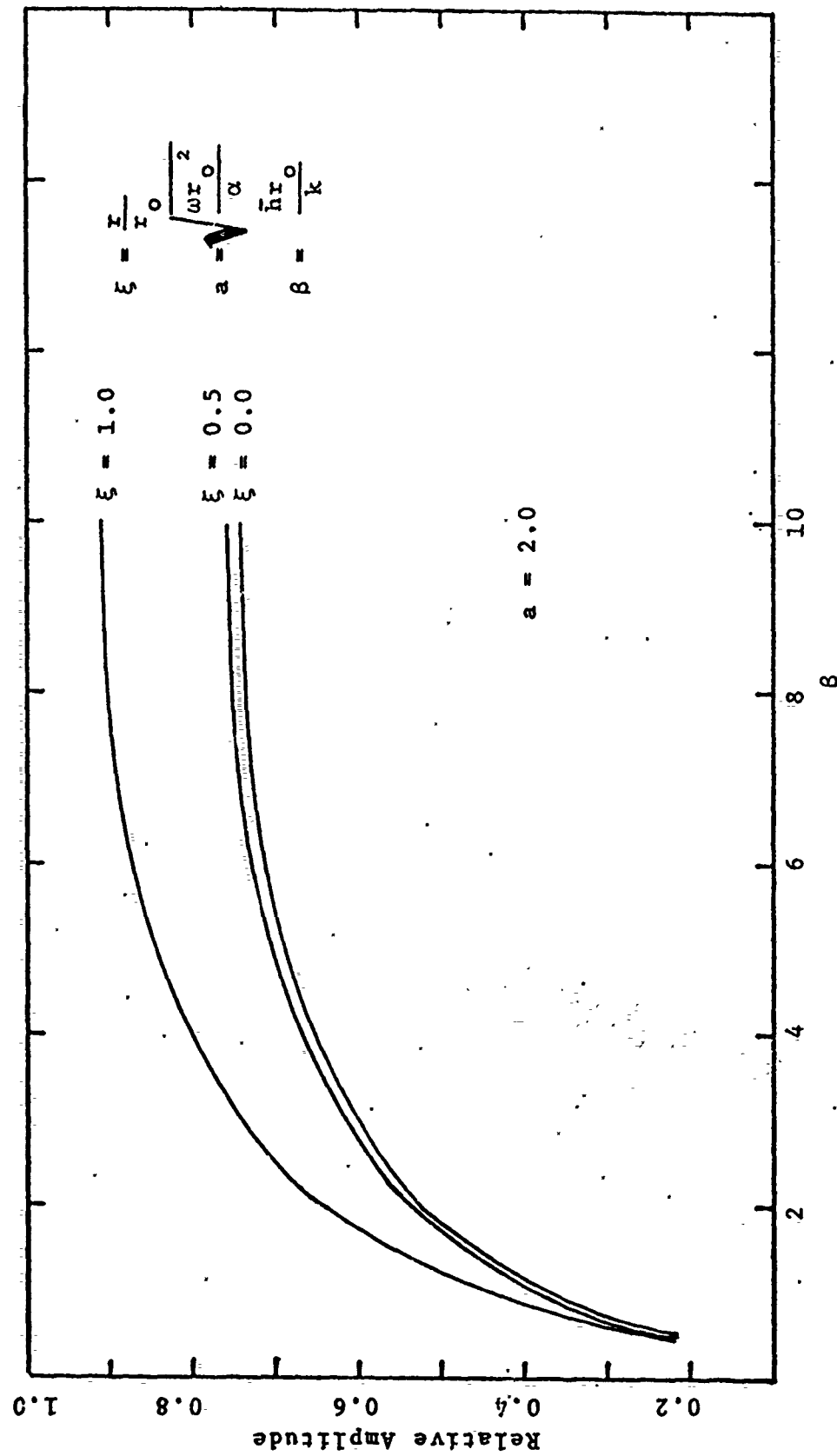


Figure 9: Variation in Relative Amplitude with Change in Biot Modulus.

studied at China Lake. The thermodynamic properties of dry sand were obtained from Ref. 6 as

$$\begin{aligned}\rho &= 94.8 \text{ lbm/ft}^3 \\ k &= 0.188 \text{ BTU/hr ft } ^\circ\text{F} \\ c &= 0.195 \text{ BTU/lbm } ^\circ\text{F}\end{aligned}$$

Substituting these values and using 1440 minutes (24 hours) as a complete cycle, the parameters α and β were calculated for this model as

$$\alpha = \sqrt{\frac{wr_o^2}{\bar{h}}} = 2.43$$

where $r_o = 5.75$ inches, the inner radius of the rocket motor.

$$\beta = \frac{\bar{h}r_o}{k} = 2.90$$

where $\bar{h} = h_{CON} + h_{RAD}$

$$\text{and } h_{CON} = \frac{k_{AIR}}{\Delta r} = 6.48 \times 10^{-2} \frac{\text{BTU}}{\text{hr ft}^2 \text{ } ^\circ\text{F}}$$

where $\Delta r = 2.94$ inches, the distance across the air gap

$$\text{and } k_{AIR} = 1.62 \times 10^{-2} \frac{\text{BTU}}{\text{hr ft } ^\circ\text{F}}$$

$$h_{RAD} = \mathcal{F}_{1-2} \sigma (T_1 + T_2) (T_1^2 + T_2^2) = 1.09 \frac{\text{BTU}}{\text{hr ft}^2 \text{ } ^\circ\text{F}}$$

where σ is the Stefan-Boltzmann constant, \mathcal{F}_{1-2} is the radiation exchange factor which for this geometry is

$$\mathcal{F}_{1-2} = \frac{1}{\frac{1}{c_1} + \frac{r_1}{r_2} \left(\frac{1}{\epsilon_2} - 1 \right)} = 0.84$$

when $\epsilon_1 = \epsilon_2 = .9$, $r_1 = 6.0$, $r_2 = 8.94$

therefore $\bar{h} = 1.15 \text{ BTU/hr ft}^2 \text{ } ^\circ\text{F}$

The average surface temperature of the storage container was found to be 104°F for a particular day at China Lake,

with a maximum temperature of 138°F. These values were obtained by averaging the readings of thermocouples 1, 8, 10, and 12 as shown in Appendix D which give the bulk temperature.

The temperatures of seven positions within the rocket motor were calculated and the results are printed at 30 minute intervals for one complete cycle in Appendix B. A graph of temperature versus time was plotted by the computer showing the relationship between the surface temperature of the storage container (TINF), the temperature on the outer skin of the rocket motor (TEDG), and the temperature at the center of the motor (TCEN). This graph is Figure 10.

B. TRUMP MODEL

The rocket motor storage container system at China Lake was modeled on TRUMP, a numerical conduction code, (See Appendix C for a description of the TRUMP program) to predict the temperature at any point in the system from a knowledge of the storage container surface temperature variation, the thermal properties and the geometrical details of the system. Two models were used to simulate the rocket motor storage container system and several variations of each model were investigated.

The first model assumed one dimensional heat transfer (radial). The system was modeled as two infinitely long concentric steel cylinders, the inner of which was filled with dry sand. A 2.94 inch air gap separated the cylinders. The model was subdivided into concentric volumetric elements

with representative nodal points as given in Figure 27, Appendix C. It was assumed that the storage container surface temperature was spacially uniform. From the data given in Appendix D and the observation of the liquid crystals' thermal mapping, it was obvious that the temperature distribution on the storage container was not spacially uniform. In order to simulate a spacially uniform condition, the readings of the thermocouples located at the 1200, 0300, 0600, and 0900 positions (#1, 8, 10, and 12) were averaged and this average value of the surface temperature (referred to as the bulk temperature) was used as the spacially uniform temperature distribution. Two methods were used to describe the container temperature. The first method used the maximum bulk temperature (138°F) and the average bulk temperature (104°F) of the storage container to generate a sine wave with a period of 24 hours (1440 minutes). The second method took the bulk temperature readings at two hour intervals and fed this data into the TRUMP program in a tabular (temperature versus time) form. The version of TRUMP used in this problem was limited to a table length of 12 tabular values. TRUMP interpolated between the tabular points. Figure 11 compares the actual bulk data with the sinusoidal approximation and the interpolated tabular values.

Several assumptions were made to simplify the solution of this problem. As the thermocouple data from the storage container gave an average value of the temperature across the $1/16$ inch steel wall, node 12 was modeled as a zero

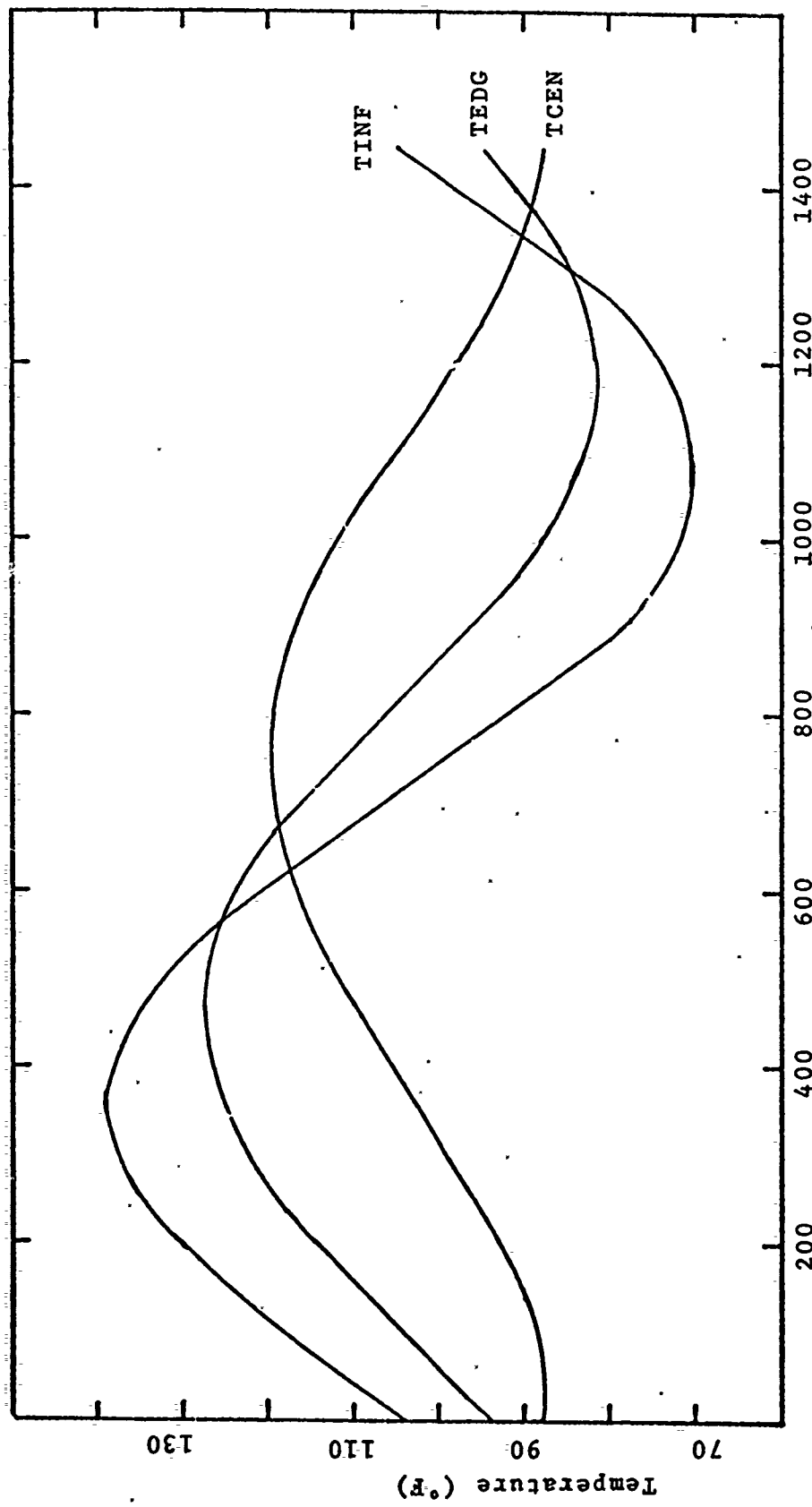


Figure 10: Analytical Prediction of Temperature Variation with Time, where TINF is the surface temperature of the storage container, TEDG is the surface temperature of the rocket motor, and TCEN is the temperature at the center of the motor.

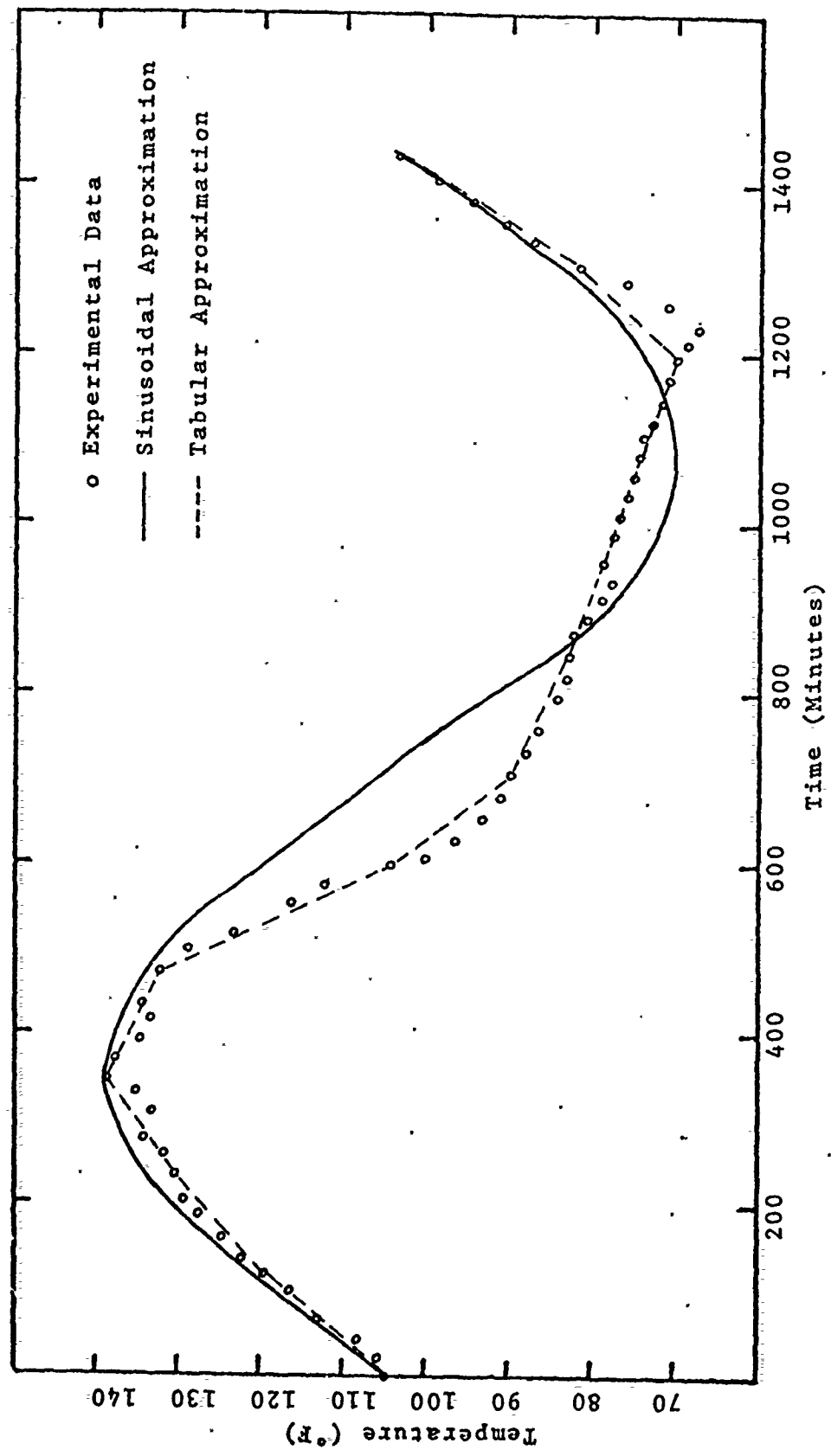


Figure 11: Comparison of Bulk Temperature to Two TRUMP Approximations.

volume boundary node with a known temperature impressed upon it. It was also assumed that heat transfer across the air gap occurred by radiation and conduction alone. Free convection effects were initially neglected. This assumption was later modified to investigate the free convection effects. All surfaces of the storage container and the outside surface of the rocket motor were painted various shades of haze gray and it was estimated that the emissivity of these surfaces was 0.9. The radiation exchange factor, \mathcal{F}_{1-2} , for this model was the same as that for the analytical solution ($\mathcal{F}_{1-2} = 0.84$). It was also assumed that there was perfect thermal contact between the rocket motor and the sand that filled it. This neglects the possibility that the sand might slightly settle after being on the site for a long period of time.

The second model assumed two dimensional heat transfer (radial and circumferential). The same physical model was used as in the one-dimensional case with the sole exception that 48 nodes were used instead of 12. The representative nodal points and an example of the thermal connections from one of the nodal points are shown in Figure 28 in Appendix C. The four nodes on the surface of the storage container were modeled as zero volume boundary nodes. The sinusoidal and tabular representations were used to describe the surface temperature of the storage container at each boundary node. Actual data taken at each position, rather than bulk data, were used as the input data for these representations.

The same assumptions made in the one dimensional case were also applicable to the two dimensional model. A complete discussion of the calculation of the radiation exchange factors in the two dimensional case is given in Appendix C.

The effect of natural convection was studied in both the one and two dimensional models. References 5 and 7 give correlations between the Grashof number based on the gap width and the effective thermal conductivity. The Grashof number was calculated from the equation

$$Gr = \frac{\rho^2 g B (\Delta T) \delta^3}{\mu^2}$$

where δ = width of the air gap

ΔT = maximum temperature difference at any instant of time in the air gap

$$B = \frac{1}{T} \text{ where } T = 565^\circ R$$

At $T = 565^\circ R$, air has the following properties

$$\rho = 0.07 \text{ lbm/ft}^3$$

$$\mu = 0.046 \text{ lbm/hr-ft}$$

The maximum Grashof number for this experiment was calculated to be 1.25×10^6 . The diameter ratio was approximately 1.5 and the $\log Gr = 6.1$. From the Beckmann correlation [Ref. 5], the effective thermal conductivity ratio $(\frac{k_c}{k})$ was approximately 3.2. Using the Liu correlation [Ref. 7]

$$\frac{k_c}{k} = 0.135 \left(\frac{Pr^2 Gr \delta}{1.36 + Pr} \right)^{0.278} = 4.5$$

where the Prandtl Number = 0.707. An effective thermal conductivity of 4.0 was assumed as the average value of these

two correlations and it was used to study the effects of free convection. This change was placed into the TRUMP program by increasing the value of the thermal conductivity of air by a factor of 4 in each of the TRUMP runs.

V. RESULTS

A. ANALYTICAL MODEL

Using the sinusoidal temperature distribution as an approximation to the actual average experimental data as shown in Figure 7, comparisons were made between predicted temperatures and actual temperatures for two radial locations in the rocket motor. Figure 12 compares the results on the surface of the rocket motor and Figure 13 does the comparison at the center of the rocket motor. An uncertainty analysis is given in Appendix E which establishes the uncertainty bounds for both the predicted and the actual temperatures. These uncertainty bounds are included in Figures 12 and 13.

It is readily seen from Figure 7 that a sine wave was not an ideal fit as an approximation to the experimental data, as it varies as much as 20°F during part of the cycle. However, it was also noted that the sine wave closely approximated the experimental data during the heating phase of the cycle and only during the cooling phase were there large variations. As the main purpose of this study was to design a model that would be useful in optimizing storage container design, the errors in the cooling phase are not critical as long as the temperatures reach the same minimum point before beginning another cycle. Figure 12 shows that the maximum surface temperature of the rocket motor predicted by the analytical model is a good approximation to the actual

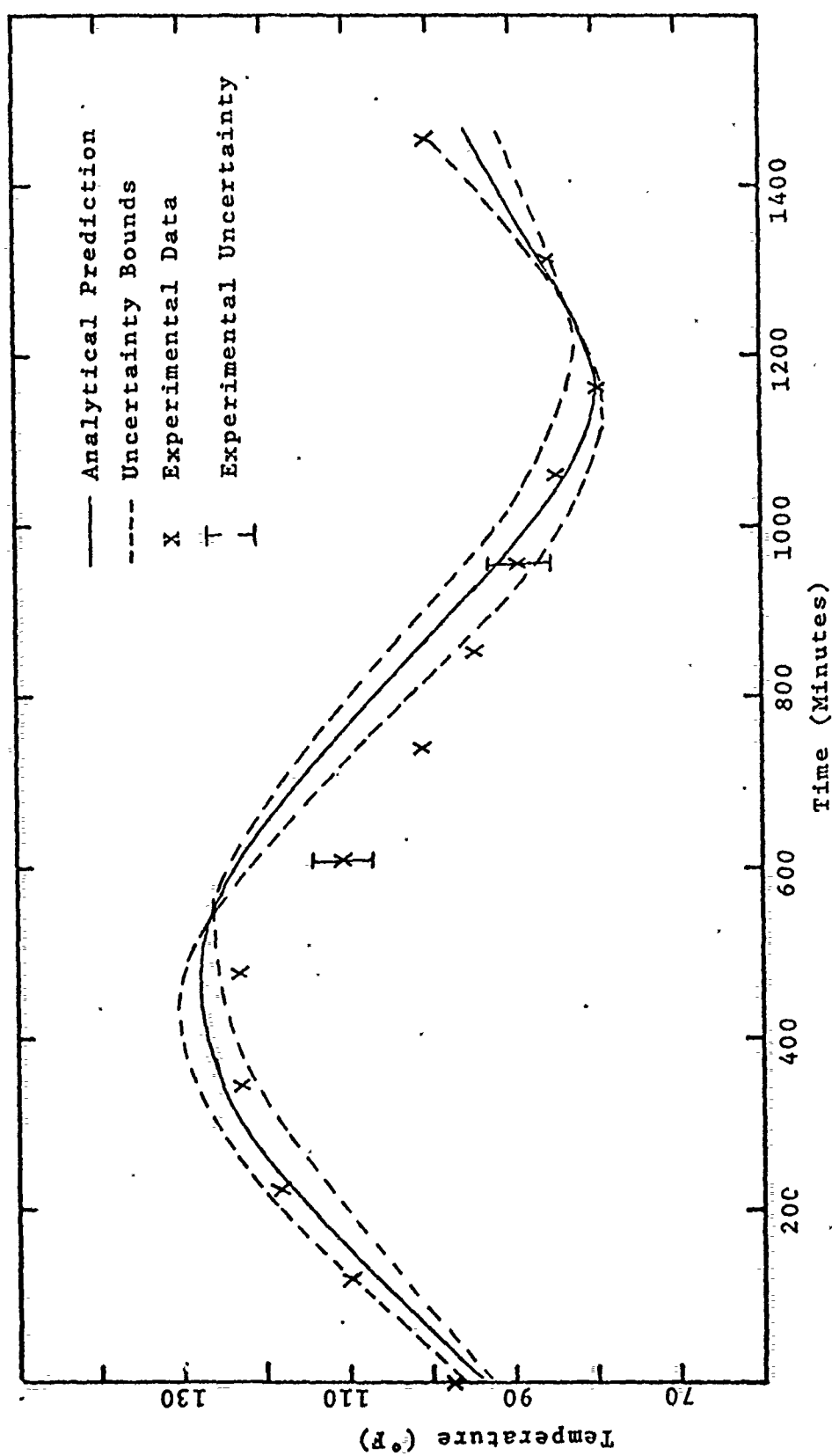


Figure 12: Comparison of Analytical and Experimental Temperatures at Surface of Rocket Motor.

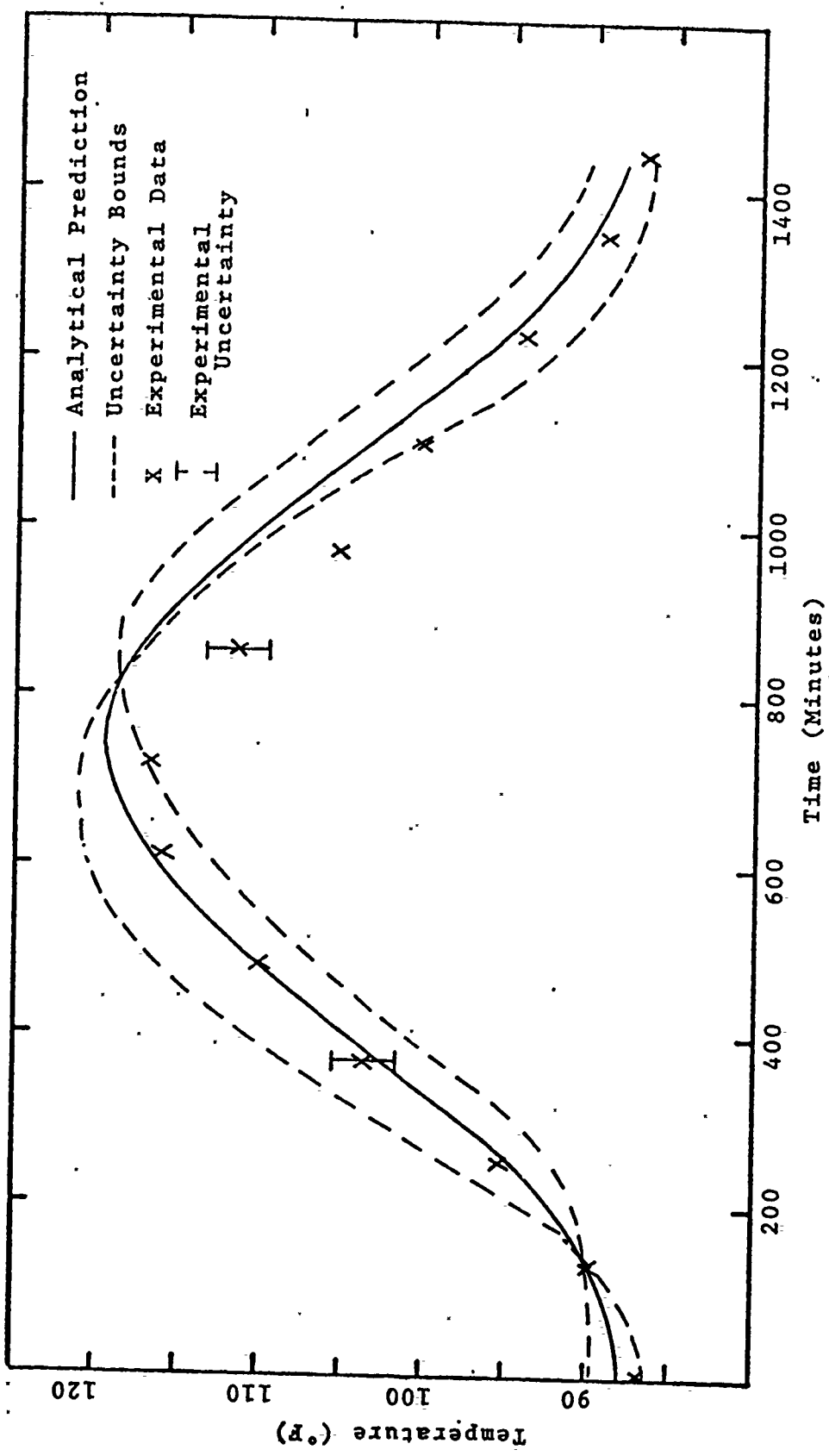


Figure 13: Comparison of Analytical and Experimental Temperature at Center of Rocket Motor.

experimental data. Again it is noted that, in actuality, the motor cools faster than the predicted value. The maximum difference in temperatures on the surface of the motor is 15°F. Figure 13 shows that the predicted value and the experimental value of the temperature at the center of the rocket motor were in close approximation except during the early stages of the cooling phase where a maximum temperature variation of about 5°F occurred.

One of the reasons the system cools faster than predicted could be the light breeze that is usually evident in the early afternoon hours at China Lake that is not present during the morning. No attempt was made to shield the system from the wind to study the effects of a light breeze on the surface temperature of the storage container.

Another point not taken into account by the analytical model is the fact that the time delay at any point in the system is not constant throughout the day as predicted in Figure 10, but varies as given by the data in Appendix D. Time delays between the peak temperature on the container surface and the peak temperature at the center of the rocket motor vary from about 250 to 400 minutes, whereas the low temperature on the surface of the container and the low temperature at the center of the rocket motor vary from about 150 to 250 minutes. The analytical model predicts a constant variation of 388 minutes at the center of the rocket motor and 159 minutes at the surface.

B. TRUMP MODEL

1. One Dimensional

Four variations of the one dimensional TRUMP model were investigated and compared to the experimental data. Figures 14 and 15 compare the TRUMP predictions to the actual experimental data at the surface and the center of the rocket motor, respectively. The TRUMP variation used for this comparison modeled the storage container temperature with tabular data (See Figure 11) and assumed convection was present ($\frac{k_c}{k} = 4.0$). The uncertainty analysis (Appendix E) established the uncertainty bounds for both the experimental and the analytical data in these Figures. The variation between the bulk temperature predicted by TRUMP and the experimental data closely matches with only two experimental points in Figure 14 falling outside the uncertainty bounds for this one dimensional model. Figure 11 shows that the tabular data that TRUMP interpolates is a good approximation to the averaged experimental data. At the center of the motor, as shown in Figure 15, all experimental points fall within the predicted error bounds. A comparison of the four one-dimensional TRUMP variations are given in Figures 16 and 17 at the surface and the center of the rocket motor respectively. It is clearly seen from these Figures that the convection assumption results in an increase of 2°F in the maximum temperature and a decrease of 2°F in the minimum temperature on the surface of the rocket motor. This temperature change drops to $\pm 1.5^{\circ}\text{F}$ at the center of the

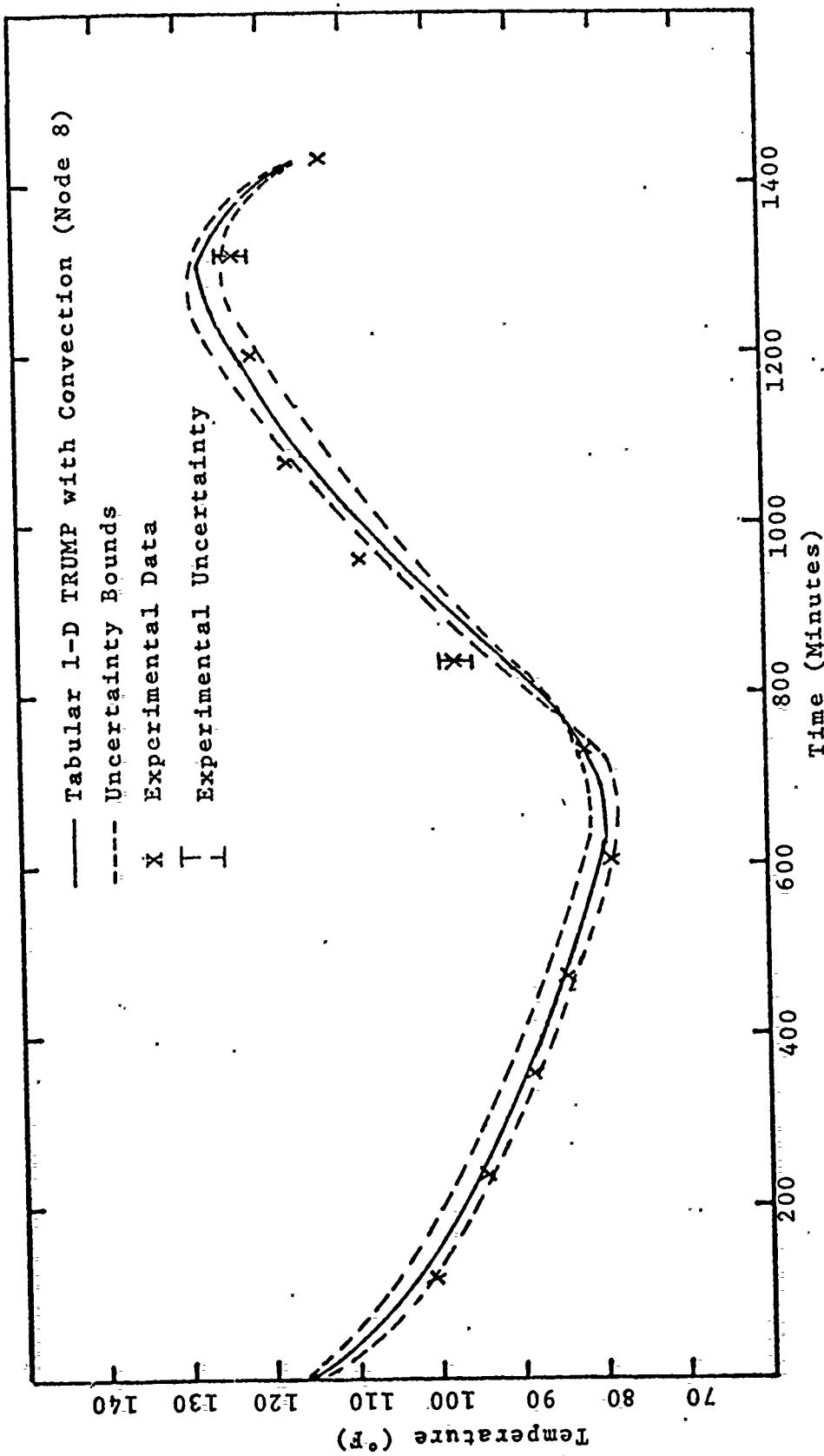


Figure 14: Comparison of 1-D TRUMP and Experimental Temperatures at Surface of the Rocket Motor.

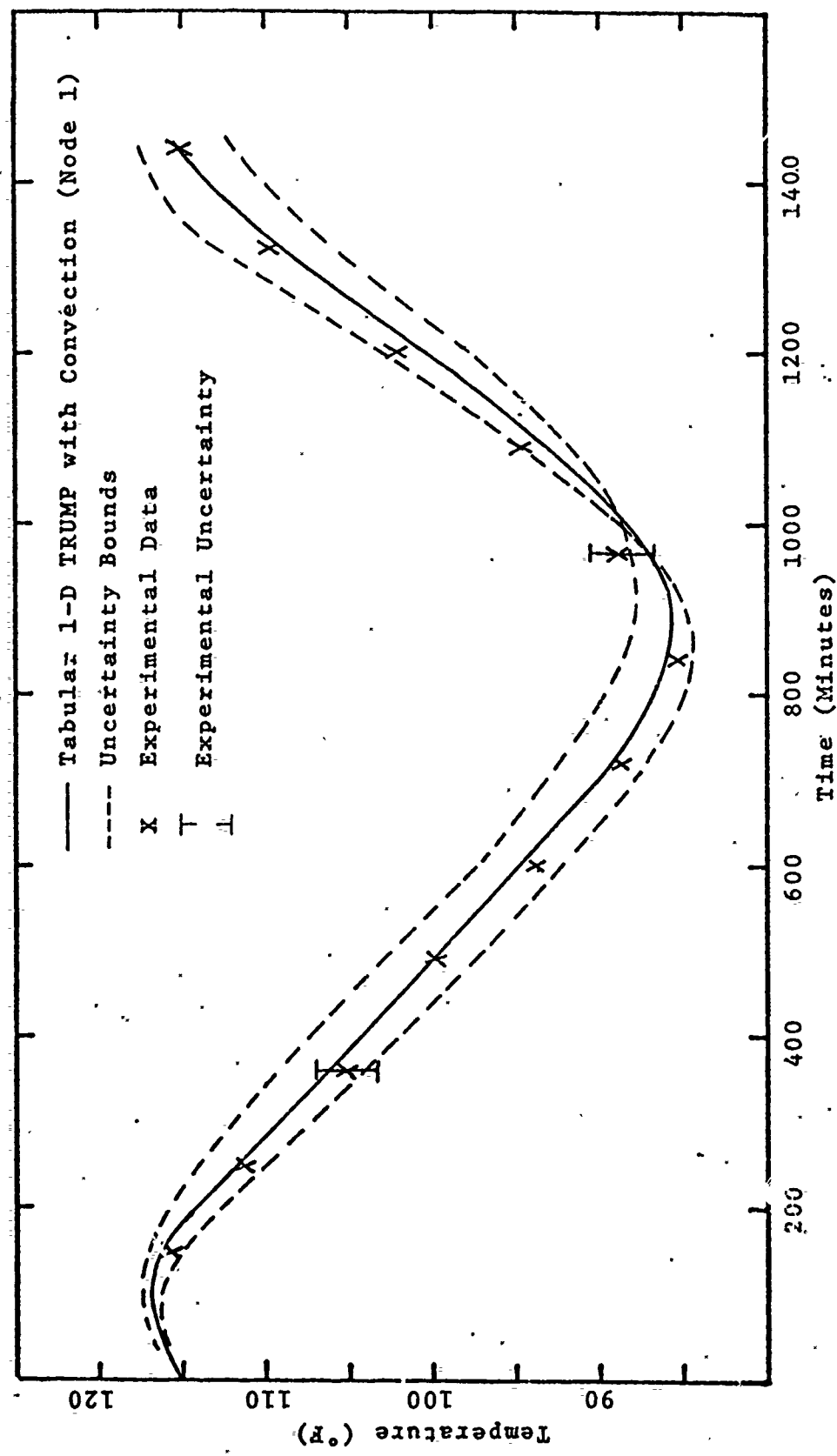


Figure 15: Comparison of 1-D TRUMP and Experimental Temperatures at Center of Rocket Motor.

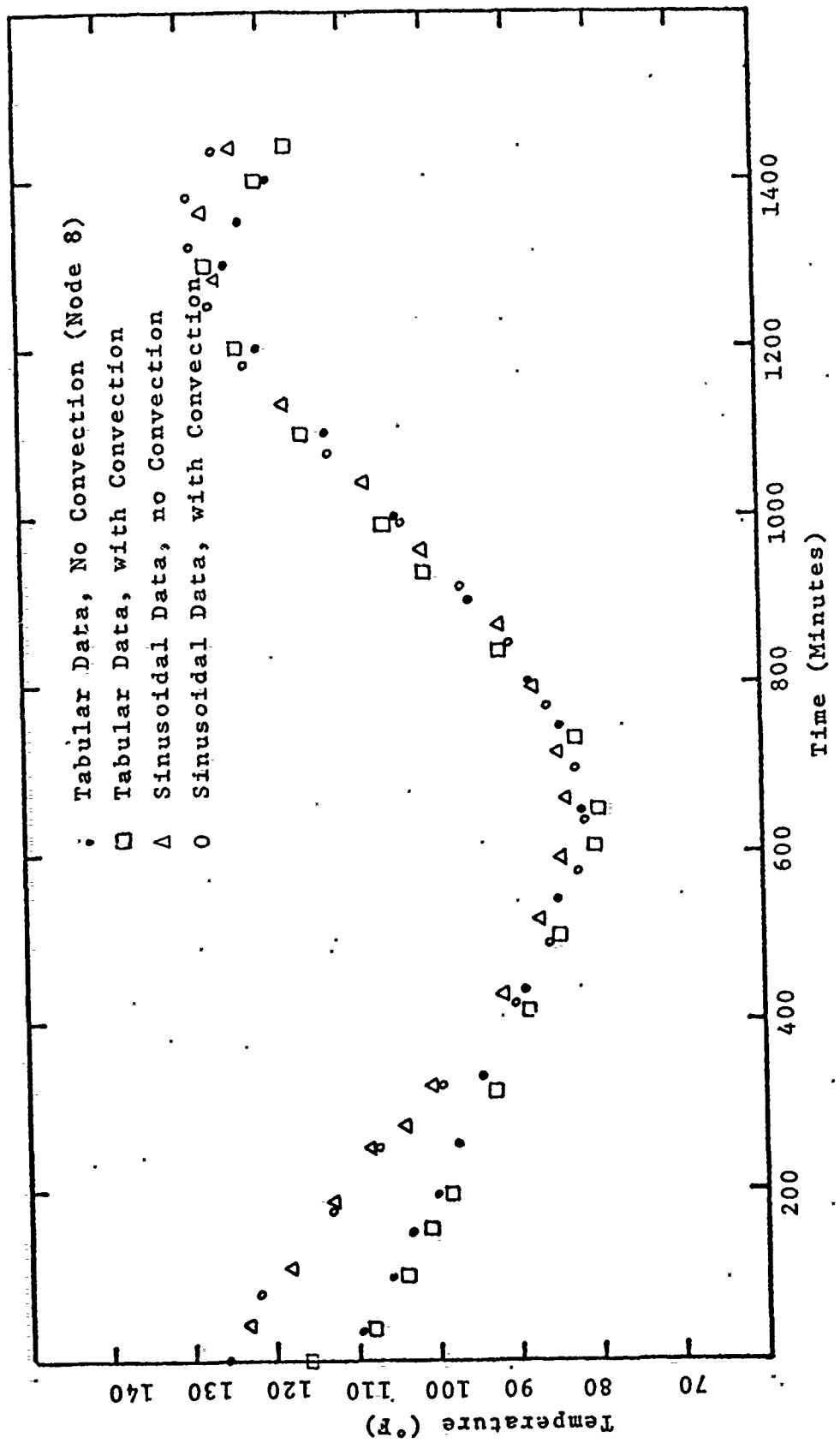


Figure 16: Comparison of Temperatures from Four 1-D TRUMP Variations at Surface of Rocket Motor.

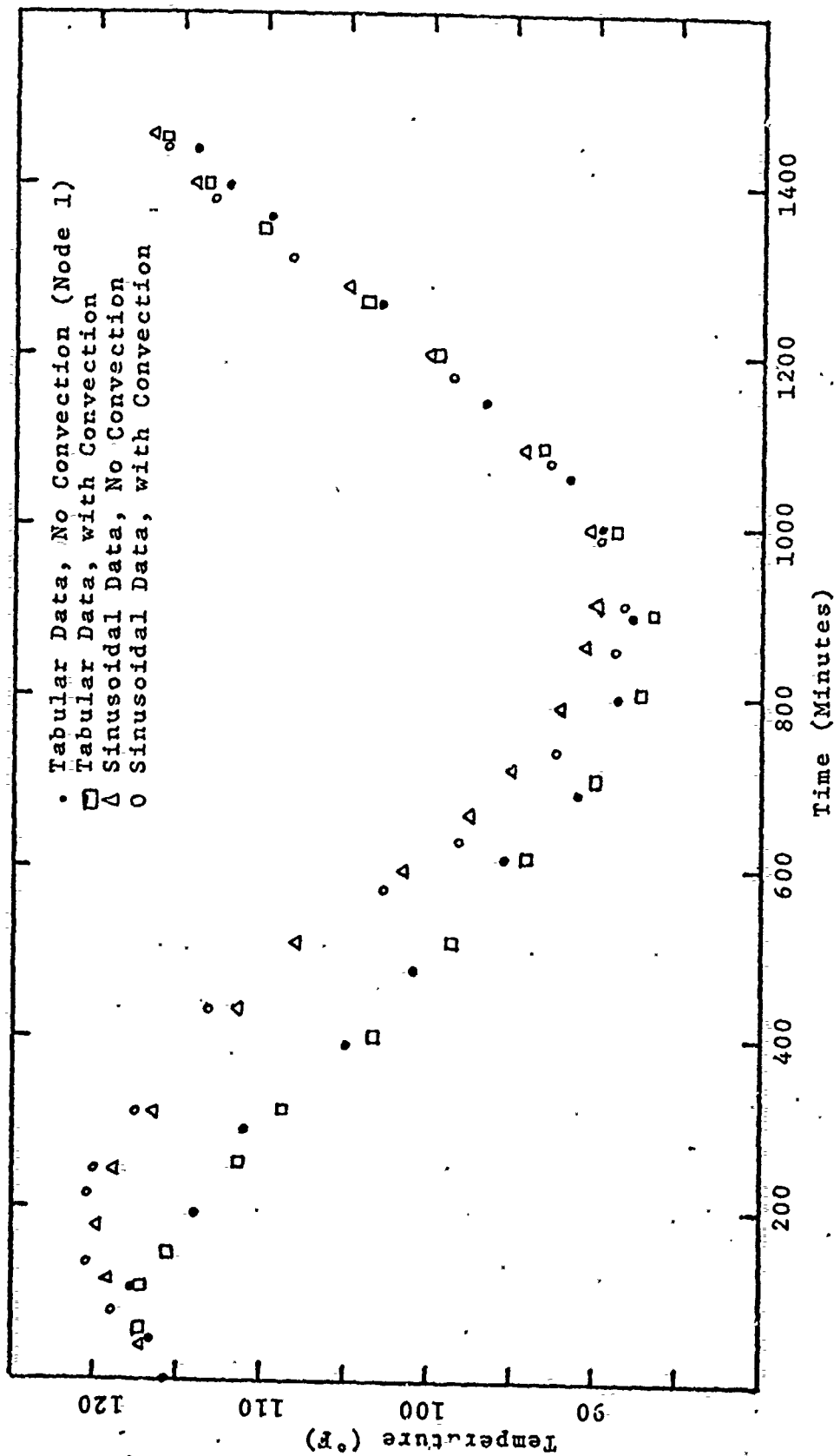


Figure 17: Comparison of Temperatures from Four 1-D TRUMP Variations at Center of Rocket Motor.

motor as shown in Figure 17. The differences between the sinusoidal approximation and the tabular approximation of the experimental data was clearly shown in Figure 11. The data in Figures 16 and 17 can be easily correlated to that in Figure 11, thereby explaining the differences in the predicted values.

2. Two Dimensional

Four variations of the two dimensional TRUMP model were investigated and compared to the experimental data. Comparisons of each TRUMP variation to the experimental data are given in Figures 18 and 19 for node 8 (located on the skin of the rocket motor at the 1200 position) and node 1 (at the center of the rocket motor) respectively. These Figures show that the TRUMP variations that used tabular data to model the surface temperature of the storage container predicted temperatures that more closely approximated the experimental values than were those predicted by TRUMP variations using sinusoidal data to model the surface temperature. Appendix D shows that all points on the surface of the storage container reach their minimum temperature at the same time; however, these points reach their maximum temperature as much as 200 minutes apart. Whereas, all the points on the surface of the storage container are in phase at the minimum temperature, they rapidly become out of phase as the container temperature rises. This varying phase shift makes it difficult to model the four boundary nodes with sinusoidal approximations which must have constant

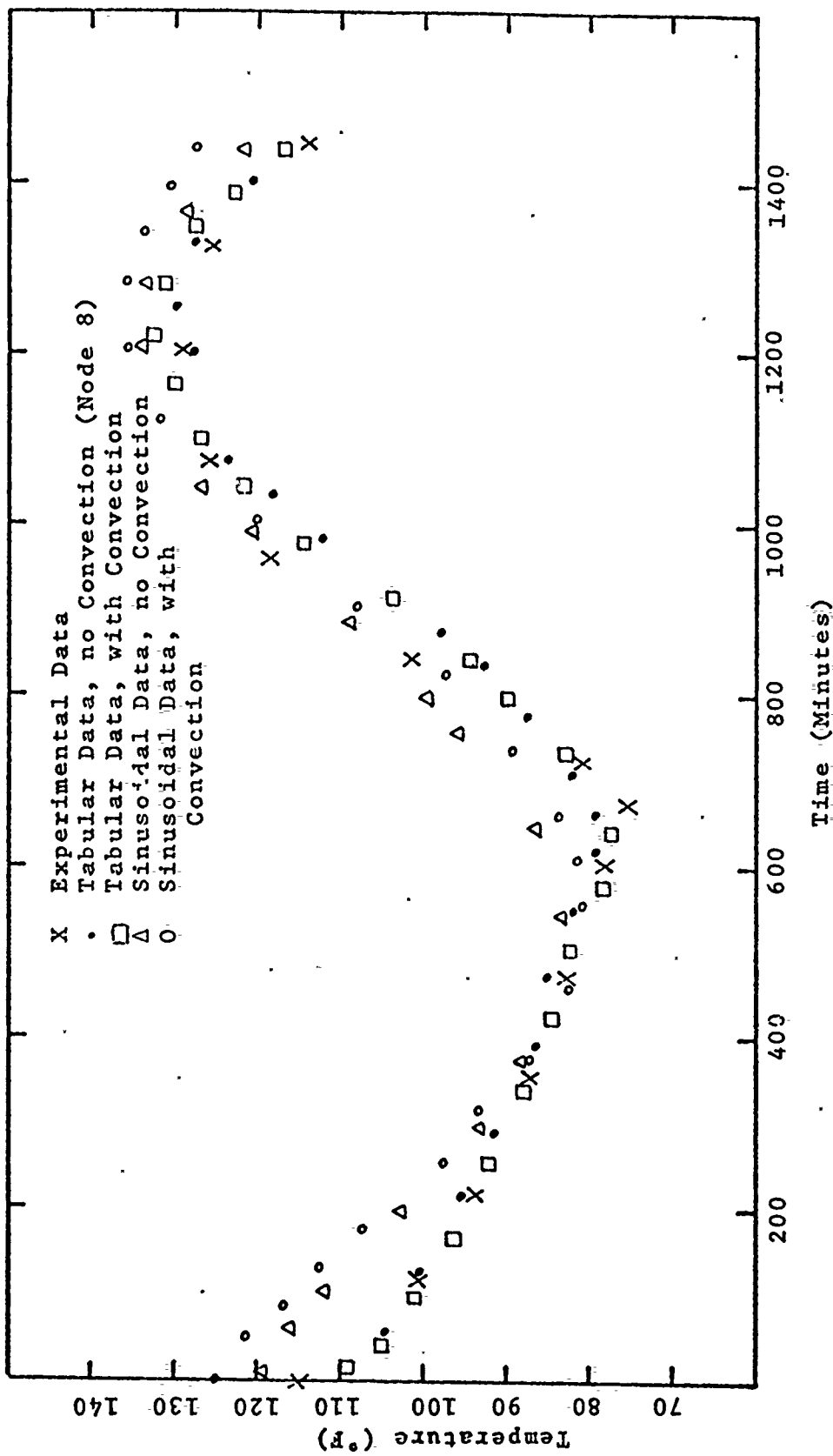


Figure 18: Comparison of 2-D TRUMP and Experimental Temperatures at Surface of Rocket Motor.

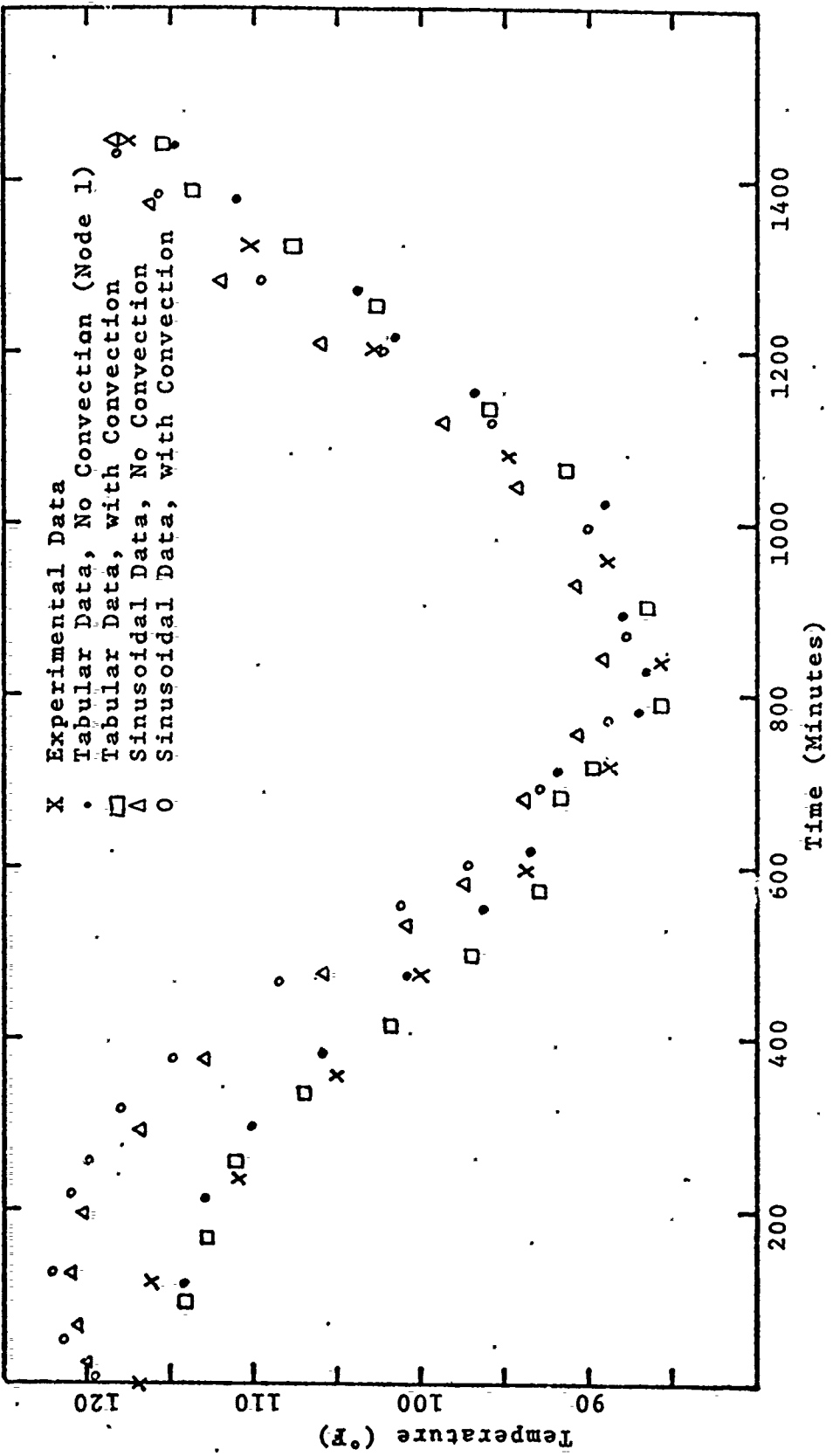


Figure 19: Comparison of 2-D TRUMP and Experimental Temperatures at Center of Rocket Motor.

phase shifts. Sizable errors in the input data during some parts of the cycle were caused by these varying phase shifts. These errors in the input data led to the variations in the predicted temperature values. As noted in the one dimensional section, the inclusion of convection effects does not produce large variations in the predicted temperatures.

Figures 20 and 21 show the actual temperature distributions on the surface of the storage container and on the surface of the rocket motor respectively at maximum bulk temperature compared to a two dimensional TRUMP program. The TRUMP variation used for this comparison assumed no free convection in the air gap and used tabular data to approximate the surface temperature of the storage container.

C. GENERAL

A comparison was made between surface temperatures on the storage container that contained the rocket motor and the storage container that was empty. The low temperature was about 4°F colder in the empty container, whereas the high temperature was about 4°F higher on the container that contained the rocket motor. The empty container had a faster response time than the one containing the motor. The differences in heat capacities, radiation effects, and natural convection all contribute to the changes in temperature noted.

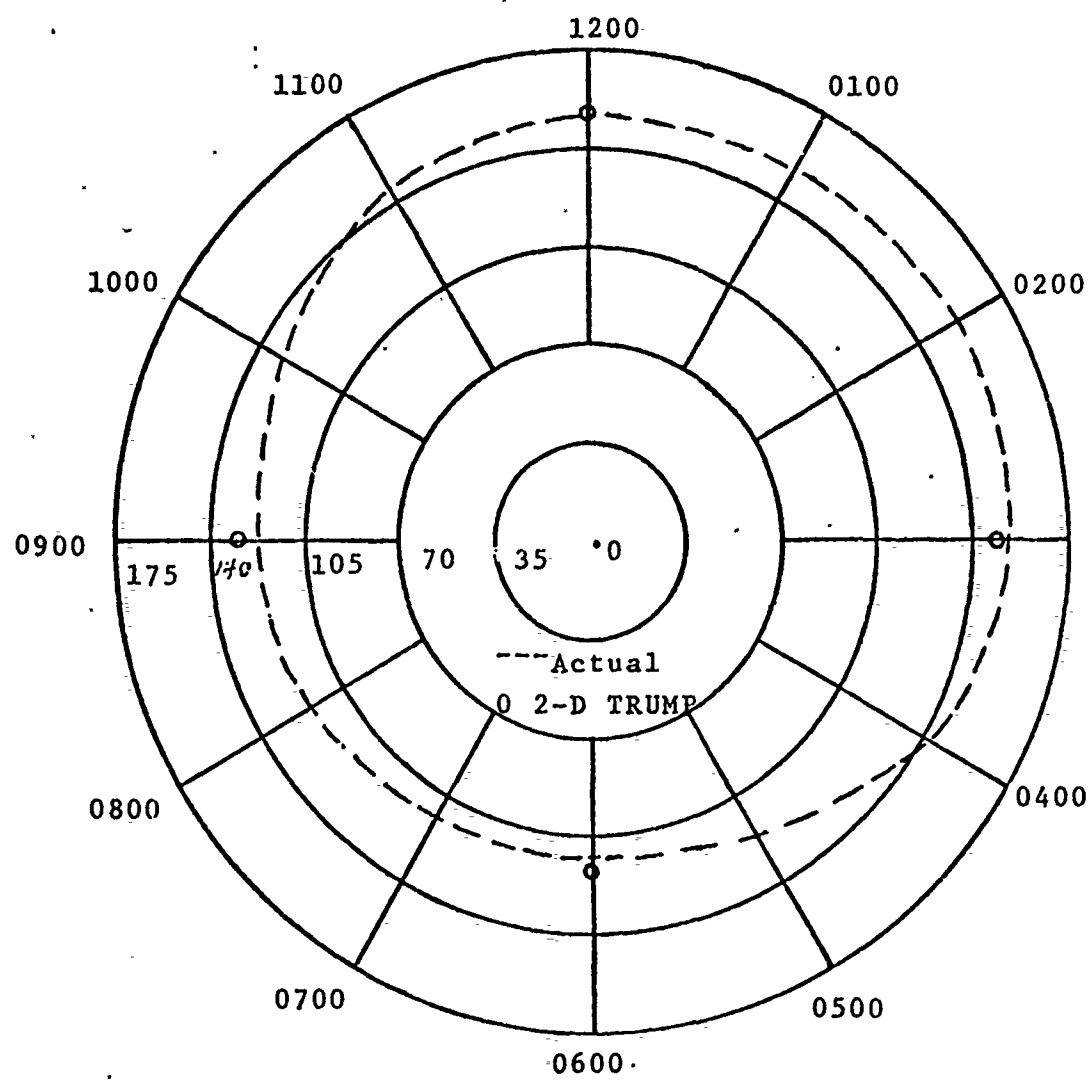


Figure 20: Temperature Distribution at Surface of Storage Container at Maximum Bulk Temperature at approximately 1500 on 2 August 1972.

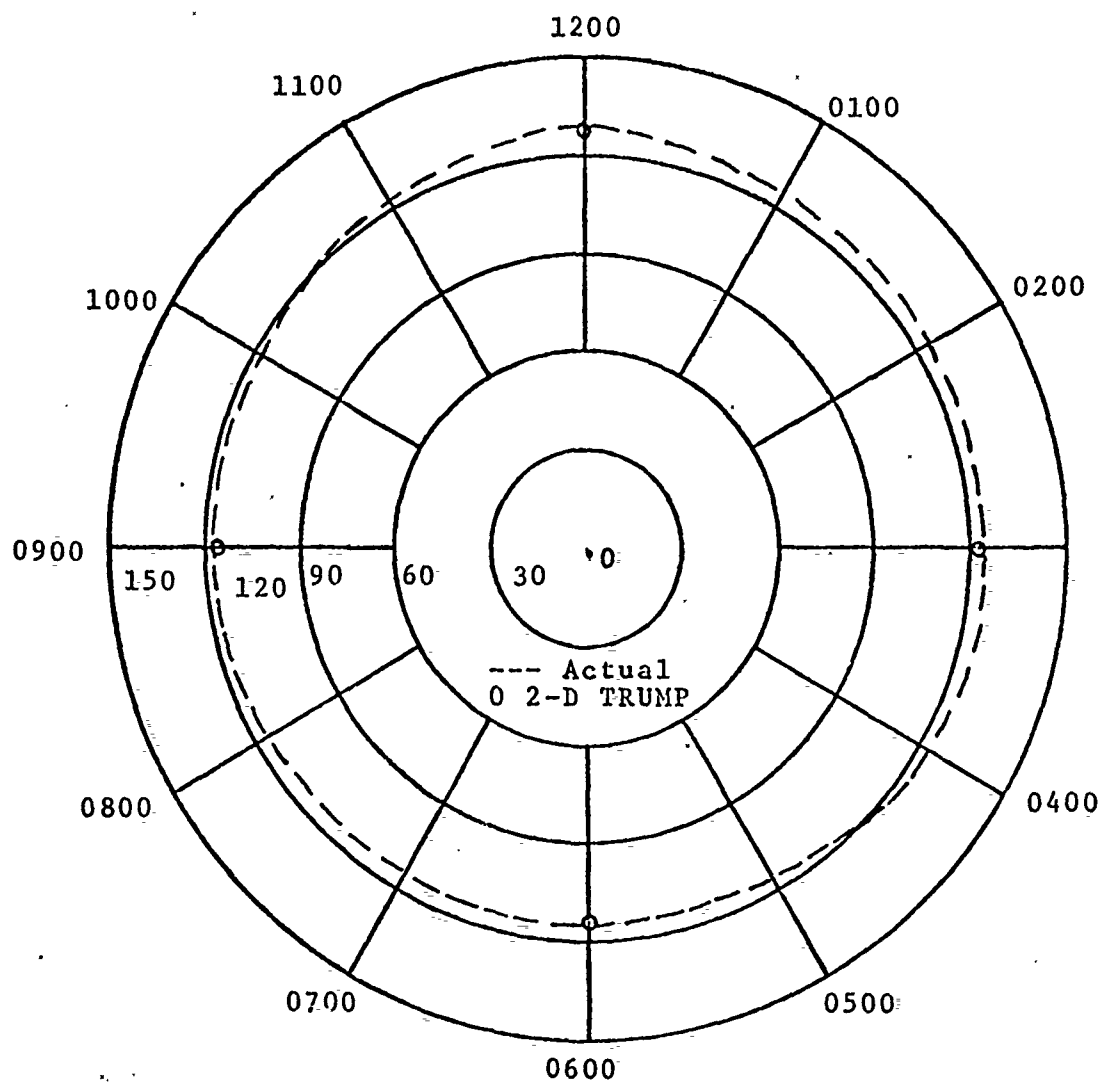


Figure 21: Temperature Distribution at Surface of the Rocket Motor at Maximum Bulk Temperature at approximately 1500 on 2 August 1972.

D. LIQUID CRYSTALS

The encapsulated cholesteric liquid crystals applied to the surface of the storage container gave brilliant colors under the intense desert sun. These colors were much clearer and brighter than the same crystals viewed under laboratory lighting conditions. The liquid crystals photographed well in both the color movies and the color slides. The movies showed by time lapse photography the rapidly changing surface temperature of the storage container. Two sample color prints made from the color slides are enclosed as Figures 22 and 23 to show the brilliance of the colors and the feasibility of obtaining data from color photos. The only photographic problem encountered was the intense reflection of the sunlight from the polyurethane film. This problem was partially overcome by taking the photographs from angles where the reflection was less intense. Qualitatively the liquid crystals were not adversely affected by the sun's rays after two weeks of desert exposure. No accurate quantitative determination was attempted; however, rough approximations were made at the site. These approximations were made by noting the color exhibited by a crystal at a certain time and then comparing the calibration of the crystal (Table 1) to the temperature recorded by the thermocouple located directly beneath the region of color change. The readings were within $\pm 2^{\circ}\text{F}$, which was very encouraging, especially considering the approximations made while taking these measurements. Although photos were taken only during

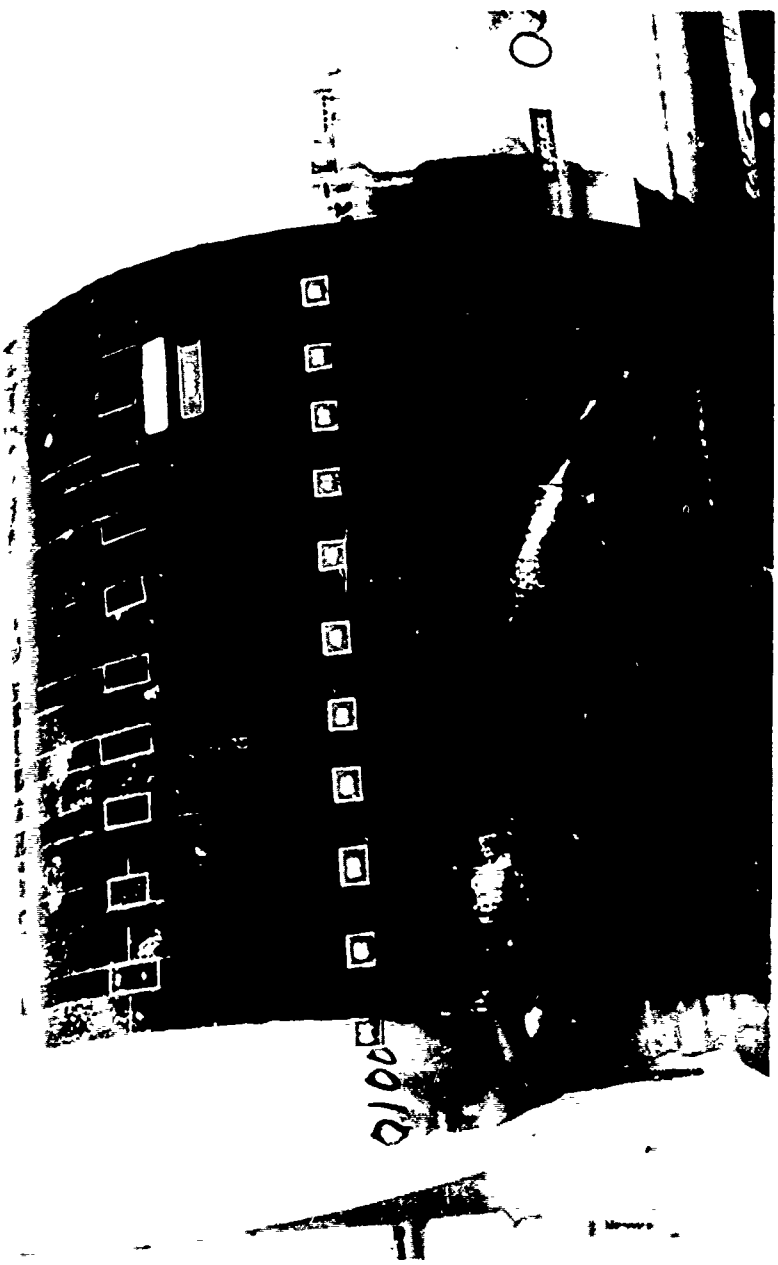


Figure 22. Thermal Mapping with Liquid Crystals.

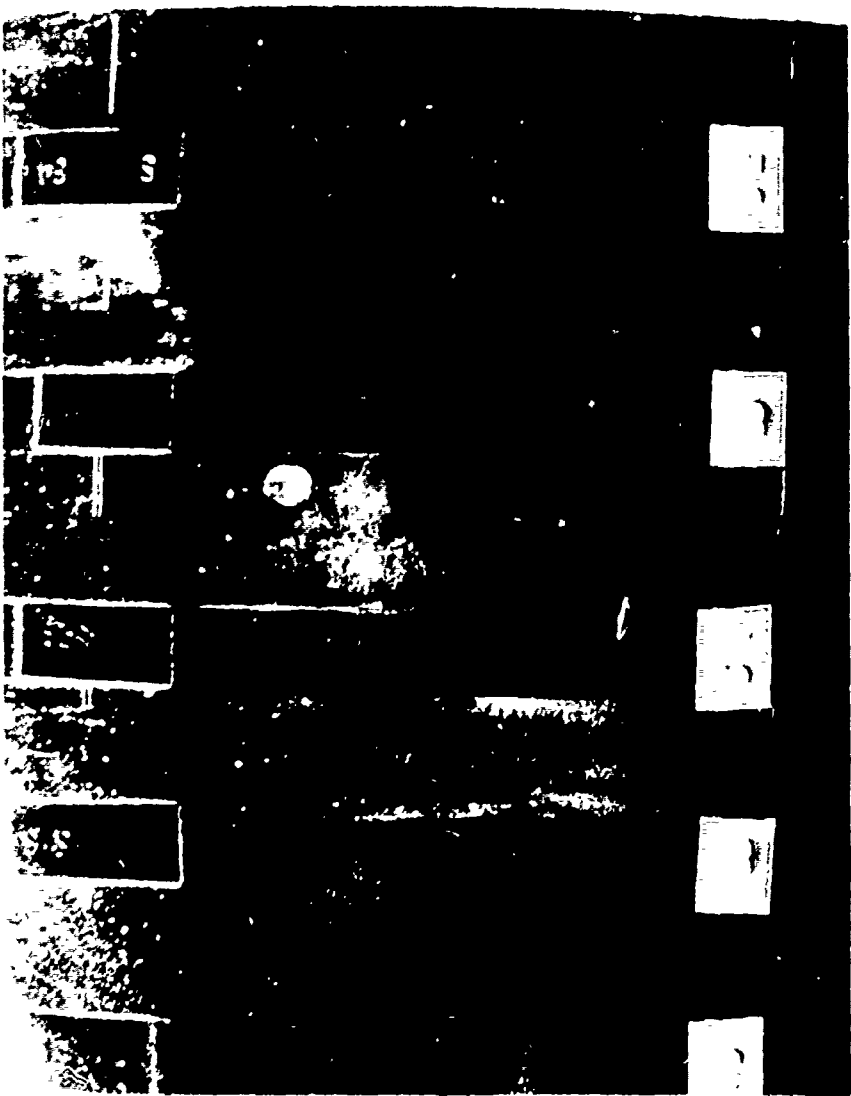


Figure 23. Liquid Crystals Feasible Under Hostile Environment.

the initial two weeks of the study, on site observations indicate that the crystals are still showing brilliant colors after 3-1/2 months. Preliminary evidence indicates that the polyurethane film did protect the crystals from decomposing from the sun's rays and from being worn away by the wind blown sand.

It was noted that the surface temperature of the storage container under the liquid crystals reached temperatures up to 15°F higher than a similar point not under the crystals. This 15°F difference was only evident when maximum temperatures were obtained. During sunlight hours the temperature under the liquid crystals was always somewhat higher; however, at night both temperatures were equal. The difference in the container surface temperatures led to a difference of 4°F on the surface of the rocket motor and 1°F at the center of the motor. It is believed that the difference in emissivities of the gray and black surfaces resulted in the difference in container surface temperature.

VI. CONCLUSIONS

From the results of this investigation, the following conclusions were drawn:

1. Although a sine wave is not a perfect fit for the experimental data at all points, it is useful in predicting bulk temperatures in the rocket motor, especially if only the high and low bulk temperatures are of concern. This is especially true in the one dimensional case. In the two dimensional case, the problem of phase shift variations make the method of sinusoidal variation less desirable, although still useful.

2. The simulation of the actual data by a table of temperatures gave the most accurate predictions of the experimental data. This method should be used whenever tabulated data are available; however, this will generally not be the case for design work, in which case the sinusoidal approximations must be used.

3. The flexibility of both the analytical and computer simulations allow the changing of many parameters. The resulting effects of these changes on rocket motor temperature can be studied with the models.

4. The convection assumption for this system resulted in only small changes in temperature and can be neglected when predicting design temperatures. Either the Liu or Beckmann correlation should be used to determine if convection can be neglected in a particular system.

5. The use of an empty storage container to obtain surface temperature data is a good approximation to using one with a rocket motor inside.

6. It is feasible to use liquid crystals for thermal mapping under desert conditions. Color photography with standard equipment gives excellent results since brilliant colors were observed.

7. The liquid crystals appear to be stable for at least two weeks under the desert conditions when protected with a polyurethane coating.

8. The application of the liquid crystal system to the surface of the storage container resulted in large increases in the surface temperature of the container throughout the hottest part of the day. Care must be taken in applying and interpreting thermal readings from liquid crystals when exposed to radiant heating.

VII. RECOMMENDATIONS

From the results of this basic study, the following recommendations for future work are offered:

1. To refine the results of this project, a second rocket motor storage container system should be instrumented with the following changes:

a. Liquid crystals should not be applied to the system used as the experimental model. As steel is a good thermal conductor, axial conduction on the surface of the storage container may be significant. Heat flow from the area where the crystals are applied may lead to higher than normal temperatures at other points on the surface of the container.

b. The rocket motor should be weighed before and after the loading of the dry sand so that an accurate determination of the density of the propellant simulant can be determined.

c. Four additional thermocouples should be located on the surface of the storage container to better enable the averaging of data. At present, the #1 thermocouple which was used as the average temperature reading of the top quarter of the surface of the container, in actuality is its hottest point; likewise the #10 thermocouple was used as the average temperature of the bottom quarter of the surface, in actuality it's the coldest point. For averaging data, it is recommended that thermocouples be placed at 0130,

0430, 0730, and 1030 and the quarters of the system be divided at 0300, 0600, 0900, and 1200 to give a more realistic bulk temperature. Thermocouples at 1200 and 0600 will provide the maximum and minimum temperature of the system.

2. The TRUMP program should be rerun in both the one and two dimensional form, varying the mesh sizes to determine the optimum number of nodes.

3. A long term study of the effects of the desert environment on liquid crystals should be done. The crystals should be calibrated before being placed in the desert and then brought to a laboratory for recalibration at specific intervals.

4. Several modifications should be made to the TRUMP program to make it comparable to the version used at Lawrence Radiation Laboratory. The variable conductivity section (BLOCK 2) and the PLOT subroutine (BLOCK 11) need to be corrected. The TIMEP subroutine which allows the setting of the problem time interval between data output should be added to this version of TRUMP. It would also be advantageous to increase the amount of tabular data that could be read in as boundary temperatures.

5. From an academic standpoint, the effects of free convection in an air gap with varying boundary temperatures should be investigated.

APPENDIX A

Introduction to Liquid Crystals

Liquid crystals were first discovered in 1889 by Reinitzer [Ref. 8] and the investigations of Lehmann which continued to 1915. Liquid crystals were considered to be laboratory curiosities with no scientific or practical merit until the 1950's. They share some of the properties of both liquids and crystals; for example, a typical liquid crystal substance scatters light in symmetrical patterns and reflects different colors depending on the angle from which it is viewed. Studies in the last few years have helped to clarify the unusual molecular structure of liquid crystals. Many applications arise from their ability to detect minute fluctuations in temperature, mechanical stress, electromagnetic radiation and chemical environment by changes in their color.

Liquid crystals are divided into three classes; smectic, nematic, and cholesteric, depending on the degree of spatial arrangement of the molecules in the mass of the material and the type of the material [Ref. 9]. In this project only cholesteric liquid crystals were used and therefore only their properties will be mentioned. The molecular structure of cholesteric liquid crystals is characteristic of the esters of cholesterol (Figure 24). The molecular layers are very thin with the long axis of the molecules parallel to the plane of the layers. The individual molecules are

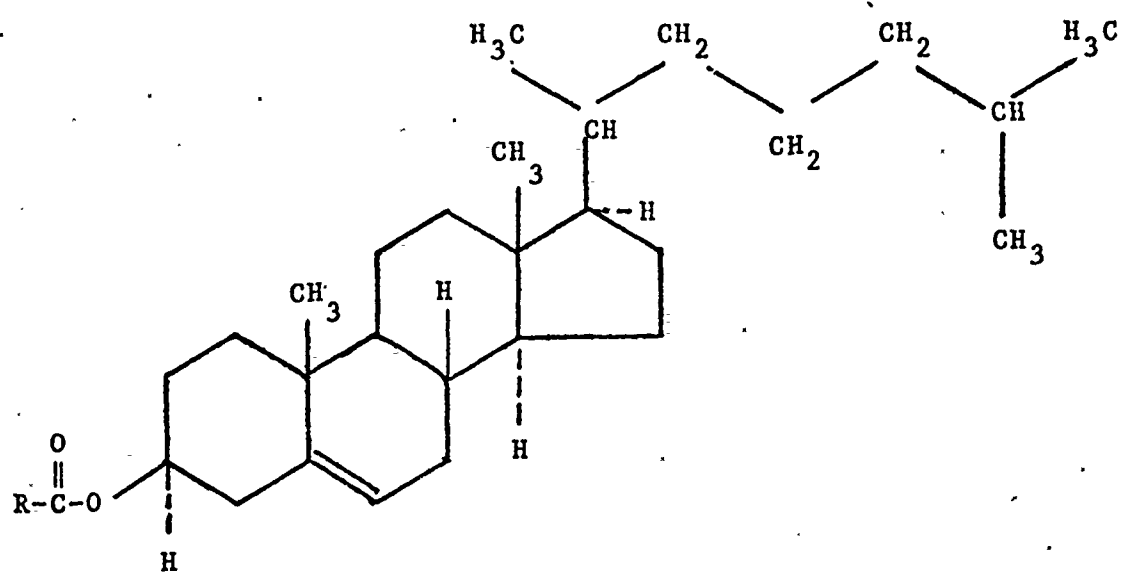


Figure 24: Molecular Structure of Cholesteric Ester

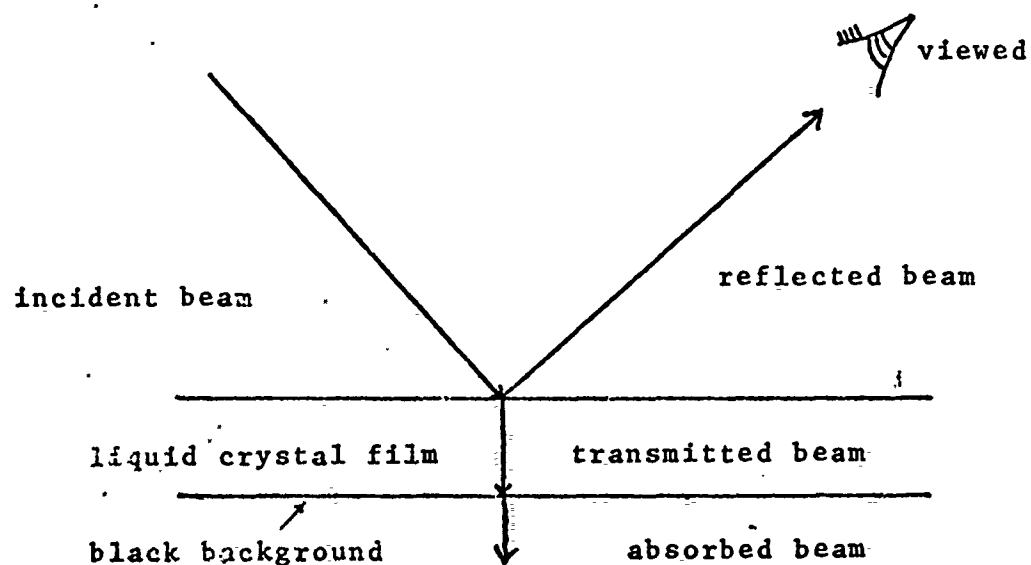


Figure 25. Light Reflection from Liquid Crystals.

basically flat, with a side chain of methyl groups ($-\text{CH}_3$) projecting upward from the plane of each molecule. This configuration causes the direction of the long axis of the molecules in each layer to be displaced slightly from the corresponding direction in adjacent layers. This displacement, which averages about fifteen minutes of arc per layer, is cumulative through successive layers, and the overall displacement traces out a helical path.

The molecular structure of cholesteric liquid crystals gives rise to many peculiar optical properties. If linearly polarized light is transmitted perpendicularly to the molecular layers, the direction of the electric vector of the light will be rotated to the left in a helical path. Therefore, the plane of polarization will also be rotated to the left, through an angle proportional to the thickness of the transmitting material. Liquid crystals are the most optically active substances known. Another strictly crystalline optical property exhibited by cholesteric liquid crystals is circular dichroism. When ordinary white light is incident to a cholesteric material, the light is separated into two components, one with the electric vector rotating clockwise, the other rotating counterclockwise. Depending on the material, one of these components is transmitted, and the other is reflected. It is this property that gives the cholesteric phase its iridescent color when it is illuminated by white light. The particular combination of colors depends on the material, the temperature, and the angle of the incident light.

The molecular structure of a cholesteric substance is very delicately balanced and is easily upset. Any small disturbance that interferes with the weak forces between the molecules can produce marked changes in optical properties such as reflection, transmission, birefringence, circular dichroism, optical activity and color. The most striking optical transformation that occurs in a cholesteric substance, in response to small changes in its environment, is the variation of color with temperature. The crystal lattice is disrupted by the thermal vibrations giving successive transitions between the solid, the mesophase, and the isotropic liquid with rising temperature. The change from the three dimensional order of the crystal lattice to the disorder of the isotropic liquid occurs via one or more intermediate states, each of which has a particular temperature range at which it is stable [Ref. 10].

A cholesteric liquid crystal system responds to changes in temperature by sequentially passing through the complete visual spectrum (red through violet) in fractions or multi-degrees, depending on which cholesterol esters comprise the formulation. This color phenomenon is reversible and has been reported to function over a temperature range of -20°C to 250°C. A very important point to note is that at a certain temperature a given material or combination of materials will always exhibit the same color. Also, the rate of change from color to color as well as the exact temperature at which the specific color changes occur are invariable. By

mixing cholesteric substances in various proportions, any desired temperature combination can be obtained. The thickness of the cholesteric film does not affect the predominant wave length of the reflected light; the light becomes circularly polarized [Ref. 11].

The colors scattered by the liquid crystals represent only a fraction of the incident light (Figure 25). The remaining portion of the incident light is transmitted by the liquid crystals. Therefore, an absorptive black background must be used to prevent reflection of the transmitted light, thereby enhancing the resolution of the scattered colors or wavelengths reflected by the liquid crystal system.

The cholesteric liquid crystal systems often present a number of problems due to the fact that they are viscous liquids. Some problems associated with the handling and the use of these materials are:

1. The tendency of the liquid crystal system to flow during application can cause variations in applied film thickness. This may result in non-uniform thermal patterns.
2. Direct exposure of liquid crystals to adverse environmental effects can cause variations in their sensitivity and deteriorate their color response in a few days.

These problems can be partially overcome by using an encapsulated liquid crystal material system. The capsules are 20-30 microns in diameter and are a water-based slurry suitable for application by conventional coating techniques such as brushing or spraying.

Encapsulated liquid crystals offer several advantages:

1. They convert the liquid crystal system to a pseudo-solid, which provides for easier handling, application, and use.
2. They provide longer shelf life by minimizing surface contamination and giving protection from ultraviolet light [Ref. 12].
3. They exhibit relatively unlimited fatigue life.
4. They reduce the angular dependence of the color observed.

APPENDIX B

Analytical Solution

The method of complex temperature as presented by Arpaci [Ref. 1] was used to find the steady periodic solution of a body experiencing a periodic sinusoidal disturbance. The general heat conduction equation in cylindrical coordinates was the basis for this derivation. It was assumed that no heat sources existed in this problem, that the rocket motor storage container system was infinitely long, that there was no heat conduction in the axial or circumferential directions, and that the container surface temperature was spatially uniform. Figure 26 gives a basic sketch of the system. The assumptions reduced the heat conduction equation to

$$\frac{1}{r} \frac{\partial(r \frac{\partial T}{\partial r})}{\partial r} = \frac{1}{\alpha} \frac{\partial T}{\partial t} \quad (1)$$

where r is the radial distance from the center of the rocket motor, T is the temperature of the rocket motor at time t and position r , and α is the thermal diffusivity, a property of the conducting material.

$$\alpha = \frac{k}{\rho c} \quad (2)$$

where k is the thermal conductivity of the conducting material, ρ is the density of the material, and c is the specific heat. All thermal properties were assumed to be constant over the temperature range of this problem.

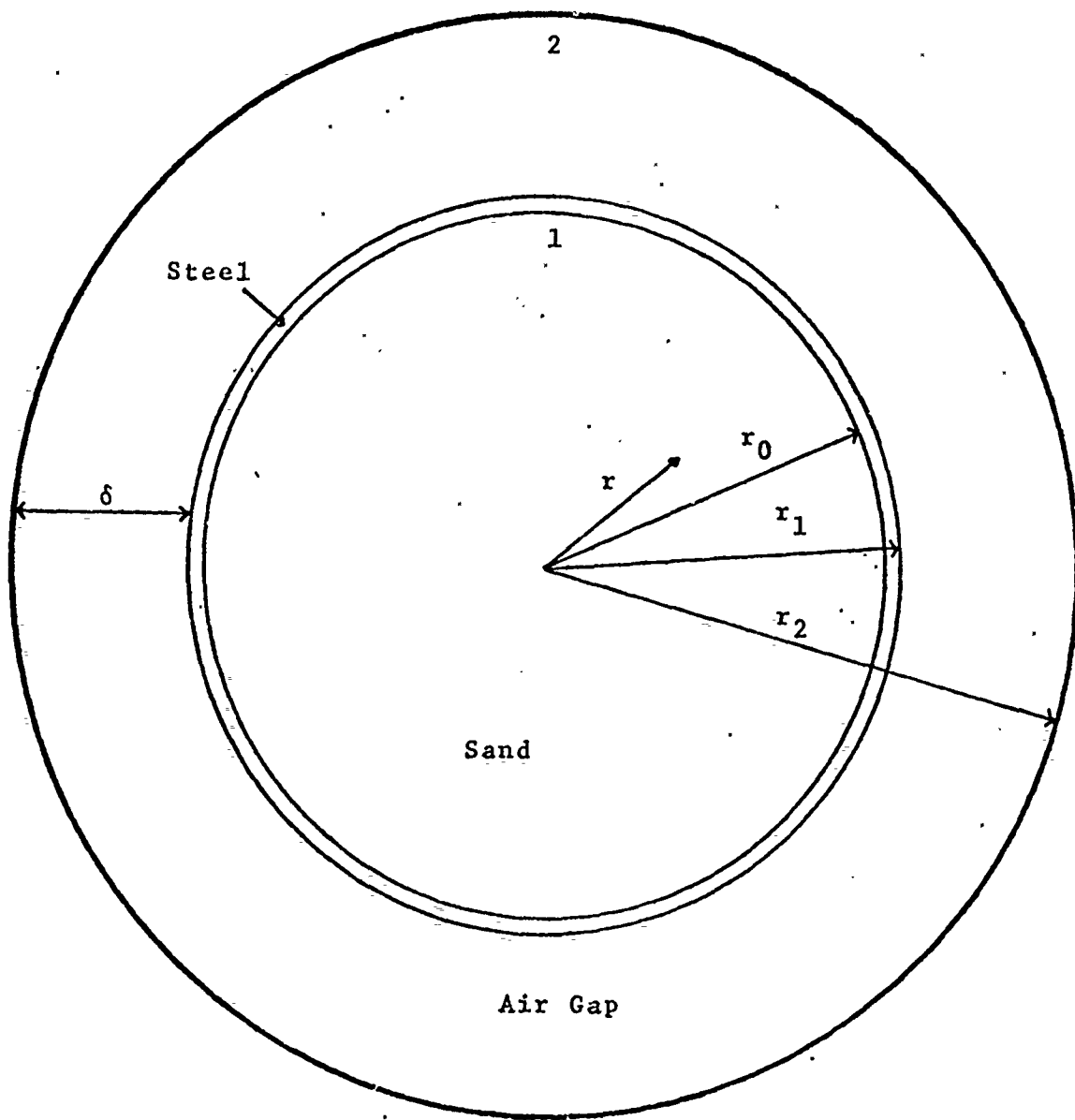


Figure 26. Analytical Model of Experimental System.

The boundary conditions used in this derivation were

$$\frac{dT}{dr} = 0 \quad \text{at } r = 0$$

$$\text{and } \frac{dT}{dr} = -\frac{\bar{h}}{k} (T - T_{\infty}) \quad \text{at } r = r_0$$

where r_0 is the inner radius of the rocket motor.

T_{∞} is the known storage container temperature which is assumed to vary as

$$T_{\infty} = (T_M - T_A) \sin \omega t + T_A$$

where

T_M = maximum bulk temperature of the storage container

T_A = average bulk temperature of the storage container

ω = frequency of the sinusoidal variation ($\frac{2\pi}{24 \text{ hours}}$)

t = time

\bar{h} is the effective heat transfer coefficient across the air gap between the storage container and the rocket motor. It combines the heat transfer effects of radiation, convection, and conduction into one coefficient. The radiation coefficient was linearized by assuming constant temperatures (T_1, T_2), representative of the average temperatures expected in the problem, in the equation

$$h_{RAD} = \mathcal{F}_{1-2} \sigma (T_1 + T_2) (T_1^2 + T_2^2)$$

where σ is the Stefan-Boltzmann constant and \mathcal{F}_{1-2} is the radiation exchange factor between surfaces 1 and 2. The convection coefficient is

$$h_{CON} = \frac{k_c}{\delta}$$

where k_c is the effective conductivity of air as obtained from the Beckmann and Liu correlations [Ref. 5 and 7] and δ is the width of the air gap. In the analytical model,

the effective conductivity was assumed to equal the conductivity, thereby treating it as pure conduction and

$$\bar{h} = h_{RAD} + h_{CON}$$

Equation (1) was non-dimensionalized using the following relationships

$$\theta = \frac{T - T_A}{T_M - T_A} \quad (\text{a non-dimensional temperature})$$

$$\xi = \frac{r}{r_o} \quad (\text{a non-dimensional distance})$$

to give

$$\frac{1}{\xi} \frac{d(\xi \frac{d\theta}{d\xi})}{d\xi} = \frac{r_o^2}{a} \frac{d\theta}{dt}$$

with boundary conditions

$$\frac{d\theta}{d\xi} = 0 \quad \text{at } \xi = 0$$

$$\text{and } \frac{d\theta}{d\xi} = -\beta(\theta - \sin \omega t) \text{ at } \xi = 1$$

where $\beta = \frac{hr_o}{k}$ is the Biot modulus (which compares the relative magnitudes of the effective heat transfer coefficient across the air gap and the internal conduction resistances to heat transfer).

An initial condition was not specified as the only concern was with the steady state, periodic behavior. Following Arpaci [Ref. 1], a complex temperature was defined as

$$\psi(r, t) = \theta^*(r, t) + i\theta(r, t)$$

where $\psi(r, t)$ satisfied

$$\frac{1}{\xi} \frac{d(\xi \frac{d\psi}{d\xi})}{d\xi} = \frac{r_o^2}{a} \frac{d\psi}{dt} \quad (3)$$

with boundary conditions

$$\frac{d\psi}{d\xi} = \frac{d\theta^*}{d\xi} + i \frac{d\theta}{d\xi} = 0 \quad \text{at } \xi = 0$$

$$\text{and } \frac{d\psi}{d\xi} = -\beta(\psi - e^{i\omega t}) = -\beta(\theta^* - \cos \omega t) + i\{-\beta(\theta - \sin \omega t)\} \text{ at } \xi = 1$$

This leads to $\theta(r, t)$ which satisfied

$$\frac{1}{\xi} \frac{d(\xi \frac{d\theta}{d\xi})}{d\xi} = \frac{r_o^2}{a} \frac{d\theta}{dt}$$

with boundary conditions

$$\frac{d\theta}{d\xi} = 0 \quad \text{at } \xi = 0$$

$$\text{and } \frac{d\theta}{d\xi} = -\beta(\theta - \sin \omega t) \quad \text{at } \xi = 1$$

also $\theta^*(r, t)$ which satisfied

$$\frac{1}{\xi} \frac{d(\xi \frac{d\theta^*}{d\xi})}{d\xi} = \frac{r_o^2}{a} \frac{d\theta^*}{dt}$$

with boundary conditions

$$\frac{d\theta^*}{d\xi} = 0 \quad \text{at } \xi = 0$$

$$\text{and } \frac{d\theta^*}{d\xi} = -\beta(\theta^* - \cos \omega t) \quad \text{at } \xi = 1$$

A solution of the form

$$\psi(r, t) = \phi(r)\tau(t)$$

was assumed, where for large values of time $\tau(t)$ was assumed to equal $e^{i\omega t}$; therefore,

$$\psi(r, t) = \phi(r)e^{i\omega t} \tag{4}$$

Equation (4) was then substituted into equation (3)

$$\frac{1}{\xi} \frac{d(\xi \frac{d\phi}{d\xi})}{d\xi} - \frac{i\omega r_o^2 \phi}{a} = 0 \tag{5}$$

with boundary conditions

$$\frac{d\phi}{d\xi} = 0 \quad \text{at } \xi = 0$$

and $\frac{d\phi}{d\xi} = -\beta(\phi-1) \quad \text{at } \xi = 1$

Equation (5) was expanded to give

$$\frac{d^2\phi}{d\xi^2} + \frac{1}{\xi} \frac{d\phi}{d\xi} - \frac{i\omega r_0^2}{\alpha} \phi = 0 \quad (6)$$

Now, let $Z = \sqrt{\frac{i\omega r_0^2}{\alpha}} \xi$

and substitute into equation (6)

$$\frac{d^2\phi}{dz^2} + \frac{1}{z} \frac{d\phi}{dz} - \phi = 0 \quad (7)$$

with boundary conditions

$$\frac{d\phi}{dz} = 0 \quad \text{at } z = 0$$

and

$$\frac{d\phi}{dz} = -\frac{\beta}{\sqrt{\frac{i\omega r_0^2}{\alpha}}} (\phi-1) \quad \text{at } z = \sqrt{\frac{i\omega r_0^2}{\alpha}}$$

The general solution of equation (7) is

$$\phi = C_1 I_0(z) + C_2 K_0(z) \quad (8)$$

as given in Ref. 13 with

$$I_0(z) = 1 + \left(\frac{1}{2}z\right)^2 + \frac{\left(\frac{1}{2}z\right)^4}{(2!)^2} + \dots = \sum_{n=0}^{\infty} \frac{\left(\frac{1}{2}z\right)^{2n}}{(n!)^2}$$

and

$$K_0(z) = -\{\gamma + \log(\frac{1}{2}z)\} I_0(z) + \sum_{n=1}^{\infty} \frac{\left(\frac{1}{2}z\right)^{2n}}{(n!)^2} - \{1 + \frac{1}{2} + \frac{1}{3} + \dots + \frac{1}{n}\}$$

Now using the boundary condition

$$\frac{d\phi}{dz} = 0 \quad \text{at } z = 0$$

and differentiating equation (8) yields

$$\frac{d\phi}{dz} = C_1 \frac{d(I_o(z))}{dz} + C_2 \frac{d(K_o(z))}{dz}$$

where

$$\frac{d(I_o(z))}{dz} = 0 \quad \text{at } z = 0$$

and

$$\frac{d(K_o(z))}{dz} \neq 0 \quad \text{at } z = 0$$

therefore $C_2 \equiv 0$

and

$$\phi = C_1 I_o(z) \quad (9)$$

Now using the second boundary condition that

$$\frac{d\phi}{dz} = - \frac{\beta}{\sqrt{\frac{i\omega r_o^2}{\alpha}}} (\phi - 1) \quad \text{at } z = \sqrt{\frac{i\omega r_o^2}{\alpha}} \quad (10)$$

and differentiating equation (9) gives

$$\frac{d\phi}{dz} = C_1 \frac{d(I_o(z))}{dz}$$

Noting that $\frac{d(I_o(z))}{dz} = I_1(z)$ and substituting into

equation (10)

$$C_1 I_1 \left(\sqrt{\frac{i\omega r_o^2}{\alpha}} \right) = \frac{\beta}{\sqrt{\frac{i\omega r_o^2}{\alpha}}} \left(C_1 I_o \left(\sqrt{\frac{i\omega r_o^2}{\alpha}} \right) - 1 \right)$$

Rearranging and solving for C_1

$$C_1 = \frac{1}{\sqrt{\frac{i\omega r_o^2}{\alpha\beta^2}} I_1 \left(\sqrt{\frac{i\omega r_o^2}{\alpha}} \right) + I_o \left(\sqrt{\frac{i\omega r_o^2}{\alpha}} \right)}$$

and then substituting into equation (9)

$$\phi = \frac{I_o(z)}{I_o \left(\sqrt{\frac{i\omega r_o^2}{\alpha}} \right) + \frac{1}{\beta} \sqrt{\frac{i\omega r_o^2}{\alpha}} I_1 \left(\sqrt{\frac{i\omega r_o^2}{\alpha}} \right)} \quad (11)$$

Now as

$$J_V(imx) = i^V I_V(mx) \quad [\text{Ref. 3, p. 135}]$$

$$I_o \left(\sqrt{\frac{\omega r_o^2}{\alpha}} i^{1/2} \xi \right) = J_o \left(\sqrt{\frac{\omega r_o^2}{\alpha}} i^{3/2} \xi \right)$$

and

$$I_1 \left(\sqrt{\frac{\omega r_o^2}{\alpha}} i^{1/2} \xi \right) = \frac{1}{i} J_1 \left(\sqrt{\frac{\omega r_o^2}{\alpha}} i^{3/2} \xi \right)$$

Let $a = \sqrt{\frac{\omega r_o^2}{\alpha}}$ and substitute into equation (11)

$$\phi = \frac{J_o(i^{3/2} a\xi)}{J_o(i^{3/2} a) - \frac{a}{\beta} i^{3/2} J_1(i^{3/2} a)} \quad (12)$$

$$\text{Now } i^{3/2} = e^{i\frac{3\pi}{4}} = \cos \frac{3\pi}{4} + i \sin \frac{3\pi}{4} = \frac{1}{\sqrt{2}} (-1 + i)$$

Substituting this into equation (12)

$$\phi = \frac{J_o(i^{3/2} a\xi)}{J_o(i^{3/2} a) + \frac{a}{\sqrt{2}\beta} (1-i) J_1(i^{3/2} a)} \quad (13)$$

$$\text{As } J_o(a\xi i^{3/2}) = J_o(a\xi e^{i\frac{3\pi}{4}}) = \text{BER}_o(a\xi) + i\text{BEI}_o(a\xi)$$

and

$$J_1(a\xi i^{3/2}) = J_1(a\xi e^{i\frac{3\pi}{4}}) = \text{BER}_1(a\xi) + i\text{BEI}_1(a\xi)$$

Substituting these results into equation (13) yields

$$\phi = \frac{\text{BER}_o(a\xi) + i\text{BEI}_o(a\xi)}{\text{BER}_o(a) + i\text{BEI}_o(a) + \frac{a}{\sqrt{2}\beta} (1-i)(\text{BER}_1(a) + i\text{BEI}_1(a))} \quad (14)$$

After rearrangement.

$$\phi = \frac{\text{BER}_o(a\xi) + i\text{BEI}_o(a\xi)}{[\text{BER}_o(a) + \frac{a}{\sqrt{2}\beta}\text{BER}_1(a) + \frac{a}{\sqrt{2}\beta}\text{BEI}_1(a)] + i[\text{BEI}_o(a) + \frac{a}{\sqrt{2}\beta}\text{BEI}_1(a) - \frac{a}{\sqrt{2}\beta}\text{BER}_1(a)]}$$

Letting

$$x_R = \text{BER}_o(a) + \frac{a}{\sqrt{2}\beta}\text{BER}_1(a) + \frac{a}{\sqrt{2}\beta}\text{BEI}_1(a)$$

and

$$x_i = \text{BEI}_o(a) + \frac{a}{\sqrt{2}\beta}\text{BEI}_1(a) - \frac{a}{\sqrt{2}\beta}\text{BER}_1(a)$$

and substituting into equation (14) gives

$$\phi = \frac{\text{BER}_o(a\xi) + i\text{BEI}_o(a\xi)}{x_R + ix_i}$$

Rationalizing the denominator yields

$$\phi = \frac{\text{BER}_o(a\xi) + i\text{BEI}_o(a\xi)}{x_R^2 + x_i^2} (x_R - ix_i) \quad (15)$$

Now

$$\phi = \frac{(\text{BER}_o(a\xi)x_R + \text{BEI}_o(a\xi)x_i) + i(\text{BEI}_o(a\xi)x_R - \text{BER}_o(a\xi)x_i)}{x_R^2 + x_i^2}$$

which after rearrangement gives

$$\phi = \sqrt{\frac{\text{BER}_o^2(a\xi) + \text{BEI}_o^2(a\xi)}{x_R^2 + x_i^2}} e^{i\delta^*} \quad (16)$$

where

$$\delta^* = \tan^{-1} \frac{\text{BEI}_o(a\xi)x_R - \text{BER}_o(a\xi)x_i}{\text{BER}_o(a\xi)x_R + \text{BEI}_o(a\xi)x_i}$$

Substituting into equation (4) gives

$$\psi(r,t) = \sqrt{\frac{BER_o^2(a\xi) + BEi_o^2(a\xi)}{x_R^2 + x_i^2}} e^{i(\omega t + \delta^*)}$$

which also equals

$$\psi(r,t) = \sqrt{\frac{BER_o^2(a\xi) + BEi_o^2(a\xi)}{x_R^2 + x_i^2}} [\cos(\omega t + \delta^*) + i \sin(\omega t + \delta^*)]$$

As this problem was modeled as a sine wave, the imaginary part of $\psi(r,t)$ was used.

$$I(\psi(r,t)) = \theta(r,t) = \sqrt{\frac{BER_o^2(a\xi) + BEi_o^2(a\xi)}{x_R^2 + x_i^2}} \sin(\omega t + \delta^*) \quad (17)$$

which is the analytical solution of infinitely long concentric cylinders experiencing a periodic sinusoidal temperature variation on its outermost surface when heat conduction is assumed to be radial only.

In summary

$$\theta(r,t) = \frac{T - T_A}{T_M - T_A} = \sqrt{\frac{BER_o^2(a\xi) + BEi_o^2(a\xi)}{x_R^2 + x_i^2}} \sin(\omega t + \delta^*)$$

where

T = the temperature of a point r in the rocket motor at time t

T_A = average bulk temperature of the storage container

T_M = maximum bulk temperature of the storage container

ω = frequency of the sinusoidal variation ($2\pi/24$ hours)

t = time

$\xi = \frac{r}{r_o}$ = dimensionless distance from the center of the rocket motor

r_o = distance to the surface of the rocket motor

r = distance from the center of the rocket motor

$a = \sqrt{\frac{\omega r_o^2}{\alpha}}$ = conduction parameter

$$\alpha = \frac{k}{\rho c} = \text{thermal diffusivity}$$

ρ = density

k = thermal conductivity

c = specific heat

BER = real Bessel Function

BEi = imaginary Bessel Function

$$X_R = BER_0(a) + \frac{a}{\sqrt{2}\beta} BER_1(a) + \frac{a}{\sqrt{2}\beta} BEi_1(a)$$

$$X_i = \frac{BEi_0(a)}{hr} + \frac{a}{\sqrt{2}\beta} BEi_1(a) - \frac{a}{\sqrt{2}\beta} BER_1(a)$$

$$\beta = \frac{\rho}{k} = \text{Biot modulus}$$

$$\delta^* = \tan^{-1} \frac{BEi_0(a\xi)X_R - BER_0(a\xi)X_i}{BER_0(a\xi)X_R + BEi_0(a\xi)X_i}$$

The following computer programs were used to investigate a wide variety of parameters. The outputs are samples of some of these parameter studies.

ANALYTICAL SOLUTION PARAMETER STUDY

```

DO 2 K=1,5
READ(5,F10.6)
FORMAT(6.31)
31 FORMAT(19X,A,'4X','B','4X','DISTANCE FROM CENTER',4X,'TIME DELAY
11 IN RADIAN S,3X,'RELATIVE AMPLITUDE')
DO 3 L=1,10
READ(5,F10.6)
INPUT VALUES OF A AND B, CALCULATE THE DENOMINATOR(DENOM) OF EQUATION 17.
Y=SQRT(2.0)
Z=A
BEROZ=(1.0-(Z**4/64.0)+(Z**8/147500.0))
BERIZ=0.25*Z**2*(1.0-(Z**4/576.0)+(Z**8/3790000.0))
1737280*0)=Z/(2.0*Y)*(1.0+(Z**4/8.0)-(Z**6/128.0)-(Z**8/185128.0))
137230*0)=(Z**2*Y)*(1.0-(Z**4/8.0)-(Z**8/128.0)+(Z**6/9216.0)+(Z**8/7
XR=BEROZ+A/(Y*B)*BERIZ-A/(Y*B)*BERIZ
XI=BEROZ+A/(Y*B)*BERIZ-A/(Y*B)*BERIZ
Y=XR**2+XI**2
DENOM=SQRT(Y)
AT THE CENTER, HALF WAY TO THE SURFACE, AND AT THE SURFACE OF THE MOTOR,
CALCULATE THE NUMERATOR(DNUM) OF EQUATION 17.
DO 30 I=1,3
C=(I-1)/2.0
Z=A*C
BEROZ=(1.0-(Z**4/64.0)+(Z**8/147500.0))
BERIZ=0.25*Z**2*(1.0-(Z**4/576.0)+(Z**8/3790000.0))
DNUM=SORT(C)
CALCULATE THE TIME DELAY(DEL).
DNJ=XR*BEROZ-XI*BEROZ
DNO=XR*BEROZ+XI*BEROZ
X=DNU/DNO
IF(DNO.DLT.0.0) GO TO 22
DEL=DATAN(X)
GO TO 23
22 DEL=TAN(X)-3.14159
CALCULATE THE RELATIVE AMPLITUDE(S).
23 S=DNUM/DENOM
WRITE(6,32)A*B*S*DEL,S
32 FORMAT(1.18X,F3.1,IX,F5.1,12X,F3.1,19X,F5.2,18X,F4.2)
30 CONTINUE
3 CONTINUE
2 STOP
END

```


ANALYTICAL SOLUTION + SAMPLE PROBLEM

```

//WIR11687 JOB (1687:0860FT,NF12),WIRZBURGER, ALLEN
//EXEC FOR TCLGP, RESIN DD#
//FORT*SYSIN DD#
REAL*8 LABEL(12)
REAL*4 J2 A B, MAXIMUM TEMPERATURE AND AVERAGE TEMPERATURE.
INPUT VALUES ON J2(49), TINF(49), T1(49), T2(49);
DIMENSION J2(49), TM, TA
READ(5,11)A,B,TM,TA
11 FORMAT(14F10.6)
10 READ(5,10)(TITLE(I), I=1, 12)
10 DMEGA=2.0*3.14159/1440.0
FROM INPUT VALUES OF A AND B, CALCULATE THE DENOMINATOR(DENOM) OF EQUATION 17.
IY=SQR(2.0)
Z=A
BEROZ=(1.0-(Z**4/64.0)+(Z**8/14750.0*(Z**31))
BERIOZ=0.25*(Z**2*((1.0-(Z**4/576.0)+(Z**8/3790000.0)))
BERIZ=-Z/(2.0*Y)*((1.0+(Z**4/28.0)-(Z**4/128.0)-(Z**6/9216.0)+(Z**8/
1737280.0))
1 BEI1Z=Z/(2.0*Y)*(1.0-(Z**2/8.0)-(Z**4/128.0)+(Z**6/9216.0)+(Z**8/7
137280.0))
XR=BEROZ+A/(Y*B)*BER1Z+A/(Y*B)*BEI1Z
XI=BERIOZ+A/(Y*B)*BEI1Z-A/(Y*B)*BERIZ
V=XR*Y2+XI*Y2
DENOM=SQRT(V)
N=0
THE TEMPERATURE OF THE CONTAINER(TINF) IS CALCULATED AT 30 MINUTE INTERVALS.
DO 40 J=1,1441,30
N=N+1
J2(N)=J-1
TEMP=DMEGA*(J2(N))
TINF(N)=(TM-TA)*SIN(TEMP)+TA
IF(J.EQ.1441) GO TO 31
L=(N-1)/6
N2=N-1
L2=6*L
IF(N2.EQ.L2) GO TO 21
FOR SEVEN POSITIONS BETWEEN THE CENTER OF THE ROCKET MOTOR AND THE SURFACE, THE
NUMBERATOR(DNUM) OF EQUATION 17 AND THE TIME DELAY(DEL) ARE CALCULATED.
32 DO 30 I=1,7
C=(I-1)/5.75
IF(C.GT.1.0) C=1.0
Z=A*C
BEROZ=(1.0-(Z**4/64.0)+(Z**8/14750.0*(Z**31))
BERIOZ=0.25*(Z**2*((1.0-(Z**4/576.0)+(Z**8/3790000.0)))

```

```

U=BEROZ**2+6EI0Z**2
DNU=SQR(BER0Z-X*I*BER0Z
DNU=XR*BER0Z+X*I*BER0Z
X=DNU/DNU
I=F(DNU,LT,0.0) GO TO 22
DEL=ATAN(X)
GO TO 23
22 DEL=DMEGA*(J2(N)+DEL
TIME=DNUM/DNUM*SIN(CTIME)
THE TEMPERATURE AT EACH POSITION IS CALCULATED.
C=I-1
IF(C.EQ.6.0) C=5.75
DEL=DEL/DMEGA
WRITE(6,50) C,J2(N),T(I,N),TINF(N),DEL
50 FORMAT(1,50) C,2.10X,F6.1,5X,F6.2,14X,F6.2,13X,F7.2
T1(N)=T(1,N)
T2(N)=T(7,N)
IF((I.EQ.1).AND.(J.EQ.1)) GO TO 33
IF((I.EQ.7).AND.(J.EQ.1)) GO TO 34
30 CONTINUE
40 STOP
A TEMPERATURE VERSUS TIME GRAPH IS DRAWN SHOWING THE TEMPERATURE OF THE SURFACE OF THE ROCKET MOTOR(TEDG) AND
CONTAINER(TINF). THE TEMPERATURE AT THE CENTER OF THE MOTOR(TCEN).
31 READ(5,9) LABEL
32 FORMAT(A4)
33 CALL DRAW(49,J2,TINF,1,0,LABEL,ITITLE,0,0,0,0,9,15,1,LAST)
34 READ(5,9) LABEL
35 CALL DRAW(49,J2,T1,2,0,LABEL,ITITLE,0,0,0,0,9,15,1,LAST)
36 READ(5,9) LABEL
37 CALL DRAW(49,J2,T2,3,0,LABEL,ITITLE,0,0,0,0,9,15,1,LAST)
38 WRITE(6,7) ///////////////
39 FORMAT(6,20)
40 WRITE(6,19X,'DISTANCE FROM CENTER',3X,'TIME',3X,'TEMPERATURE',2
41 X,'TEMPERATURE OF CONTAINER',3X,'TIME',3X,'DELAY')
42 WRITE(6,60)
43 FORMAT(4,19X,
44 3X,3X,3X,3X,7,7)
45 GO TO 32
46 END

```

The graph illustrates the temperature increase over time for two different containers. Both containers start at an initial temperature of 20°C. Container 1 (solid line) reaches a final temperature of 100°C at approximately 60 minutes. Container 2 (dashed line) reaches the same final temperature of 100°C at approximately 100 minutes. The x-axis represents time in minutes, and the y-axis represents temperature in degrees Celsius.

Time (min)	Temperature (°C) - Container 1	Temperature (°C) - Container 2
0	20	20
20	22	22
40	24	24
60	26	26
80	28	28
100	30	30
120	32	32

DISTANCE FROM CENTRE	TIME	TEMPERATURE	TEMPERATURE OF CONTAINER	TIME DELAY
0	0	0	0	-388.40
12m45°	0	0	0	-388.47
24m50°	0	0	0	-388.52
36m55°	0	0	0	-388.59
48m60°	0	0	0	-388.65
60m65°	0	0	0	-388.70
72m70°	0	0	0	-388.75
84m75°	0	0	0	-388.80
96m80°	0	0	0	-388.85
108m85°	0	0	0	-388.90
120m90°	0	0	0	-388.95
132m95°	0	0	0	-388.97
144m100°	0	0	0	-388.99
156m105°	0	0	0	-389.00
168m110°	0	0	0	-389.00
180m115°	0	0	0	-389.00
192m120°	0	0	0	-389.00
204m125°	0	0	0	-389.00
216m130°	0	0	0	-389.00
228m135°	0	0	0	-389.00
240m140°	0	0	0	-389.00
252m145°	0	0	0	-389.00
264m150°	0	0	0	-389.00
276m155°	0	0	0	-389.00
288m160°	0	0	0	-389.00
300m165°	0	0	0	-389.00
312m170°	0	0	0	-389.00
324m175°	0	0	0	-389.00
336m180°	0	0	0	-389.00
348m185°	0	0	0	-389.00
360m190°	0	0	0	-389.00
372m195°	0	0	0	-389.00
384m200°	0	0	0	-389.00
396m205°	0	0	0	-389.00
408m210°	0	0	0	-389.00
420m215°	0	0	0	-389.00
432m220°	0	0	0	-389.00
444m225°	0	0	0	-389.00
456m230°	0	0	0	-389.00
468m235°	0	0	0	-389.00
480m240°	0	0	0	-389.00
492m245°	0	0	0	-389.00
504m250°	0	0	0	-389.00
516m255°	0	0	0	-389.00
528m260°	0	0	0	-389.00
540m265°	0	0	0	-389.00
552m270°	0	0	0	-389.00
564m275°	0	0	0	-389.00
576m280°	0	0	0	-389.00
588m285°	0	0	0	-389.00
600m290°	0	0	0	-389.00
612m295°	0	0	0	-389.00
624m300°	0	0	0	-389.00
636m305°	0	0	0	-389.00
648m310°	0	0	0	-389.00
660m315°	0	0	0	-389.00
672m320°	0	0	0	-389.00
684m325°	0	0	0	-389.00
696m330°	0	0	0	-389.00
708m335°	0	0	0	-389.00
720m340°	0	0	0	-389.00
732m345°	0	0	0	-389.00
744m350°	0	0	0	-389.00
756m355°	0	0	0	-389.00
768m360°	0	0	0	-389.00
780m365°	0	0	0	-389.00
792m370°	0	0	0	-389.00
804m375°	0	0	0	-389.00
816m380°	0	0	0	-389.00
828m385°	0	0	0	-389.00
840m390°	0	0	0	-389.00
852m395°	0	0	0	-389.00
864m400°	0	0	0	-389.00
876m405°	0	0	0	-389.00
888m410°	0	0	0	-389.00
900m415°	0	0	0	-389.00
912m420°	0	0	0	-389.00
924m425°	0	0	0	-389.00
936m430°	0	0	0	-389.00
948m435°	0	0	0	-389.00
960m440°	0	0	0	-389.00
972m445°	0	0	0	-389.00
984m450°	0	0	0	-389.00
996m455°	0	0	0	-389.00
1008m460°	0	0	0	-389.00
1020m465°	0	0	0	-389.00
1032m470°	0	0	0	-389.00
1044m475°	0	0	0	-389.00
1056m480°	0	0	0	-389.00
1068m485°	0	0	0	-389.00
1080m490°	0	0	0	-389.00
1092m495°	0	0	0	-389.00
1104m500°	0	0	0	-389.00
1116m505°	0	0	0	-389.00
1128m510°	0	0	0	-389.00
1140m515°	0	0	0	-389.00
1152m520°	0	0	0	-389.00
1164m525°	0	0	0	-389.00
1176m530°	0	0	0	-389.00
1188m535°	0	0	0	-389.00
1200m540°	0	0	0	-389.00
1212m545°	0	0	0	-389.00
1224m550°	0	0	0	-389.00
1236m555°	0	0	0	-389.00
1248m560°	0	0	0	-389.00
1260m565°	0	0	0	-389.00
1272m570°	0	0	0	-389.00
1284m575°	0	0	0	-389.00
1296m580°	0	0	0	-389.00
1308m585°	0	0	0	-389.00
1320m590°	0	0	0	-389.00
1332m595°	0	0	0	-389.00
1344m600°	0	0	0	-389.00
1356m605°	0	0	0	-389.00
1368m610°	0	0	0	-389.00
1380m615°	0	0	0	-389.00
1392m620°	0	0	0	-389.00
1404m625°	0	0	0	-389.00
1416m630°	0	0	0	-389.00
1428m635°	0	0	0	-389.00
1440m640°	0	0	0	-389.00
1452m645°	0	0	0	-389.00
1464m650°	0	0	0	-389.00
1476m655°	0	0	0	-389.00
1488m660°	0	0	0	-389.00
1500m665°	0	0	0	-389.00
1512m670°	0	0	0	-389.00
1524m675°	0	0	0	-389.00
1536m680°	0	0	0	-389.00
1548m685°	0	0	0	-389.00
1560m690°	0	0	0	-389.00
1572m695°	0	0	0	-389.00
1584m700°	0	0	0	-389.00
1596m705°	0	0	0	-389.00
1608m710°	0	0	0	-389.00
1620m715°	0	0	0	-389.00
1632m720°	0	0	0	-389.00
1644m725°	0	0	0	-389.00
1656m730°	0	0	0	-389.00
1668m735°	0	0	0	-389.00
1680m740°	0	0	0	-389.00
1692m745°	0	0	0	-389.00
1704m750°	0	0	0	-389.00
1716m755°	0	0	0	-389.00
1728m760°	0	0	0	-389.00
1740m765°	0	0	0	-389.00
1752m770°	0	0	0	-389.00
1764m775°	0	0	0	-389.00
1776m780°	0	0	0	-389.00
1788m785°	0	0	0	-389.00
1800m790°	0	0	0	-389.00
1812m795°	0	0	0	-389.00
1824m800°	0	0	0	-389.00
1836m805°	0	0	0	-389.00
1848m810°	0	0	0	-389.00
1860m815°	0	0	0	-389.00
1872m820°	0	0	0	-389.00
1884m825°	0	0	0	-389.00
1896m830°	0	0	0	-389.00
1908m835°	0	0	0	-389.00
1920m840°	0	0	0	-389.00
1932m845°	0	0	0	-389.00
1944m850°	0	0	0	-389.00
1956m855°	0	0	0	-389.00
1968m860°	0	0	0	-389.00
1980m865°	0	0	0	-389.00
1992m870°	0	0	0	-389.00
2004m875°	0	0	0	-389.00
2016m880°	0	0	0	-389.00
2028m885°	0	0	0	-389.00
2040m890°	0	0	0	-389.00
2052m895°	0	0	0	-389.00
2064m900°	0	0	0	-389.00
2076m905°	0	0	0	-389.00
2088m910°	0	0	0	-389.00
2100m915°	0	0	0	-389.00
2112m920°	0	0	0	-389.00
2124m925°	0	0	0	-389.00
2136m930°	0	0	0	-389.00
2148m935°	0	0	0	-389.00
2160m940°	0	0	0	-389.00
2172m945°	0	0	0	-389.00
2184m950°	0	0	0	-389.00
2196m955°	0	0	0	-389.00
2208m960°	0	0	0	-389.00
2220m965°	0	0	0	-389.00
2232m970°	0	0	0	-389.00
2244m975°	0	0	0	-389.00
2256m980°	0	0	0	-389.00
2268m985°	0	0	0	-389.00
2280m990°	0	0	0	-389.00
2292m995°	0	0	0	-389.00
2304m1000°	0	0	0	-389.00
2316m1005°	0	0	0	-389.00
2328m1010°	0	0	0	-389.00
2340m1015°	0	0	0	-389.00
2352m1020°	0	0	0	-389.00
2364m1025°	0	0	0	-389.00
2376m1030°	0	0	0	-389.00
2388m1035°	0	0	0	-389.00
2400m1040°	0	0	0	-389.00
2412m1045°	0	0	0	-389.00
2424m1050°	0	0	0	-389.00
2436m1055°	0	0	0	-389.00
2448m1060°	0	0	0	-389.00
2460m1065°	0	0	0	-389.00
2472m1070°	0	0	0	-389.00
2484m1075°	0	0	0	-389.00
2496m1080°	0	0	0	-389.00
2508m1085°	0	0	0	-389.00
2520m1090°	0	0	0	-389.00
2532m1095°	0	0	0	-389.00
2544m1100°	0	0	0	-389.00
2556m1105°	0	0	0	-389.00
2568m1110°	0	0	0	-389.00
2580m1115°	0	0	0	-389.00
2592m1120°	0	0	0	-389.00
2604m1125°	0	0	0	-389.00
2616m1130°	0	0	0	-389.00
2628m1135°	0	0	0	-389.00
2640m1140°	0	0	0	-389.00
2652m1145°	0	0	0	-389.00
2664m1150°	0	0	0	-389.00
2676m1155°	0	0	0	-389.00
2688m1160°	0	0	0	-389.00
2700m1165°	0	0	0	-389.00
2712m1170°	0	0	0	-389.00
2724m1175°	0	0	0	-389.00
2736m1180°	0	0	0	-389.00
2748m1185°	0	0	0	-389.00
2760m1				

The figure consists of five rows of binary matrices, each representing a different parameter over a 10-day period. The columns represent days from 1 to 10.

- Row 1:** TIME DELAY
- Row 2:** TEMPERATURE OF CONTAINER
- Row 3:** TEMPERATURE
- Row 4:** TIME
- Row 5:** DISTANCE FROM CENTER

Each matrix cell contains either a 0 or a 1, indicating the presence or absence of a specific condition or value at a given time and location.

The figure consists of a 5x5 grid of small plots. The columns are labeled "DISTANCE FROM CENTER" with values 0, 100, 200, 300, and 400 mm. The rows are labeled "TIME DELAY" with values 0, 10, 20, 30, and 40 minutes. Each plot shows a bell-shaped curve representing the relative temperature profile. The peak of each curve is at 100% relative temperature. As time delay increases, the peak shifts towards the right (longer distance from center).

APPENDIX C

TRUMP Solution

TRUMP is a computer program for solving transient and steady-state temperature distributions in multidimensional systems. This program was developed in 1965 at the Lawrence Radiation Laboratory by A. L. Edwards [Ref. 2] for their CDC/3600 computer. The program was adapted to the Naval Postgraduate School IBM/360 Model 67 computer system in 1971 by C. Erbayrum [Ref. 3] from a version used by the B. F. Goodrich Corporation.

TRUMP is a multi-purpose program able to solve a wide variety of problems involving flow in various kinds of potential fields such as heat flow in a temperature field. TRUMP allows the solution of general nonlinear parabolic partial differential equations both in steady-state and transient problems. Complex geometric configurations with multidimensional flow may be solved using various coordinate systems. Initial conditions may vary with spatial position. Material properties, boundary conditions, and other problem parameters may vary with spatial position, time, or the primary dependent variable.

Input data are fed to TRUMP in "Block" form through its 12 input data blocks. A complete description of each of these blocks is given in Ref. 2. A model of the problem must be constructed and data from this model read into TRUMP through the data blocks.

Two models were used to simulate the rocket motor storage container system and several variations of each model were investigated.

The first model assumed one dimensional heat transfer (radial) with the assumptions that the system was infinitely long and that the container surface temperature was spatially uniform. The system was modeled as two infinitely long concentric cylinders separated by a 2.94 inch air gap. The inner cylinder was constructed of 4130 steel and was filled with dry wind blown sand. The thermal properties of the materials used in the experimental system are given in Table II with units most easily compared to the actual data obtained from the system at China Lake.

TABLE II
Thermal Properties of Materials

Material	Density	Specific Heat	Thermal Conductivity
Sand	0.05486 lbm/in ³	0.195 BTU/lbm°F	0.00026 BTU/min-in°F
Steel	0.2807 lbm/in ³	0.109 BTU/lbm°F	0.364 BTU/min-in°F
Air	0.0000436 "	0.240 BTU/lbm°F	0.0000225 "

The model was subdivided into volume elements or nodes with the representative nodal points given in Figure 27. Although the representative nodal point may be located anywhere in the node or on the surface of the node, in transient problems it is usually located so that the lines connecting the nodal points are perpendicularly bisected by the connected area. This gives maximum accuracy. Two boundary conditions were given to the surface node. The first was a sinusoidal disturbance which closely modeled the actual

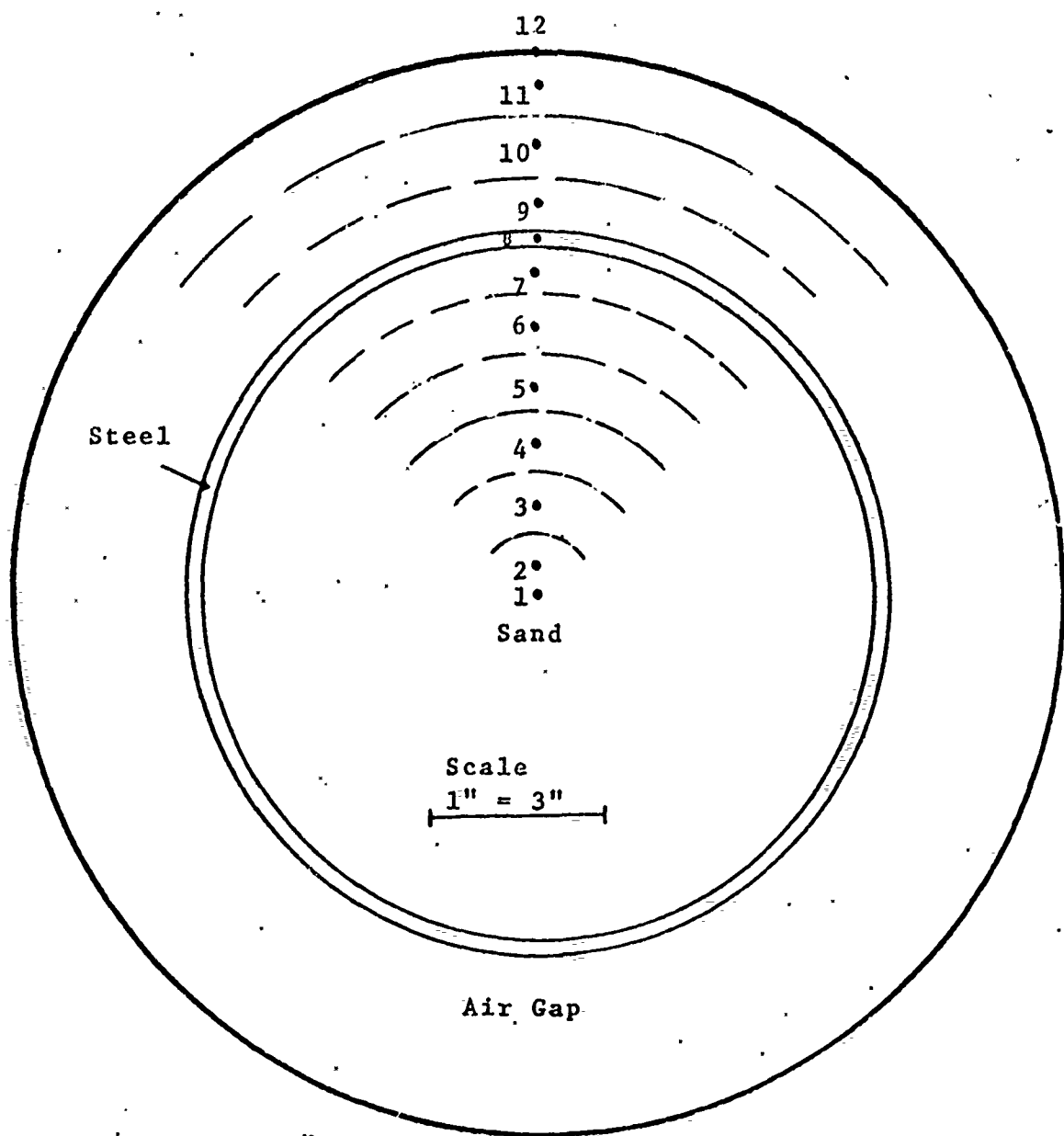


Figure 27. Location of Nodes for One Dimensional TRUMP Model.

average experimental data obtained at China Lake as given in Appendix D. The sine wave exhibited a maximum temperature of 138°F and an average temperature of 104°F. Its period was 24 hours (1440 minutes). The second boundary condition was the actual average surface temperature of the storage container given at two hour intervals. Both these boundary conditions are approximations of the actual surface temperature. Two hour intervals were the minimum allowable for the tabular data as this version of TRUMP has a maximum table size of 12.

Several assumptions were initially made. The thermocouple data obtained from the experiment at China Lake gave the average temperature at a point on the storage container and not the actual outside surface temperature. As this container wall was only 1/16 of an inch thick and made of a good thermal conductor, it was decided to model this data as a zero volume boundary node with a known temperature impressed on it. It was also assumed that heat transfer across the air gap occurred only by radiation and conduction, neglecting the effects of free convection.

It was estimated that the surface emissivities for the rocket motor and the storage container were 0.9 [Ref. 6] based on their haze gray surfaces. The radiation exchange factor for this geometry is given by

$$\mathcal{F}_{1-2} = \frac{1}{\frac{1}{\epsilon_1} + \frac{r_1}{r_2} \left(\frac{1}{\epsilon_2} - 1 \right)} = 0.84$$

A sample input deck for the tabular approximation of the boundary condition is given at the end of this appendix. Several cycles of output data for the one dimensional model are also given.

The second model assumed two dimensional heat transfer (radial and circumferential) with the assumption that the system was infinitely long. The same physical model was assumed for the system except 48 nodes were used instead of 12. The representative nodal points are given in Figure 28. The four surface nodes (12, 24, 36, and 48) each had two different temperature approximations applied, a sinusoidal representation and a tabular input taken at two hour intervals. The four surface nodes were also modeled as zero volume boundary nodes. Each internal thermal connection between nodes is described in the input data by specifying the two node identification numbers, two connector lengths, and two interface dimensional factors. An example of the thermal connections of node 4 is shown in Figure 28 and the input data in BLOCK 5 of the two dimensional TRUMP program.

The calculation of the radiosities in the two dimensional case was accomplished by using a radiation-network and the method of crossed-strings.

The radiation shape factors for the two dimensional system were determined by the method of crossed-strings [Ref. 14]. The graphical construction for this method is given in Figure 29.

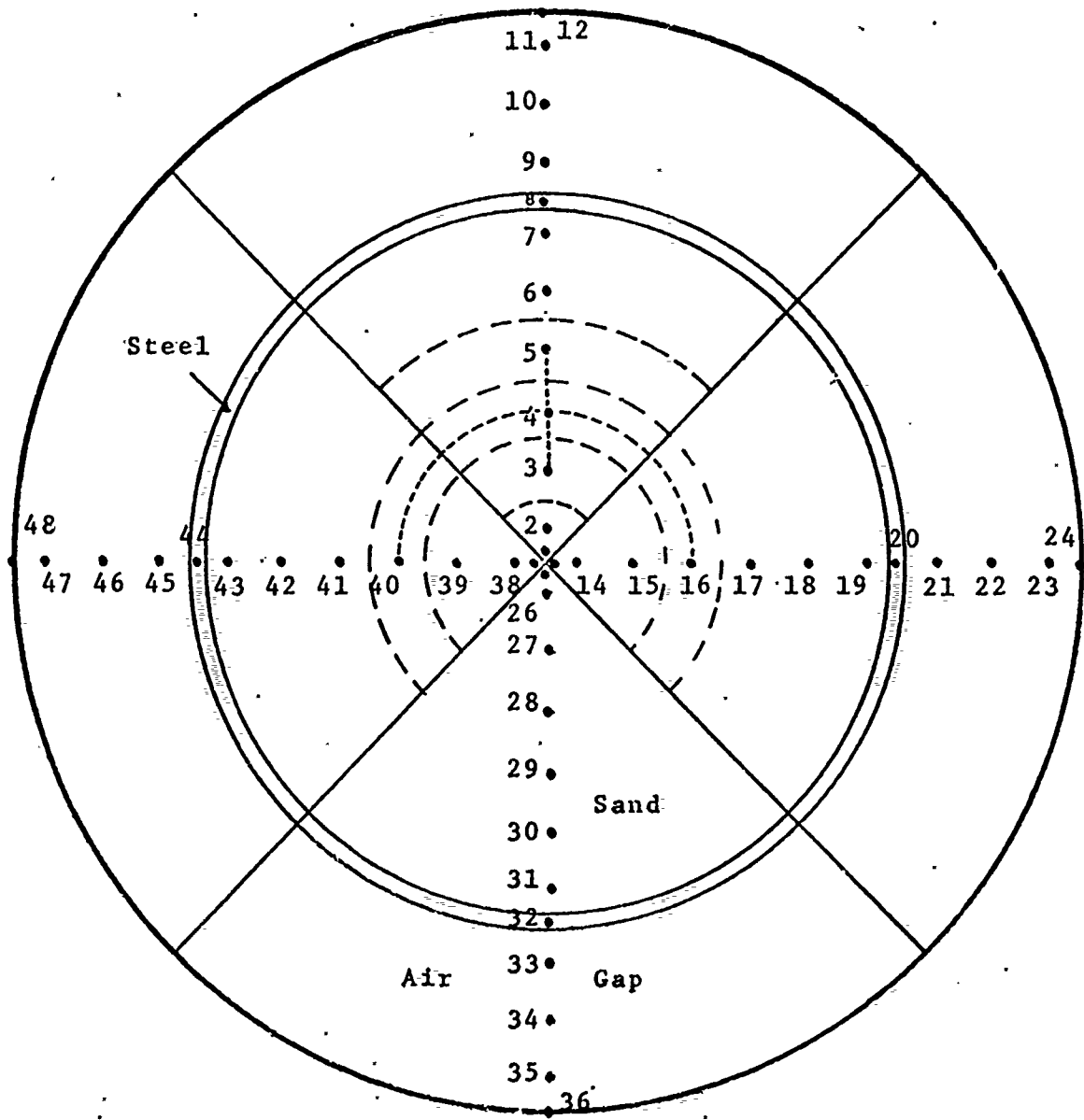


Figure 28: Location of Nodes for Two Dimensional TRUMP Model.

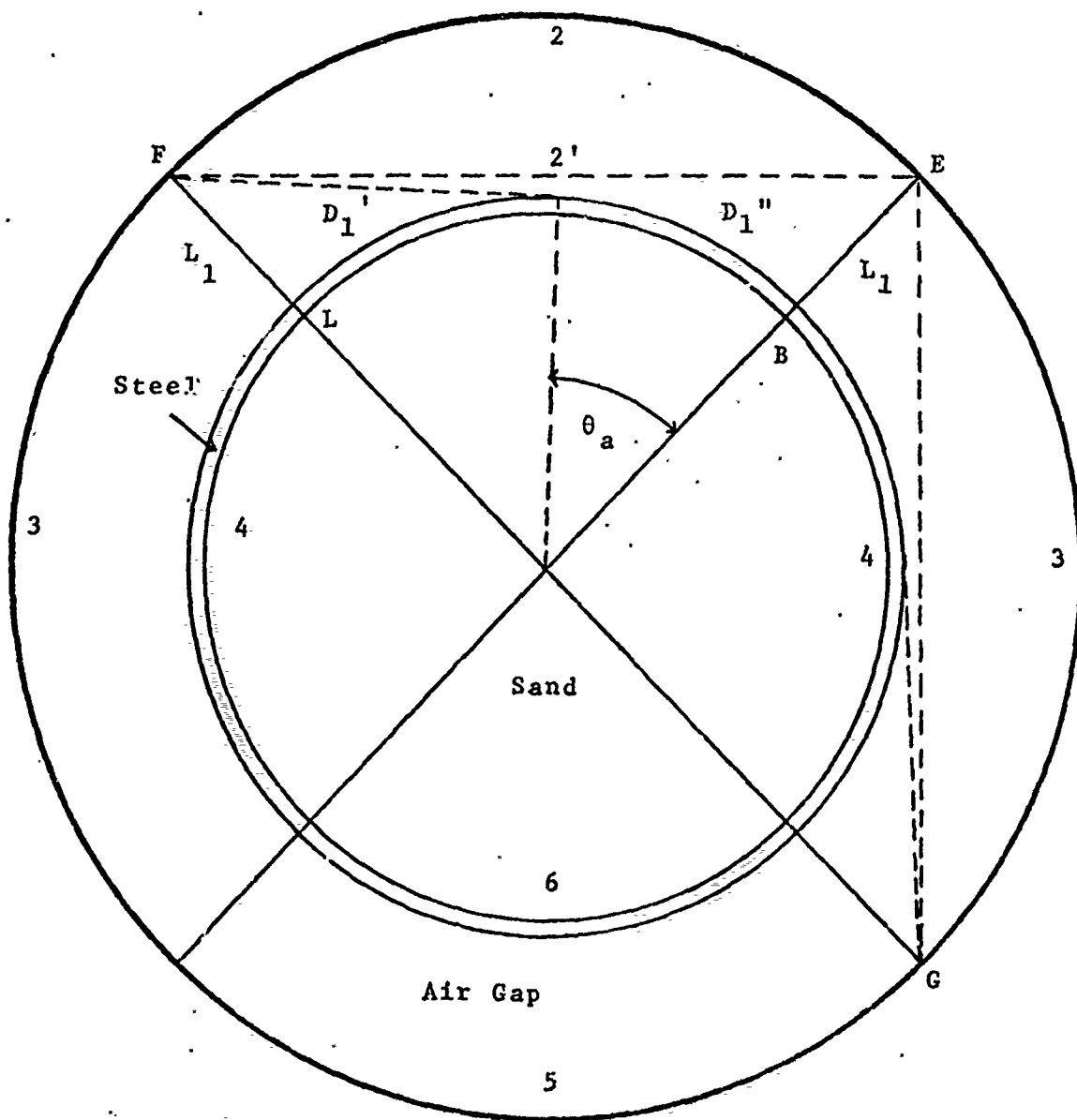


Figure 29: Graphical Construction for Crossed-Strings Method.

F_{m-n} is defined as the fraction of energy leaving surface m which directly reaches surface n. From the physical dimensions of the model $A_1 = A_4 = A_6 = 9.45 \frac{\text{sq.in}}{\text{in.}}$, $A_2 = A_3 = A_5 = 14.05 \frac{\text{sq.in}}{\text{in.}}$, $A_{2'} = 12.65 \frac{\text{sq.in}}{\text{in.}}$, assuming unit depth. Let s_i equal the length of A_i .

The crossed-string method lets each surface represent the effective surface obtained by stretching a string tightly over the radiating face between the bounding edges, to produce a surface that cannot see any of itself. For example, surface $2'$ in Figure 29 stretched over surface 2. By definition $F_{2'2} \equiv 1$, which by reciprocity leads to

$$F_{22'} = \frac{A_{2'}}{A_2} F_{2'2} = 0.9$$

and therefore since

$$F_{22} + F_{22'} = 1 \quad \text{then } F_{22} = 0.10$$

To calculate the direct radiant heat exchanged between surfaces 1 and 2, a minimum-length line was stretched connecting edge B of A_1 to edge E of A_2 and a second minimum length line from edge L of A_1 to edge F of A_2 . These lines are labeled L_1 in Figure 29 and are equal to the width of the air gap, $L_1 = 2.9375 \text{ in.}$ Minimum length lines were also stretched from point B on A_1 to F on A_2 and L on A_1 to E on A_2 . The length of these lines is D_1 and is made up of two parts; D_1' , the tangential distance from F to surface A_1 and D_1'' , the arc length from the point the tangent hits A_1 to B. From geometry $D_1' = \sqrt{r_1^2 - r_o^2} \approx 6.62"$

$$D_1'' = r_o \theta_a = 4.42"$$

therefore

$$D_1 = D_1' + D_1'' = 11.04"$$

$$\text{Now } F_{12} = \frac{2D_1 - 2L_1}{2S_1} = 0.86$$

From reciprocity, $A_1 F_{12} = A_2 F_{21}$

$$F_{21} = \frac{r_o}{r_1} F_{12} = 0.578$$

Now F_{13} is calculated from

$$F_{12} + 2F_{13} = 1$$

$$\text{therefore } F_{13} = 0.07$$

From symmetry $F_{42} = F_{13}$

and then by reciprocity

$$F_{24} = \frac{r_o}{r_1} F_{42} = 0.047$$

Now F_{23} was calculated by stretching minimum length lines from F to E, from E to G, from F to G and from E to E; where the length of the line from F to E = from E to G = S_2' , from F to G = $2D_1$, and from E to E = 0

$$F_{23} = \frac{2S_2' - 2D_1}{2S_2} = .113$$

F_{25} was now calculated from

$$F_{21} + F_{22} + F_{23} + F_{24} + F_{25} = 1$$

$$\text{therefore } F_{25} = 0.002$$

As F_{25} was much smaller than the other F_{m-n} , it was not included in the radiation-network diagram in Figure 30 [Ref. 15].

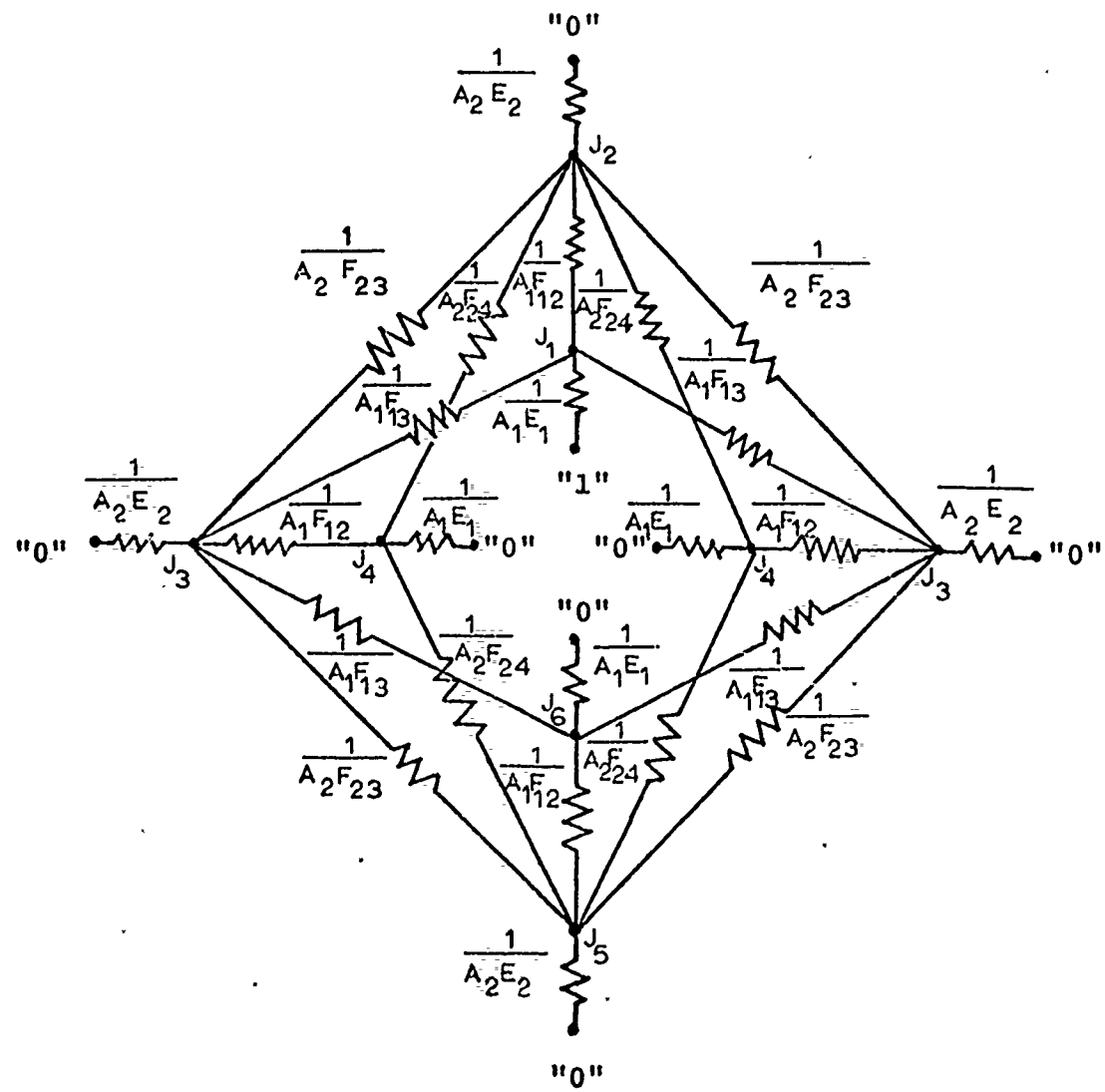


Figure 30: Radiation Network.

To calculate F_{1-n} , the blackbody potential of area 1 is set to unity and all other blackbody potentials are set as zero. An energy balance was written at each node giving a set of six simultaneous equations as follows:

Node 1

$$E_1 A_1 (1-J_1) = A_1 F_{12} (J_1 - J_2) + 2A_1 F_{13} (J_1 - J_3)$$

Node 2

$$E_2 A_2 (0-J_2) = A_1 F_{12} (J_2 - J_1) + 2A_2 F_{24} (J_2 - J_4) + 2A_2 F_{23} (J_2 - J_3)$$

Node 3

$$E_2 A_2 (0-J_3) = A_1 F_{12} (J_3 - J_4) + A_2 F_{23} (J_3 - J_2) + A_1 F_{13} (J_3 - J_1) + A_1 F_{13} (J_3 - J_6) + A_2 F_{23} (J_3 - J_5)$$

Node 4

$$E_1 A_1 (0-J_4) = A_2 F_{24} (J_4 - J_2) + A_1 F_{12} (J_4 - J_3) + A_2 F_{24} (J_4 - J_5)$$

Node 5

$$E_2 A_2 (0-J_5) = 2A_2 F_{23} (J_5 - J_3) + 2A_2 F_{24} (J_5 - J_4) + A_1 F_{12} (J_5 - J_6)$$

Node 6

$$E_1 A_1 (0-J_6) = 2A_1 F_{13} (J_6 - J_3) + A_1 F_{12} (J_6 - J_5)$$

where J_n = radiosity of node n .

$$E_1 A_1 = \frac{\epsilon_1}{1-\epsilon_1} A_1$$

$$E_2 A_2 = \frac{\epsilon_2}{1-\epsilon_2} A_2$$

F_{nm} = radiation shape factors previously calculated.

Now the values of A_1 , A_2 and F_{nm} were substituted into the energy balance equations which were then put into matrix form as shown in Table III.

TABLE III
Matrix Form of Energy Balance Equations

$\left[\frac{1}{1-\epsilon_1} \right]$	(-0.86)	(-0.14)	(0.0)	(0.0)	$\left[\frac{\epsilon_1}{1-\epsilon_1} \right]$
(-0.86)	$(1.33 + \frac{3\epsilon_2}{2(1-\epsilon_2)})$	(-0.33)	(-0.14)	(0.0)	(0.0)
(-0.07)	(-0.165)	$(1.33 + \frac{3\epsilon_2}{2(1-\epsilon_2)})$	(-0.86)	(-0.165)	(0.0)
(0.0)	(-0.07)	(-0.86)	$(\frac{1}{1-\epsilon_1})$	(-0.07)	(0.0)
(0.0)	(0.0)	(-0.14)	(0.0)	(-0.86)	$(\frac{1}{1-\epsilon_1})$
(0.0)	(0.0)	(-0.33)	(-0.14)	$(1.33 + \frac{3\epsilon_2}{2(1-\epsilon_2)})$	(-0.86)
					(0.0)

Letting $\epsilon_1 = \epsilon_2 = 0.9$, a standard computer solution for matrix problems gave the radiosities as listed in Table IV.

TABLE IV
Radiosities at Nodes

$$\begin{aligned}J_1 &= .9046 \\J_2 &= .0529 \\J_3 &= .00495 \\J_4 &= .000797 \\J_5 &= .000125 \\J_6 &= .000080\end{aligned}$$

Now to find the radiation exchange factors from node 1 to nodes n, the radiation network shown in Figure 30 was reduced to the equivalent network shown in Figure 31. Where the nodal equations are

$$\mathcal{F}_{1-2} A_1 (1-0) = E_2 A_2 (J_2 - 0)$$

where

$$\mathcal{F}_{1-2} = \frac{E_2}{A_1} A_2 J_2 = .71$$

$$\mathcal{F}_{1-3} A_1 (1-0) = E_2 A_2 (J_3 - 0)$$

$$\mathcal{F}_{1-3} = \frac{E_2}{A_1} A_2 J_3 = .066$$

These values of the radiation exchange factor are used in the two-dimensional program. A sample input deck for the sinusoidal boundary condition is included at the end of this appendix. Several cycles of output data for the tabular boundary condition are also given.

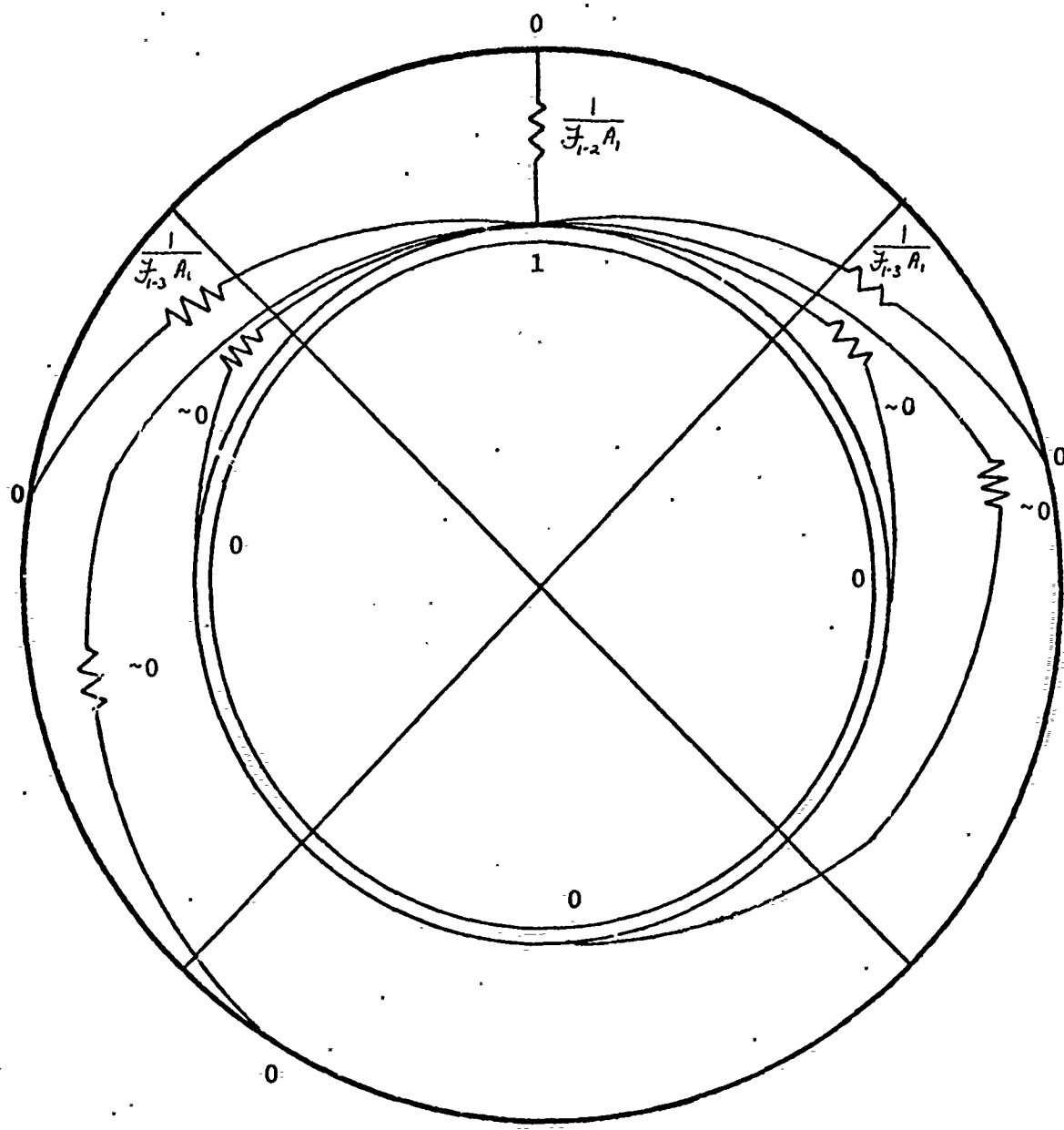


Figure 31: Equivalent Radiation Network

```

//WIRZ1687 JOB (1687,0860FT,NF12) * WIRZBURGER.A. BOX W*, TIME=(2,00)
//JOBBL DD UNIT=2321,DSNAME=SL734.KATZ,
//DISP=(OLD, PASS), VOLUME=350K
//EXEC PGM=TRUNP, REGION=350K
//FT06F001 DD SYSSOUT=A,DCB=(RECFM=FBA,LRECL=133,BLKSIZE=3325),
//FT05F001 DD

```

* NISSE PROBLEM ONE DIMENSIONAL

BLOCK 1	CONTROLS, LIMITS, CONSTANTS
1	1.000 E 00 1.000E 00
2	1440.0
3	
93.0	

BLOCK 2	MATERIAL NAMES, NUMBERS, THERMAL PROPERTIES
ASAND	0.0544 0.19 0.00027
ASTEL	0.2807 0.109 0.0364
AAIR	0.0000436 0.240 0.0000225

BLOCK 4	NODE NUMBERS, MATERIAL REFERENCES, TYPES, VOLUMES.
1	1.00 0.002 0.001
2	1.00 0.998 0.501
3	1.00 1.00 1.55
4	1.00 2.00 2.5
5	1.00 3.00 3.5
6	1.00 4.00 4.5
7	1.00 5.00 5.75
8	1.00 6.00 6.5
9	1.00 7.00 7.5
10	1.00 8.00 8.75
11	1.00 9.00 9.375
12	1.00 10.00 10.0

BLOCK 5	INTERNAL THERMAL CONNECTION NODE NUMBERS.
1	2 0.001 0.499 1.0 0.002
2	3 0.499 0.5 1.0 0
3	4 0.5 0.5 1.0 0
4	5 0.5 0.5 1.0 0
5	6 0.5 0.5 1.0 0
6	7 0.5 0.5 1.0 0
7	8 0.5 0.5 1.0 0
8	9 0.5 0.5 1.0 0
9	10 0.5 0.5 1.0 0
10	11 0.5 0.5 1.0 0
11	12 0.5 0.5 1.0 0
12	

0.00009760

8.9375
8.9375

BLOCK 6 2001 EXTERNAL THERMAL CONNECTIONS 1.0 8.9375 1.00 E6
BLOCK 7 12 BOUNDARY TEMPERATURE VARIATION 84.5 240.0 79.25 360.0
2001 12 89.5 120.0 82.25 720.0 103.75 840.0
76.0 480.0 69.75 600.0 138.0 1200.0 132.25 1320.0
119.0 960.0 130.0 1080.0
103.5 1440.0

BLOCK 9 INITIAL TEMPERATURES

1 115.2
2 115.3
3 116.0
4 117.2
5 118.4
6 118.7
7 117.3
8 115.8
9 113.2
10 108.9
11 105.1
12 103.5

ENDED-1 LAST CARD OF DATA DECK

MISSLE PROBLEM ONE DIMENSIONAL UNIT = 6.

===== CONTROLS, LIMITS, CONSTANTS
DATA BLOCK 10

IPRINT	NUM	KDATA	KSPEC	MCYC	MSEC	NPUNCH	NDOT	IRITE	SCALE	
15	0	30000	30000	0	0	0	0	0	0.1000E 01	
KD	KT	3	1.00000E 12	1.00000E 00	1.00000E 00	0.0	TAU			
KD	KSYM	1	6.283190 00	1.73300E-09	4.6000E 02					
TONE	ALCNE		BONE	GONE	PONE	HONE	RONE	PONE		
9.3500E 01	0.0		0.0	0.0	0.0	0.0	0.0	0.0		
***** MATERIAL NAMES, NUMBERS, THERMAL PROPERTIES. *****										
DATA BLOCK 20										
NAME	MATL	INDEX	KA	KB	LTABC	LTABK	DENSITY	CAPACITY	CONDUCTIVITY	TWELT
SAND	1	1	0	0	0	0	5.4400E-02	1.9000E-01	2.7000E-04	0.0
STEEL	2	2	0	0	0	0	2.8070E-01	1.0900E-01	3.6400E-02	0.0
AIR	3	3	0	0	0	0	4.3600E-05	2.4000E-01	2.2500E-05	0.0
***** NODE NUMBERS, MATERIAL REFERENCES, TYPES, VOLUMES. *****										
NODE	INDEX	MATL	NTYPE	DLONG	DWIDE	DRAD	VOLUME			
1	1	0	0	1.00000E 00	2.00000E 00	1.00000E-03	1.25664E+05			
2	1	0	0	1.00000E 00	2.00000E 00	5.00000E-03	3.14158E+00			
3	3	1	0	1.00000E 00	1.00000E 00	1.00000E 00	9.42478E+00			
4	4	1	0	1.00000E 00	1.00000E 00	1.00000E 00	1.50000E+00	1.00000E+00		
5	5	1	0	1.00000E 00	1.00000E 00	1.00000E 00	3.50000E+00	2.19911E+01		
6	6	1	0	1.00000E 00	1.00000E 00	1.00000E 00	4.50000E+00	2.82491E+01		
7	7	1	0	1.00000E 00	1.00000E 00	1.00000E 00	5.50000E+00	3.51291E+01		
8	8	1	0	1.00000E 00	1.00000E 00	1.00000E 00	6.50000E+00	4.22843E+01		
9	9	2	0	1.00000E 00	1.00000E 00	1.00000E 00	7.50000E+00	4.98647E+01		
10	10	3	0	1.00000E 00	1.00000E 00	1.00000E 00	8.50000E+00	4.71239E+01		
11	11	3	0	1.00000E 00	9.37500E-01	8.49975E+00	9.50000E+00	4.98850E+01		
12	12	2	0	0.0	0.0	8.93750E+00	1.00000E-24	1.00000E-24		
***** INTERNAL THERMAL CONNECTION NODE NUMBERS. *****										
NOD1	NOD2	INDEX	DEL1	DLONG	DRAD	HINT	RINT	AREA		
1	2	1	4.9900D-03	1.0000E 00	1.0000E 00	1.0000E 03	1.0000E 12	1.0000E 00		
2	3	2	4.9900D-01	1.0000E 00	1.0000E 00	1.0000E 00	1.0000E 12	1.0000E 00		
3	4	3	5.0000D-01	1.0000E 00	1.0000E 00	1.0000E 00	1.0000E 12	1.0000E 00		
4	5	4	5.0000D-01	1.0000E 00	1.0000E 00	1.0000E 00	1.0000E 12	1.0000E 00		
5	6	5	5.0000D-01	1.0000E 00	1.0000E 00	1.0000E 00	1.0000E 12	1.0000E 00		
6	7	6	5.0000D-01	1.0000E 00	1.0000E 00	1.0000E 00	1.0000E 12	1.0000E 00		
7	8	7	3.7500D-01	1.2500D-01	5.0000E 00	5.7500E 00	1.0000E 12	0.0	3.14159E+01	
8	9	8	1.2500D-01	5.0000D-01	6.0000E 00	6.0000E 00	1.0000E 12	0.0	3.61280E+01	
9	10	9	1.2500D-01	0.0	6.0000E 00	6.0000E 00	1.0000E 12	0.0	3.76990E+01	
10	11	10	1.2500D-01	5.0000D-01	7.0000E 00	7.0000E 00	1.0000E 12	0.0	3.98920E+01	
11	12	11	5.0000D-01	4.6875D-01	8.0000E 00	8.9375E 00	1.0000E 12	0.0	4.02650E+01	
12	13	12	4.6875D-01	0.0	8.9375E 00	8.9375E 00	1.0000E 12	0.0	5.61560E+01	
***** EXTERNAL THERMAL CONNECTIONS *****										
NODSB	INDEX	LTABK	POWER	DLONG	DRAD	HSURE	RSURE	AREAS		
12	2001	1	0.0	1.0000E 00	8.9375E 00	1.0000D 06	0.0	5.6156D 01		

DATA BLOCK 70 BOUNDARY TEMPERATURE VARIATION.

BOUNDARY TEMPERATURE VARIATION

תְּנַשֵּׁא בְּנָהָרִים

```

SUMMARY OF INPUT DATA
BLOCK NUMBER 2
TIME READ IN 1
TIME NAME MAT
MAXIMUM SIZE 15
UNMODIFIED SIZE 0
TABLES CAPT

```

MAXIMUM ALLOWED TABLE LENGTH IS 12.
 ARRAY STORAGE = 3*M11+M1*(1+M11)+2*(11+7*M9)+M3*(5+9*M9)+56*M4+12*M5+M6*(12+3*M9)+M7*(5+3*M9)

卷之三

TRUMP OUTPUT DATA

* MISSILE PROBLEM ONE DIMENSIONAL

DATA DECK 1

PRINTOUT	CYCLE	TOO FAST	TOO SLOW	KWIT	DELTAX	SMALL	TVARY	NUTS
TOTAL TIME	TIME STEP	HEAT FLOW			TEMP FROM FLUX	FLUX RATE	TEMP RATE	
1.00000E-12	1.00000E-12	-4.43992E-14			-3.24884E-02	-4.4099E-02		
AVG TEMP	HEAT CAPACITY	HEAT CONTENT			GEN RATE	HEAT GEN	TEMP FROM GEN	
1.17311E 02	1.25739E 00	1.59237E 02			0.0	0.0		
NODE	TEMP	DT	DDT	GE N RATE	W	H	F	CURE AT 286 F
2	0.11520 03	0.52240 -11	0.52240 01	0.0	0.1196E-04	0.6785E-18	0.6185E-18	0.0
3	0.11530 03	0.53629 -11	0.53629 01	0.0	0.3744E-01	0.1188E-14	0.1188E-14	0.0
4	0.11600 03	0.52959 -13	0.52959 01	0.0	0.1933E-02	0.2883E-14	0.2883E-14	0.0
5	0.11720 03	0.12940 -13	0.12940 01	0.0	0.1933E-02	0.2036E-14	0.2036E-14	0.0
6	0.11840 03	0.53179 -13	0.53179 01	0.0	0.3469E-02	0.4071E-14	0.4071E-14	0.0
7	0.11870 03	0.53410 -13	0.53410 01	0.0	0.3469E-02	0.1561E-13	0.1561E-13	0.0
8	0.11870 03	0.96630 -13	0.96630 01	0.0	0.3071E-02	0.6574E-13	0.6574E-13	0.0
9	0.11870 03	0.23630 -12	0.23630 01	0.0	0.4373E-01	0.1548E-13	0.1548E-13	0.0
10	0.11890 03	0.36220 -12	0.36220 00	0.0	0.4373E-01	0.1810E-13	0.1810E-13	0.0
11	0.10510 03	0.46420 -19	0.46420 02	0.0	0.5486E-01	0.2414E-13	0.2414E-13	0.0
12	0.94500 02	0.90000 01	0.0	0.0	0.2591E-23	0.2754E-24	0.2754E-24	0.0

NAME	MATL	TOT CAP	TOT HEAT	Avg TEMP	THELT	HNELT
SAND	1.00359E 00	1.26893E 02	1.1770E 02	0.0	0.0	0.0
STEEL	2.83356E 01	3.26697E 01	1.1580E 02	0.0	0.0	0.0
AIR	1.42446E 03	1.56938E 01	1.0879E 02	0.0	0.0	0.0

NODE	DATA
1	NAME MATL
2	RADIUS
3	STEL
4	AIR

NODE	NTYPE	RADUIS	VOLUME	MASS	CAPACITY	CONDUCTIVITY	ZIP	SLIM
1	1	0.10000 02	0.12447E-06	0.1199D-06	0.1199D-06	0.27000E-03	0.6786D-05	0.1140D-01
2	1	0.15000 01	0.15000 00	0.15000 00	0.15000 00	0.27000E-03	0.6786D-05	0.1140D-01
3	1	0.20000 01	0.20000 00	0.20000 00	0.20000 00	0.27000E-03	0.6786D-05	0.1140D-01
4	1	0.25000 01	0.25000 00	0.25000 00	0.25000 00	0.27000E-03	0.6786D-05	0.1140D-01
5	1	0.30000 01	0.30000 00	0.30000 00	0.30000 00	0.27000E-03	0.6786D-05	0.1140D-01
6	1	0.35000 01	0.35000 00	0.35000 00	0.35000 00	0.27000E-03	0.6786D-05	0.1140D-01
7	1	0.40000 01	0.40000 00	0.40000 00	0.40000 00	0.27000E-03	0.6786D-05	0.1140D-01
8	1	0.45000 01	0.45000 00	0.45000 00	0.45000 00	0.27000E-03	0.6786D-05	0.1140D-01
9	1	0.50000 01	0.50000 00	0.50000 00	0.50000 00	0.27000E-03	0.6786D-05	0.1140D-01
10	1	0.55000 01	0.55000 00	0.55000 00	0.55000 00	0.27000E-03	0.6786D-05	0.1140D-01
11	2	0.60000 02	0.60000 00	0.60000 00	0.60000 00	0.36400E-01	0.5610D-08	0.1000D-23
12	2	0.65000 02	0.65000 00	0.65000 00	0.65000 00	0.36400E-01	0.5610D-08	0.1000D-23

INTERNAL CONNECTION DATA								
NODE1	NODE2	AREA	HINT	RINT	TRAN	HEAT FLOW	AVG RATE	
1	2	0.12570E-01	0.10000 13	0.0	0.6786D-05	0.6786E-18	0.6185E-06	
2	3	0.62237E-01	0.10000 13	0.0	0.1199D-02	0.1189E-14	0.1189E-06	
3	4	0.16855E-01	0.10000 13	0.0	0.1199D-02	0.2036E-14	0.2036E-06	
4	5	0.25142E-01	0.10000 13	0.0	0.1199D-02	0.1357E-13	0.1357E-06	
5	6	0.36770E-01	0.10000 13	0.0	0.1199D-02	0.3892E-13	0.3892E-06	
6	7	0.50277E-01	0.10000 13	0.0	0.1199D-02	0.4410E-14	0.4410E-06	
7	8	0.69129E-01	0.10000 13	0.0	0.1199D-02	0.1002E-14	0.1002E-06	
8	9	0.92170E-01	0.10000 13	0.0	0.1199D-02	0.4256E-14	0.4256E-06	
9	10	0.90277E-01	0.10000 13	0.0	0.1199D-02	0.4436E-14	0.4436E-06	
10	11	0.56160E-02	0.10000 13	0.0	0.1670E-02	0.2857E-13	0.2857E-06	
11	12	0.56160E-02	0.10000 13	0.0	0.1695D-02	0.2857E-13	0.2857E-06	

BOUNDARY NODE DATA								
NCNB	TEMPB	HEAT FLOW	Avg RATE					
2001	9.4503E 01	-4.4399D-14	-4.4099E-02					
SYSTEM TOTAL		-4.4399E-14	-4.4099E-02					
EXTERNAL CONNECTION DATA								
NON3	NODES	AREAS	RSURE	TRANS	HEAT FLOW	AVG RATE		
12	2001	5.6156D 01	1.0000D 06	0.0	5.6156D 07	-4.4099E-14		
CYCLE	1 MADE NODE	1 A SPECIAL NODE						

TRUMP OUTPUT DATA

* MISSLE PROBLEM ONE DIMENSIONAL

PRINTOUT	CYCLE	TOO FAST	TOO SLOW	KNT	DELTMAX	SMALL	TVARY	NUTS	
2	1	0	0	0	9.00062E-02	9.00062E-02	1.30330E 00		
TOTAL TIME	TIME STEP	HEAT FLOW	TEMP FROM FLUX	FLUX RATE	TEMP RATE				
1.27665E-02	-1.9315E03	-1.1769E-03	-1.24830E-01	-9.1978E-02					
Avg TEMP	HEAT CAPACITY	HEAT CONTENT	GEN RATE	HEAT GEN	TEMP FROM GEN				
1.17310E 02	1.35739E 00	1.52235E 02	0.0	0.0					
NODE	TEMP	DT	DDT	GE N RATE	H			CURE AT 280 F	
1	0.11530 03	0.66660 -03	0.1344D 01	0.1497E-04	0.8658E-08			0.0	
2	0.11600 03	0.4669D -03	0.1659D 01	0.3144E 01	0.1516E-04			0.0	
3	0.11670 03	0.3776D -03	0.1959D 01	0.1303E 02	0.3679E-04			0.0	
4	0.11740 03	0.2866D -03	0.1226D 01	0.1903E 02	0.2599E-04			0.0	
5	0.11810 03	0.2265D -03	0.1791D 01	0.1901E 02	0.2049E-04			0.0	
6	0.11870 03	0.1685D -03	0.2410D 01	0.1901E 02	0.1909E-04			0.0	
7	0.11930 03	0.1286D -02	0.1260D 01	0.1901E 02	0.1809E-04			0.0	
8	0.11980 03	0.8624D -02	0.2444D 00	0.1901E 02	0.1709E-04			0.0	
9	0.12030 03	0.4662D -02	0.2444D 00	0.1901E 02	0.1609E-04			0.0	
10	0.10890 03	0.4665D -02	0.6720D 00	0.1901E 02	0.1509E-04			0.0	
11	0.10450 02	-0.5188D 03	0.0	0.0	0.2291E-03			0.0	
12	0.94500 02	-0.319D 02	0.0	0.0	0.2291E-03			0.0	
MATERIAL DATA									
NAME	MATL	TOT CAP	TOT HEAT	AVG TEMP	TWELT	HMET			
SAND	1	1.00000E 00	1.2683E 02	1.1570E 02	0.0	0.0			
STFL	2	2.00000E 01	3.2689E 02	1.1570E 02	0.0	0.0			
AIR	3	1.00000E 03	1.5650E 02	1.0850E 02	0.0	0.0			
NODE DATA									
NODE	NATL	NTYPE	RADIUS	VOLUME	MASS	CAPACITY	CONDUCT	IVTY	SLIM
1	1	4	0.10000 02	0.1250E-04	0.1790D-06	0.1299D-06	0.3441D-01	0.1944D-01	
2	1	4	0.15000 01	0.3427E-02	0.2700D-03	0.2700D-03	0.1705E-02	0.1950D-02	
3	1	4	0.15000 01	0.9427E-02	0.5441D-03	0.5441D-03	0.5091E-02	0.1930D-02	
4	1	4	0.15000 01	0.1592E-02	0.8555D-03	0.8555D-03	0.8482E-02	0.1944D-02	
5	1	4	0.15000 01	0.2827E-02	0.1596D-03	0.1596D-03	0.1888E-01	0.1944D-02	
6	1	4	0.15000 01	0.4578E-02	0.2523D-03	0.2523D-03	0.1648E-01	0.1743D-02	
7	1	4	0.15000 01	0.7587E-02	0.4082D-03	0.4082D-03	0.3562E-01	0.1743D-02	
8	2	3	0.75000 01	0.9225E-02	0.2500D-03	0.2500D-03	0.3268E-01	0.1521D-02	
9	3	3	0.75000 01	0.4082E-02	0.1706D-03	0.1706D-03	0.2253E-02	0.2156D-02	
10	3	3	0.75000 01	0.4712E-02	0.2151D-03	0.2151D-03	0.2253E-02	0.2156D-02	
11	3	3	0.75000 01	0.4989E-02	0.2150D-03	0.2150D-03	0.2253E-02	0.2156D-02	
12	3	3	0.8938E-01	0.1000E-23	0.2800D-24	0.3000D-25	0.3640E-01	0.1000D-23	
INTERNAL CONNECTION DATA									
NODE1	NOD2	AREA	HINT	RINT	TRANS	HEAT FLOW	Avg RATE		
1	2	0.1257D-01	0.1000E 13	0.0	0.8658D-05	0.8658E-05	0.6700E-06		
2	3	0.6283D-01	0.1000E 13	0.0	0.6980E-05	0.6980E-05	0.1407E-06		
3	4	0.1257D-02	0.1000E 13	0.0	0.3930E-05	0.3930E-05	0.7798E-06		
4	5	0.1835D-02	0.1000E 13	0.0	0.5089E-05	0.5089E-05	0.1303E-06		
5	6	0.2513D-02	0.1000E 13	0.0	0.9860E-05	0.9860E-05	0.1924E-06		
6	7	0.3142D-02	0.1000E 13	0.0	0.2084E-05	0.2084E-05	0.2403E-06		
7	8	0.3613D-02	0.1000E 13	0.0	0.9760E-04	0.9760E-04	0.2403E-06		
8	9	0.3717D-02	0.1000E 13	0.0	0.4966E-04	0.4966E-04	0.2403E-06		
9	10	0.4379D-02	0.1000E 13	0.0	0.1000E-04	0.1000E-04	0.2403E-06		
10	11	0.5027D-02	0.1000E 13	0.0	0.2000E-04	0.2000E-04	0.2403E-06		
11	12	0.5616D-02	0.1000E 13	0.0	0.4000E-04	0.4000E-04	0.2403E-06		
BOUNDARY NODE DATA									
NODEB	TEMPB	HEAT FLOW	AVG RATE						
2001	9.4499E 01	-1.5911D-03	-1.2485E-01						
SYSTEM TOTAL									
		-1.5315E-03	-1.2405E-01						
EXTERNAL CONNECTION DATA									
NODS	NODSB	AREAS	HSURR	POWER	RSURE	TRANS	HEAT FLOW		
12	2001	5.615D 01	1.0000E 06	0.0	0.0	5.615D 01	-1.5911E-03		
CYCLE 5 MADE NODE 9 A SPECIAL NODE									

TRAINING OUTPUT CAT

ONE DIMENSIONAL

DATA DECK 1

```

***** MISSILE PROBLEM ONE DIMENSIONAL

PRINTOUT CYCLE TOO FAST TOO SLOW KWT DELTAX 0.1822E 01 SMALL 1.0000E 00 TVARY NUTS 7
TOTAL TIME 15 TIME STEP 0 HEAT FLOW 0.6360E 01 1.0787E 01 1.0700E 00 8.6195E-01
3.10774E 01 7.1561E 00 3.6360E 01 2.6787E 01 1.1700E 00 8.6195E-01
AVG TEMP 1.15130E 02 HEAT CAPACITY 1.35739E 00 1.5627E 02 GEN RATE 0.0 HEAT GEN 0.0 TEMP FROM GEN 0.0
***** MATERIAL DATA
NODE 1 TEMP 0.1630 03 DT 0.1909D 00 DDT 0.2675D 01 GEN RATE 0.0 H 0.1510E 04 CURE AT 280 F
2. 0.1630 03 0.1909D 00 0.2675D 01 0.3776E 04 0.395E 04
3. 0.1747 03 0.1828D 00 0.1790D 01 0.3776E 04 0.395E 04
4. 0.1747 03 0.1828D 00 0.1790D 01 0.3776E 04 0.395E 04
5. 0.1760 03 0.1632D 02 0.1929D 02 0.2700D 01 0.3047E 04
6. 0.1760 03 0.1632D 02 0.1929D 02 0.2700D 01 0.3047E 04
7. 0.1750 03 0.1734D 00 0.1800D 01 0.2600D 01 0.3047E 04
8. 0.1750 03 0.1734D 00 0.1800D 01 0.2600D 01 0.3047E 04
9. 0.1750 03 0.1734D 00 0.1800D 01 0.2600D 01 0.3047E 04
10. 0.1750 03 0.1734D 00 0.1800D 01 0.2600D 01 0.3047E 04
11. 0.1750 03 0.1734D 00 0.1800D 01 0.2600D 01 0.3047E 04
12. 0.1750 03 0.1734D 00 0.1800D 01 0.2600D 01 0.3047E 04
***** INTERNAL CONNECTION DATA
NODE 1 NAME MATL TOT CAP 1.0715E 02 TOT HEAT 1.4215E 02 AVE TEMP 0.02 MELT 0.0
SSAB 1 1.0715E 00 1.0715E 01 1.0715E 02 0.0 0.0
SSAR 1 1.0715E 00 1.0715E 01 1.0715E 02 0.0 0.0
***** NODE DATA
NODE 1 MATL NTYP VOLUME 0.1425E -04 MASS 0.6360E -06 CONDUCTIVITY 0.2700D -03 ZIP 0.1394D -02
2 1 1 0.1500E 01 0.6170D 01 0.3247D -01 0.1394D -02
3 1 1 0.1500E 01 0.6170D 01 0.3247D -01 0.1394D -02
4 1 1 0.1500E 01 0.6170D 01 0.3247D -01 0.1394D -02
5 1 1 0.1500E 01 0.6170D 01 0.3247D -01 0.1394D -02
6 1 1 0.1500E 01 0.6170D 01 0.3247D -01 0.1394D -02
7 1 1 0.1500E 01 0.6170D 01 0.3247D -01 0.1394D -02
8 1 1 0.1500E 01 0.6170D 01 0.3247D -01 0.1394D -02
9 1 1 0.1500E 01 0.6170D 01 0.3247D -01 0.1394D -02
10 1 1 0.1500E 01 0.6170D 01 0.3247D -01 0.1394D -02
11 1 1 0.1500E 01 0.6170D 01 0.3247D -01 0.1394D -02
12 1 1 0.1500E 01 0.6170D 01 0.3247D -01 0.1394D -02
***** INTERNAL CONNECTION DATA
NODE 1 NODE 2 AREA 0.2570D -01 HINT 1.000E 13 RINT 0.6787D -05 HEAT FLOW 0.1390E -03
2 3 0.6257D -01 0.2000E 13 0.0 0.1698D 02 0.1390E -03
4 5 0.2865D 02 0.2000E 13 0.0 0.5989D 02 0.1390E -03
6 7 0.000142D 00 0.1800E 13 0.0 0.6789D 02 0.1390E -03
8 8 0.000142D 00 0.1800E 13 0.0 0.2592D 02 0.1390E -03
9 9 0.000142D 00 0.1800E 13 0.0 0.1493D 02 0.1390E -03
10 10 0.000142D 00 0.1800E 13 0.0 0.0796D 02 0.1390E -03
11 11 0.000142D 00 0.1800E 13 0.0 0.0364D 02 0.1390E -03
12 12 0.000142D 00 0.1800E 13 0.0 0.0182D 02 0.1390E -03
***** BOUNDARY NODE DATA
NODE 9 TEMPB 9.235E 01 HEAT FLOW 3.6361D 01 AVG RATE 1.1700E 00
SYSTEM TOTAL 3.6361E 01 1.1700E 00
***** EXTERNAL CONNECTION DATA
NODES NODSB 1.0000E 06 HSURE 0.0 RSURE 0.0
NODES NODSB 5.6156D 01 1.0000E 06 HSURE 0.0 RSURE 0.0
CYCLE 21 MADE NODE 2 A SPECIAL NODE

```

TUTORIAL

TRUMP OUTPUT DATA

DATA DECK 1

MATERIAL DATA

MATERIAL DATA									
NAME	MATL	TOT	HEAT	TOT	HEAT	AVG	TEMP	TWELT	HMEU
SAND	1	0.359E-00	1.1358E-02	1.0580E-02	0.0	0.0	0.0	0.0	0.0
STAIN	2	0.824E-03	9.8304E-01	9.8304E-01	0.0	0.0	0.0	0.0	0.0
ALR	3	1.442E-03	1.3053E-01	9.0493E-01	0.0	0.0	0.0	0.0	0.0

NODE DATA								
NODE	NODE	RADIUS	VOLUME	MASS	CAPACITY	CONDUCTIVITY	ZIP	SLIM
1	1	0.100E-01	0.1299D-06	0.1914D-01	0.0	0.0	0.0	0.0
2	2	0.100E-01	0.3249D-01	0.1905D-02	0.0	0.0	0.0	0.0
3	3	0.100E-01	0.9744D-01	0.1909D-02	0.0	0.0	0.0	0.0
4	4	0.100E-01	0.1626D-01	0.1914D-02	0.0	0.0	0.0	0.0
5	5	0.100E-01	0.2292D-01	0.1914D-02	0.0	0.0	0.0	0.0
6	6	0.100E-01	0.2958D-01	0.1914D-02	0.0	0.0	0.0	0.0
7	7	0.100E-01	0.3624D-01	0.1914D-02	0.0	0.0	0.0	0.0
8	8	0.100E-01	0.4290D-01	0.1914D-02	0.0	0.0	0.0	0.0
9	9	0.100E-01	0.4956D-01	0.1914D-02	0.0	0.0	0.0	0.0
10	10	0.100E-01	0.5622D-01	0.1914D-02	0.0	0.0	0.0	0.0
11	11	0.100E-01	0.6288D-01	0.1914D-02	0.0	0.0	0.0	0.0
12	12	0.100E-01	0.6954D-01	0.1914D-02	0.0	0.0	0.0	0.0
13	13	0.100E-01	0.7620D-01	0.1914D-02	0.0	0.0	0.0	0.0
14	14	0.100E-01	0.8286D-01	0.1914D-02	0.0	0.0	0.0	0.0
15	15	0.100E-01	0.8952D-01	0.1914D-02	0.0	0.0	0.0	0.0
16	16	0.100E-01	0.9618D-01	0.1914D-02	0.0	0.0	0.0	0.0
17	17	0.100E-01	0.10284D-01	0.1914D-02	0.0	0.0	0.0	0.0
18	18	0.100E-01	0.10950D-01	0.1914D-02	0.0	0.0	0.0	0.0
19	19	0.100E-01	0.11616D-01	0.1914D-02	0.0	0.0	0.0	0.0
20	20	0.100E-01	0.12282D-01	0.1914D-02	0.0	0.0	0.0	0.0
21	21	0.100E-01	0.12948D-01	0.1914D-02	0.0	0.0	0.0	0.0
22	22	0.100E-01	0.13614D-01	0.1914D-02	0.0	0.0	0.0	0.0
23	23	0.100E-01	0.14280D-01	0.1914D-02	0.0	0.0	0.0	0.0
24	24	0.100E-01	0.14946D-01	0.1914D-02	0.0	0.0	0.0	0.0
25	25	0.100E-01	0.15612D-01	0.1914D-02	0.0	0.0	0.0	0.0
26	26	0.100E-01	0.16278D-01	0.1914D-02	0.0	0.0	0.0	0.0
27	27	0.100E-01	0.16944D-01	0.1914D-02	0.0	0.0	0.0	0.0
28	28	0.100E-01	0.17610D-01	0.1914D-02	0.0	0.0	0.0	0.0
29	29	0.100E-01	0.18276D-01	0.1914D-02	0.0	0.0	0.0	0.0
30	30	0.100E-01	0.18942D-01	0.1914D-02	0.0	0.0	0.0	0.0
31	31	0.100E-01	0.19608D-01	0.1914D-02	0.0	0.0	0.0	0.0
32	32	0.100E-01	0.20274D-01	0.1914D-02	0.0	0.0	0.0	0.0
33	33	0.100E-01	0.20940D-01	0.1914D-02	0.0	0.0	0.0	0.0
34	34	0.100E-01	0.21606D-01	0.1914D-02	0.0	0.0	0.0	0.0
35	35	0.100E-01	0.22272D-01	0.1914D-02	0.0	0.0	0.0	0.0
36	36	0.100E-01	0.22938D-01	0.1914D-02	0.0	0.0	0.0	0.0
37	37	0.100E-01	0.23604D-01	0.1914D-02	0.0	0.0	0.0	0.0
38	38	0.100E-01	0.24270D-01	0.1914D-02	0.0	0.0	0.0	0.0
39	39	0.100E-01	0.24936D-01	0.1914D-02	0.0	0.0	0.0	0.0
40	40	0.100E-01	0.25602D-01	0.1914D-02	0.0	0.0	0.0	0.0
41	41	0.100E-01	0.26268D-01	0.1914D-02	0.0	0.0	0.0	0.0
42	42	0.100E-01	0.26934D-01	0.1914D-02	0.0	0.0	0.0	0.0
43	43	0.100E-01	0.27600D-01	0.1914D-02	0.0	0.0	0.0	0.0
44	44	0.100E-01	0.28266D-01	0.1914D-02	0.0	0.0	0.0	0.0
45	45	0.100E-01	0.28932D-01	0.1914D-02	0.0	0.0	0.0	0.0
46	46	0.100E-01	0.29598D-01	0.1914D-02	0.0	0.0	0.0	0.0
47	47	0.100E-01	0.30264D-01	0.1914D-02	0.0	0.0	0.0	0.0
48	48	0.100E-01	0.30930D-01	0.1914D-02	0.0	0.0	0.0	0.0
49	49	0.100E-01	0.31596D-01	0.1914D-02	0.0	0.0	0.0	0.0
50	50	0.100E-01	0.32262D-01	0.1914D-02	0.0	0.0	0.0	0.0
51	51	0.100E-01	0.32928D-01	0.1914D-02	0.0	0.0	0.0	0.0
52	52	0.100E-01	0.33594D-01	0.1914D-02	0.0	0.0	0.0	0.0
53	53	0.100E-01	0.34260D-01	0.1914D-02	0.0	0.0	0.0	0.0
54	54	0.100E-01	0.34926D-01	0.1914D-02	0.0	0.0	0.0	0.0
55	55	0.100E-01	0.35592D-01	0.1914D-02	0.0	0.0	0.0	0.0
56	56	0.100E-01	0.36258D-01	0.1914D-02	0.0	0.0	0.0	0.0
57	57	0.100E-01	0.36924D-01	0.1914D-02	0.0	0.0	0.0	0.0
58	58	0.100E-01	0.37590D-01	0.1914D-02	0.0	0.0	0.0	0.0
59	59	0.100E-01	0.38256D-01	0.1914D-02	0.0	0.0	0.0	0.0
60	60	0.100E-01	0.38922D-01	0.1914D-02	0.0	0.0	0.0	0.0
61	61	0.100E-01	0.39588D-01	0.1914D-02	0.0	0.0	0.0	0.0
62	62	0.100E-01	0.40254D-01	0.1914D-02	0.0	0.0	0.0	0.0
63	63	0.100E-01	0.40920D-01	0.1914D-02	0.0	0.0	0.0	0.0
64	64	0.100E-01	0.41586D-01	0.1914D-02	0.0	0.0	0.0	0.0
65	65	0.100E-01	0.42252D-01	0.1914D-02	0.0	0.0	0.0	0.0
66	66	0.100E-01	0.42918D-01	0.1914D-02	0.0	0.0	0.0	0.0
67	67	0.100E-01	0.43584D-01	0.1914D-02	0.0	0.0	0.0	0.0
68	68	0.100E-01	0.44250D-01	0.1914D-02	0.0	0.0	0.0	0.0
69	69	0.100E-01	0.44916D-01	0.1914D-02	0.0	0.0	0.0	0.0
70	70	0.100E-01	0.45582D-01	0.1914D-02	0.0	0.0	0.0	0.0
71	71	0.100E-01	0.46248D-01	0.1914D-02	0.0	0.0	0.0	0.0
72	72	0.100E-01	0.46914D-01	0.1914D-02	0.0	0.0	0.0	0.0
73	73	0.100E-01	0.47580D-01	0.1914D-02	0.0	0.0	0.0	0.0
74	74	0.100E-01	0.48246D-01	0.1914D-02	0.0	0.0	0.0	0.0
75	75	0.100E-01	0.48912D-01	0.1914D-02	0.0	0.0	0.0	0.0
76	76	0.100E-01	0.49578D-01	0.1914D-02	0.0	0.0	0.0	0.0
77	77	0.100E-01	0.50244D-01	0.1914D-02	0.0	0.0	0.0	0.0
78	78	0.100E-01	0.50910D-01	0.1914D-02	0.0	0.0	0.0	0.0
79	79	0.100E-01	0.51576D-01	0.1914D-02	0.0	0.0	0.0	0.0
80	80	0.100E-01	0.52242D-01	0.1914D-02	0.0	0.0	0.0	0.0
81	81	0.100E-01	0.52908D-01	0.1914D-02	0.0	0.0	0.0	0.0
82	82	0.100E-01	0.53574D-01	0.1914D-02	0.0	0.0	0.0	0.0
83	83	0.100E-01	0.54240D-01	0.1914D-02	0.0	0.0	0.0	0.0
84	84	0.100E-01	0.54906D-01	0.1914D-02	0.0	0.0	0.0	0.0
85	85	0.100E-01	0.55572D-01	0.1914D-02	0.0	0.0	0.0	0.0
86	86	0.100E-01	0.56238D-01	0.1914D-02	0.0	0.0	0.0	0.0
87	87	0.100E-01	0.56904D-01	0.1914D-02	0.0	0.0	0.0	0.0
88	88	0.100E-01	0.57570D-01	0.1914D-02	0.0	0.0	0.0	0.0
89	89	0.100E-01	0.58236D-01	0.1914D-02	0.0	0.0	0.0	0.0
90	90	0.100E-01	0.58902D-01	0.1914D-02	0.0	0.0	0.0	0.0
91	91	0.100E-01	0.59568D-01	0.1914D-02	0.0	0.0	0.0	0.0
92	92	0.100E-01	0.60234D-01	0.1914D-02	0.0	0.0	0.0	0.0
93	93	0.100E-01	0.60899D-01	0.1914D-02	0.0	0.0	0.0	0.0
94	94	0.100E-01	0.61565D-01	0.1914D-02	0.0	0.0	0.0	0.0
95	95	0.100E-01	0.62231D-01	0.1914D-02	0.0	0.0	0.0	0.0
96	96	0.100E-01	0.62897D-01	0.1914D-02	0.0	0.0	0.0	0.0
97	97	0.100E-01	0.63563D-01	0.1914D-02	0.0	0.0	0.0	0.0
98	98	0.100E-01	0.64229D-01	0.1914D-02	0.0	0.0	0.0	0.0
99	99	0.100E-01	0.64895D-01	0.1914D-02	0.0	0.0	0.0	0.0
100	100	0.100E-01	0.65561D-01	0.1914D-02	0.0	0.0	0.0	0.0

卷之三

INTERNAL CONNECTION DATA									
NOD1	NOD2	AREA	MINT	RINT	HT	FLW	AVG RATE	HT	FLW
2	3	0.25750-21	0.0000E+00	1.3	0.0	0.0	0.0000E+00	0.0000E+00	0.0000E+00
3	4	0.62830-21	0.0000E+00	1.3	0.0	0.0	0.0000E+00	0.0000E+00	0.0000E+00
4	5	0.12550-21	0.0000E+00	1.3	0.0	0.0	0.0000E+00	0.0000E+00	0.0000E+00
5	6	0.35130-21	0.0000E+00	1.3	0.0	0.0	0.0000E+00	0.0000E+00	0.0000E+00
6	7	0.15420-21	0.0000E+00	1.3	0.0	0.0	0.0000E+00	0.0000E+00	0.0000E+00
7	8	0.36130-21	0.0000E+00	1.3	0.0	0.0	0.0000E+00	0.0000E+00	0.0000E+00
8	9	0.35770-21	0.0000E+00	1.3	0.0	0.0	0.0000E+00	0.0000E+00	0.0000E+00
9	10	0.3980-21	0.0000E+00	1.3	0.0	0.0	0.0000E+00	0.0000E+00	0.0000E+00
10	11	0.27070-21	0.0000E+00	1.3	0.0	0.0	0.0000E+00	0.0000E+00	0.0000E+00
11	12	0.56160-21	0.0000E+00	1.3	0.0	0.0	0.0000E+00	0.0000E+00	0.0000E+00

TRUMP OUTPUT DATA

* MISSLE PROBLEM ONE DIMENSIONAL

PRINTOUT	CYCLE	TCD	TOO FAST	TOO SLOW	KWIT	DELTMX	0	SHALL	TVARY	NUTS
5	45				0	1.00000E-12		1.00000E-33	1.00000E-33	
TOTAL TIME	TIME STEP		HEAT FLOW		TEMP FROM FLUX	1.66963E-03	FLUX RATE			
5.51874E-32	1.7817E-31		2.26636E-33		4.1366E-30		3.02543E-03			
Avg TEMP	HEAT CAPACITY		HEAT CONTENT		GEN RATE		TEMP FROM GEN			
9.06828E-01	1.25739E-09		1.33092E-32		0.5		0.0			

NODE	TEMP	0	0.0	0.0	0.0	0.0	0.0	0.0	0.0	0.0
1	0.863	0.0	0.0	0.0	0.0	0.0	0.0	0.0	0.0	0.0
2	0.900	0.0	0.0	0.0	0.0	0.0	0.0	0.0	0.0	0.0
3	0.947	0.0	0.0	0.0	0.0	0.0	0.0	0.0	0.0	0.0
4	0.994	0.0	0.0	0.0	0.0	0.0	0.0	0.0	0.0	0.0
5	0.000	0.0	0.0	0.0	0.0	0.0	0.0	0.0	0.0	0.0
6	0.000	0.0	0.0	0.0	0.0	0.0	0.0	0.0	0.0	0.0
7	0.000	0.0	0.0	0.0	0.0	0.0	0.0	0.0	0.0	0.0
8	0.000	0.0	0.0	0.0	0.0	0.0	0.0	0.0	0.0	0.0
9	0.000	0.0	0.0	0.0	0.0	0.0	0.0	0.0	0.0	0.0
10	0.000	0.0	0.0	0.0	0.0	0.0	0.0	0.0	0.0	0.0
11	0.000	0.0	0.0	0.0	0.0	0.0	0.0	0.0	0.0	0.0
12	0.000	0.0	0.0	0.0	0.0	0.0	0.0	0.0	0.0	0.0

NAME	MATL	TOT CAP	0.0	TOT HEAT	0.01	Avg TEMP	0.01	MELT	0.0	MELT
SAND	1.0E-32	0.00000E+00								
STEEL	2.0E-32	0.00000E+00								
AIR	3.0E-32	0.00000E+00								

NAME	MATL	DATA	NAME	MATL	DATA
------	------	------	------	------	------

NODE	MATL	NTYPE	RADIUS	VOLUME	MASS	CAPACITY	CONDUCTIVITY	ZIP	SLIM
1	1	4	0.1000E-02	0.1557E-04	0.68360E-06	0.1299D-06	0.270CD-03	0.686D-05	0.194D-01
2	1	4	0.0500E-01	0.3422E-01	0.00000E+00	0.327D-01	0.705D-03	0.193D-02	0.193D-02
3	3	4	0.0000E+00	0.0000E+00	0.00000E+00	0.971D-01	0.270D-03	0.591D-02	0.591D-02
4	4	4	0.0000E+00	0.0000E+00	0.00000E+00	0.104D-01	0.270D-03	0.194D-02	0.194D-02
5	5	4	0.0000E+00	0.0000E+00	0.00000E+00	0.104D-01	0.270D-03	0.194D-02	0.194D-02
6	6	4	0.0000E+00	0.0000E+00	0.00000E+00	0.104D-01	0.270D-03	0.194D-02	0.194D-02
7	7	4	0.0000E+00	0.0000E+00	0.00000E+00	0.104D-01	0.270D-03	0.194D-02	0.194D-02
8	8	3	0.0000E+00	0.0000E+00	0.00000E+00	0.202D-01	0.270D-03	0.194D-02	0.194D-02
9	9	3	0.0000E+00	0.0000E+00	0.00000E+00	0.202D-01	0.270D-03	0.194D-02	0.194D-02
10	10	3	0.0000E+00	0.0000E+00	0.00000E+00	0.202D-01	0.270D-03	0.194D-02	0.194D-02
11	11	3	0.0000E+00	0.0000E+00	0.00000E+00	0.202D-01	0.270D-03	0.194D-02	0.194D-02
12	12	3	0.0000E+00	0.0000E+00	0.00000E+00	0.202D-01	0.270D-03	0.194D-02	0.194D-02

INTC1	NOID	AREA	INT	INT	INT	TRAN	HEAT FLOW	AVG RATE
1	1	0.1257E-01	0.1000E-13	0.00	0.696D-05	-0.696D-05	0.696D-05	0.1895E-08
2	3	0.02628E-01	0.0200E-13	0.00	0.333D-02	-0.333D-02	0.333D-02	0.906E-03
3	4	0.01257E-01	0.0100E-13	0.00	0.333D-02	-0.333D-02	0.333D-02	0.906E-03
4	5	0.00628E-01	0.0020E-13	0.00	0.333D-02	-0.333D-02	0.333D-02	0.906E-03
5	6	0.00314E-01	0.0010E-13	0.00	0.333D-02	-0.333D-02	0.333D-02	0.906E-03
6	7	0.00157E-01	0.0002E-13	0.00	0.333D-02	-0.333D-02	0.333D-02	0.906E-03
7	8	0.000787E-01	0.0001E-13	0.00	0.333D-02	-0.333D-02	0.333D-02	0.906E-03
8	9	0.000393E-01	0.00002E-13	0.00	0.333D-02	-0.333D-02	0.333D-02	0.906E-03
9	10	0.000197E-01	0.00001E-13	0.00	0.333D-02	-0.333D-02	0.333D-02	0.906E-03
10	11	0.0000987E-01	0.000002E-13	0.00	0.333D-02	-0.333D-02	0.333D-02	0.906E-03
11	12	0.0000493E-01	0.000001E-13	0.00	0.333D-02	-0.333D-02	0.333D-02	0.906E-03

NOID	TEMPB	HEAT FLOW	AVG RATE
200	7.2257E-01	2.2664D-03	4.1067E-00
SYSTEM TOTAL		664E-03	4.1067E-00
EXTERNAL CONNECTION DATA			
NOIDS	AREAS	HSURE	POWER
12	2001	5.6156D-01	1.0000D-06
		0.0	
		5.616D-07	4.1067E-00
INTERNAL CONNECTION DATA			
NOIDS	AREAS	HSURE	RSURE
12	2001	5.6156D-01	1.0000D-06
		0.0	
		5.616D-07	4.1067E-00
WILL REPEAT CYCLE			
49	DIMAX	2.29E-00	DTRE
	DTMAX	2.109E-00	DELT = 2.109E-00
	DTMIN	2.083E-02	DELT = 2.083E-02
	DTMAX	2.109E-00	DELT = 2.109E-00

TRUMP OUTPUT DATA

* MISSLE PROBLEM ONE DIMENSIONAL

DATA DECK 1

PRINTOUT									
60	CYCLE	TOO FAST	TOO SLOW	KWIT	DELTMAX	1 SMALL	TIVARY	RUTS	
6.97239E 02	9.34838E 00	-7.26409E 03	-5.35153E 03	-1.04488E 01	1.00000E 00	1.00000E 00	1.00000E 00		
Avg TEMP	HEAT CAPACITY	HEAT CONTENT	HEAT GEN	TEMP FROM GEN					
8.6275E 01	1.35739E 00	1.115E 02	0.0	0.0					
NODE									
1	TEMP	DT	DDT	GE N RATE	H	H	F	CURE AT 280 F	
2	0.9253D 02	-0.371D 00	-0.185D 01	0.0	0.025E 04	0.2945E 05	0.2042E 05	0.0	
3	0.9177D 02	-0.366D 00	-0.172D 01	0.0	0.025E 04	0.2945E 05	0.2042E 05	0.0	
4	0.9028D 02	-0.3269D 00	-0.1386D 01	0.0	0.025E 04	0.2945E 05	0.2042E 05	0.0	
5	0.8819D 02	-0.1259D 00	-0.0533D 01	0.0	0.025E 04	0.2945E 05	0.2042E 05	0.0	
6	0.8572D 02	-0.1552D 00	-0.0561D 01	0.0	0.025E 04	0.2945E 05	0.2042E 05	0.0	
7	0.8362D 02	-0.1577D 00	-0.0561D 01	0.0	0.025E 04	0.2945E 05	0.2042E 05	0.0	
8	0.8226D 02	-0.3366D 00	-0.3476D 01	0.0	0.025E 04	0.2945E 05	0.2042E 05	0.0	
9	0.8216D 02	-0.6346D 00	-0.6347D 01	0.0	0.025E 04	0.2945E 05	0.2042E 05	0.0	
10	0.8025D 02	-0.8647D 00	-0.8647D 01	0.0	0.025E 04	0.2945E 05	0.2042E 05	0.0	
11	0.7981D 02	-0.9577D 00	-0.9577D 01	0.0	0.025E 04	0.2945E 05	0.2042E 05	0.0	
12	0.7924D 02	-0.9817D 00	-0.9817D 01	0.0	0.025E 04	0.2945E 05	0.2042E 05	0.0	
MATERIAL DATA									
NAME	MATL	TOT CAP	TOT HEAT	AVG TEMP	TOT MELT	TOT MELT	SLIM		
SAND	1	1.9235E 03	9.01	8.7172E 01	0.0	0.0	0.194D-01	0.194D-01	0.194D-01
AIR	2	1.9244E 03	9.01	8.7172E 01	0.0	0.0	0.194D-01	0.194D-01	0.194D-01
NODE DATA									
NODE	NATL	NTYPE	RADIUS	VOLUME	MASS	CONDUCTIVITY	ZIP	TRAN	Avg RATE
1	1	4	0.1000E-02	0.0314E-04	0.6816D-06	0.2990D-06	0.194D-05	0.194D-05	0.194D-05
2	1	4	0.5000E-02	0.0000E-04	0.1990D-06	0.2470D-06	0.170D-03	0.170D-03	0.170D-03
3	1	4	0.2500E-02	0.0000E-04	0.9952D-06	0.1241D-06	0.509D-02	0.509D-02	0.509D-02
4	1	4	0.1250E-02	0.0000E-04	0.4976D-06	0.6240D-06	0.2648D-02	0.2648D-02	0.2648D-02
5	1	4	0.0625E-02	0.0000E-04	0.2498D-06	0.3123D-06	0.1324D-02	0.1324D-02	0.1324D-02
6	1	4	0.0312E-02	0.0000E-04	0.1250D-06	0.1618D-06	0.6622D-02	0.6622D-02	0.6622D-02
7	1	4	0.0156E-02	0.0000E-04	0.6250D-06	0.8196D-06	0.3309D-02	0.3309D-02	0.3309D-02
8	1	4	0.0078E-02	0.0000E-04	0.3125D-06	0.4098D-06	0.1654D-02	0.1654D-02	0.1654D-02
9	1	4	0.0039E-02	0.0000E-04	0.15625D-06	0.2049D-06	0.8272D-03	0.8272D-03	0.8272D-03
10	1	4	0.0019E-02	0.0000E-04	0.78125D-06	0.1024D-06	0.4136D-03	0.4136D-03	0.4136D-03
11	1	4	0.0009E-02	0.0000E-04	0.390625D-06	0.5020D-06	0.2068D-03	0.2068D-03	0.2068D-03
12	2	4	0.8938E-01	0.4983E-02	0.2075D-02	0.931D-03	0.1000D-01	0.1000D-01	0.1000D-01
INTERNAL CONNECTION DATA									
NODE1	NODE2	AREA	HINT	RINT	TRAN	HEAT FLOW	Avg RATE		
1	2	0.1257D-01	0.1000E 13	0.0	0.1257D-05	0.1257D-05	0.1257D-05		
2	3	0.6283D-01	0.1000E 13	0.0	0.6283D-05	0.6283D-05	0.6283D-05		
3	4	0.1257D-02	0.1000E 13	0.0	0.1257D-05	0.1257D-05	0.1257D-05		
4	5	0.1858D-02	0.1000E 13	0.0	0.1858D-05	0.1858D-05	0.1858D-05		
5	6	0.2515D-02	0.1000E 13	0.0	0.2515D-05	0.2515D-05	0.2515D-05		
6	7	0.3142D-02	0.1000E 13	0.0	0.3142D-05	0.3142D-05	0.3142D-05		
7	8	0.3770D-02	0.1000E 13	0.0	0.3770D-05	0.3770D-05	0.3770D-05		
8	9	0.4398D-02	0.1000E 13	0.0	0.4398D-05	0.4398D-05	0.4398D-05		
9	10	0.4926D-02	0.1000E 13	0.0	0.4926D-05	0.4926D-05	0.4926D-05		
10	11	0.5554D-02	0.1000E 13	0.0	0.5554D-05	0.5554D-05	0.5554D-05		
11	12	0.5616D-02	0.1000E 13	0.0	0.5616D-05	0.5616D-05	0.5616D-05		
BOUNDARY NODE DATA									
NODE	TEMP	HEAT FLOW	Avg RATE						
2001	7.987E 01	7.2641D 03	-1.0419E 01						
SYSTEM TOTAL									
EXTERNAL CONNECTION DATA									
NOODS NOOSB	AREAS	HSURE	POWER	RSURE	TRANS	HEAT FLOW	Avg RATE		
120	5.616D 01	1.0000D 06	0.0	5.616D 07	-7.2641E 03	-1.0419E 01			

TRUMP OUTPUT DATA

* MISSE PROBLEM ONE DIMENSIONAL

DATA DECK 1

PRINTOUT	CYCLE	TOO FAST	TOO SLOW	KWT	DELMX	1.0000E 12	SMALL	1.0000E 00	1.0000E 00	TVALY	NUTS
TOTAL TIME	5.5791E 00	-7.5614E 03			TEMP FROM FLOH	-5.6794E 03	FLUX RATE	-9.7467E 00	-7.1805E 00		
7.9094E 02											
Avg TEMP	HEAT CAPACITY	HEAT CONTENT	GEN RATE	HEAT GEN							
8.7013E 01	1.1573E 00	1.1811E 02	0.0	0.0							
NODE	TEMP	DT	DOT	GDN	RATE		H	1.160E-04	-0.3354E-05	F	CURE AT 280 F
1	0.8931E 02	-0.1498E 00	-0.2684E 01	0.0	0.0		0.2901E 01	-0.8435E 00	0.0	0.8435E 00	0.0
2	0.8998E 02	-0.1280E 00	-0.1493E 01	0.0	0.0		0.8614E 01	-0.2646E 01	0.0	0.2646E 01	0.0
3	0.8997E 02	-0.1280E 00	-0.1473E 01	0.0	0.0		0.8614E 02	-0.4751E 01	0.0	0.4751E 01	0.0
4	0.8996E 02	-0.1280E 00	-0.1473E 01	0.0	0.0		0.8614E 02	-0.7158E 01	0.0	0.7158E 01	0.0
5	0.8996E 02	-0.1280E 00	-0.1473E 01	0.0	0.0		0.8614E 02	-0.9504E 01	0.0	0.9504E 01	0.0
6	0.8996E 02	-0.1280E 00	-0.1473E 01	0.0	0.0		0.8614E 02	-0.8084E 01	0.0	0.8084E 01	0.0
7	0.8996E 02	-0.1280E 00	-0.1473E 01	0.0	0.0		0.8614E 02	-0.8135E 01	0.0	0.8135E 01	0.0
8	0.8996E 02	-0.1280E 00	-0.1473E 01	0.0	0.0		0.8614E 02	-0.1049E 01	0.0	0.1049E 01	0.0
9	0.8996E 02	-0.1280E 00	-0.1473E 01	0.0	0.0		0.8614E 02	-0.8123E 02	0.0	0.8123E 02	0.0
10	0.8996E 02	-0.1280E 00	-0.1473E 01	0.0	0.0		0.8614E 02	-0.5857E 02	0.0	0.5857E 02	0.0
11	0.8996E 02	-0.1280E 00	-0.1473E 01	0.0	0.0		0.8614E 02	-0.2613E 24	0.0	0.2613E 24	0.0
12	0.8996E 02	-0.1280E 00	-0.1473E 01	0.0	0.0		0.8614E 02	-0.7666E 34	0.0	0.7666E 34	0.0
MATERIAL DATA											
	NAME	MATL	TOT CAP	TOT HEAT	Avg TEMP	THLT	HWELET				
	SAND	1.01359E 00	9.23396E 01	8.69948E 01	0.0	0.0	0.0				
	STEL	2.08256E -03	2.4193E -01	8.70594E 01	0.0	0.0	0.0				
	AR	1.01246E -03	1.3193E -01	9.15055E 01	0.0	0.0	0.0				
NODE DATA											
NODE	MATL	NTYPE	RADIUS	VOLUME	MASS	CAPACITY	CONDUCT	ITY	ZIP	SLIN	
1	1	1	0.1257E -02	0.3142E -04	0.6830E -36	0.1257E -06	0.2424E 00	1	0.1914E 00	0.1914E 00	
2	1	1	0.1510E -02	0.3142E -04	0.1709E 00	0.1510E -06	0.9140E -01	1	0.1914E 00	0.1914E 00	
3	1	1	0.1500E -02	0.1571E 01	0.8514E 00	0.1500E -06	0.1440E 00	1	0.1914E 00	0.1914E 00	
4	1	1	0.1500E -02	0.1571E 01	0.1190E 00	0.1500E -06	0.2123E 00	1	0.1914E 00	0.1914E 00	
5	1	1	0.1500E -02	0.1571E 01	0.1530E 00	0.1500E -06	0.2123E 00	1	0.1914E 00	0.1914E 00	
6	1	1	0.1500E -02	0.1571E 01	0.1537E 00	0.1500E -06	0.2123E 00	1	0.1914E 00	0.1914E 00	
7	1	1	0.1500E -02	0.1571E 01	0.1537E 00	0.1500E -06	0.2123E 00	1	0.1914E 00	0.1914E 00	
8	1	1	0.1500E -02	0.1571E 01	0.1537E 00	0.1500E -06	0.2123E 00	1	0.1914E 00	0.1914E 00	
9	3	2	0.6500E 01	0.4712E 01	0.1781E 02	0.4712E 03	0.2914E 03	0.2186E 02	0.2186E 02	0.2186E 02	
10	3	4	0.6500E 01	0.4712E 01	0.2052E 02	0.4712E 03	0.4291E 03	0.2500E 02	0.2500E 02	0.2500E 02	
11	3	4	0.6500E 01	0.4712E 01	0.2807E 02	0.4712E 03	0.5264E 03	0.3600E 02	0.3600E 02	0.3600E 02	
12	2	2	0.8938E 01	0.1000E -02	0.2807E 02	0.1000E -02	0.3600E -02	0.2807E 02	0.3600E 02	0.3600E 02	
INTERNAL CONNECTION DATA											
NODE1	NODE2	AREA	HINT	RINT	TRN1	HEAT FLOW	Avg RATE				
1	2	0.1257E 01	0.1000E 13	0.0	0.1257E 05	0.1257E 05	0.1257E 05				
2	3	0.1257E 01	0.1000E 13	0.0	0.1257E 05	0.1257E 05	0.1257E 05				
3	4	0.1257E 01	0.1000E 13	0.0	0.1257E 05	0.1257E 05	0.1257E 05				
4	5	0.1257E 01	0.1000E 13	0.0	0.1257E 05	0.1257E 05	0.1257E 05				
5	6	0.1257E 01	0.1000E 13	0.0	0.1257E 05	0.1257E 05	0.1257E 05				
6	7	0.1257E 01	0.1000E 13	0.0	0.1257E 05	0.1257E 05	0.1257E 05				
7	8	0.1257E 01	0.1000E 13	0.0	0.1257E 05	0.1257E 05	0.1257E 05				
8	9	0.1257E 01	0.1000E 13	0.0	0.1257E 05	0.1257E 05	0.1257E 05				
9	10	0.1257E 01	0.1000E 13	0.0	0.1257E 05	0.1257E 05	0.1257E 05				
10	11	0.1257E 01	0.1000E 13	0.0	0.1257E 05	0.1257E 05	0.1257E 05				
11	12	0.1257E 01	0.1000E 13	0.0	0.1257E 05	0.1257E 05	0.1257E 05				
BOUNDARY NODE DATA											
NOOD	TEMPB	HEAT FLOW	Avg RATE								
2001	9.4960E 01	-7.0792E 03	-9.7468E 00								
SYSTEM TOTAL											
		-7.7092E 03	-9.7468E 00								
EXTERNAL CONNECTION DATA											
NOOD	NOOSB	AREAS	HSURE	POWER	RSURE	TRANS	HEAT FLOW	Avg RATE			
12	2001	5.6156E 01	1.0330E 36	0.0	0.0	5.6156E 07	-7.7091E 03	-9.7468E 00			

DATA DECK 1

TRUMP OUTPUT DATA
* MISSLE PROBLEM ONE DIMENSIONAL

PRINTOUT CYCLE TOO FAST TOO SLOW KWIT DELTMX SMALL 1.0000E 30 TVARY NUTS

8 90 TOTAL TIME TIME STEP HEAT FLOW 1.02246E 04 -7.5325E 03 -1.15632E 01 -8.5176E 00

8.84236E 02 7.0307E 00 AVG TEMP HEAT CAPACITY HEAT CONTENT GEN RATE TEMP FROM GEN

9.09457E 01 1.35739E 00 1.2348E 32 0.0 0.0 0.0

NODE TEMP DT DDT GE N RATE H 1.163E-04 H 3.237E-05 CURE AT 280 F

1 0.87970 02 -0.2100D-01 -0.20970-01 -0.2670-02 0.0 0.0 0.0

2 0.87940 02 0.21590-01 0.25450-01 0.28830-02 0.0 0.0 0.0

3 0.88040 02 0.25450-01 0.31450-01 0.36830-02 0.0 0.0 0.0

4 0.88620 02 0.43100-01 0.53100-01 0.62000-02 0.0 0.0 0.0

5 0.90170 02 0.66400-01 0.83700-01 0.99400-02 0.0 0.0 0.0

6 0.92940 02 0.94760-01 0.97700-01 0.99400-02 0.0 0.0 0.0

7 0.97700 02 0.10300-01 0.85400-01 0.7460-02 0.0 0.0 0.0

8 0.10740 03 0.10940-01 0.99160-00 0.1210-00 0.0 0.0 0.0

9 0.10940 03 0.10940-01 0.99160-00 0.1210-00 0.0 0.0 0.0

10 0.10940 03 0.10940-01 0.99160-00 0.1210-00 0.0 0.0 0.0

11 0.10940 03 0.10940-01 0.99160-00 0.1210-00 0.0 0.0 0.0

12 0.10940 03 0.10940-01 0.99160-00 0.1210-00 0.0 0.0 0.0

***** MATERIAL DATA *****

NAME MATL TOT CAP HEAT 01 AVG TEMP 31 MELT 0.0

SAND 1 1.03359E 03 2.67550E 01 8.9273E 31 0.0

STEEL 2 2.83266E 03 1.4246E 03 1.4866E 01 1.4030E 02 0.0

AIR 3 1.4030E 02 0.0 0.0 0.0

***** NODE DATA *****

NODE MATL NTYP RADIUS VOLUME MASS CONDUCTIVITY SLIM ZIP

1 1 4 0.10000-01 0.12540-01 0.69000-06 0.19140-01 0.67860-05

2 1 4 0.10000-01 0.31450-01 0.49000-06 0.19140-01 0.67860-05

3 1 4 0.10000-01 0.31450-01 0.49000-06 0.19140-01 0.67860-05

4 1 4 0.10000-01 0.31450-01 0.49000-06 0.19140-01 0.67860-05

5 1 4 0.10000-01 0.31450-01 0.49000-06 0.19140-01 0.67860-05

6 1 4 0.10000-01 0.31450-01 0.49000-06 0.19140-01 0.67860-05

7 1 4 0.10000-01 0.31450-01 0.49000-06 0.19140-01 0.67860-05

8 1 4 0.10000-01 0.31450-01 0.49000-06 0.19140-01 0.67860-05

9 1 4 0.10000-01 0.31450-01 0.49000-06 0.19140-01 0.67860-05

10 1 4 0.10000-01 0.31450-01 0.49000-06 0.19140-01 0.67860-05

11 1 4 0.10000-01 0.31450-01 0.49000-06 0.19140-01 0.67860-05

12 1 4 0.10000-01 0.31450-01 0.49000-06 0.19140-01 0.67860-05

***** INTERNAL CONNECTION DATA *****

NOD1 NOD2 AREA HINT RINT TRAN HEAT FLOW AVG RATE

1 2 0.12570-01 0.10000-01 0.0 0.0 0.67860-05 -0.91313E 00 -0.1053E 02

2 3 0.62830-01 0.10000-01 0.0 0.0 0.1980-02 -0.1930-02 -0.1930-02

3 4 0.12570-01 0.10000-01 0.0 0.0 0.50890-02 -0.8747E 01 -0.9293E 02

4 5 0.18850-01 0.10000-01 0.0 0.0 0.67860-02 -0.91581E 02 -0.1782E 01

5 6 0.31450-01 0.10000-01 0.0 0.0 0.25550-02 -0.311903E 02 -0.3522E 01

6 7 0.31450-01 0.10000-01 0.0 0.0 0.1660-02 -0.49436E 02 -0.3283E 02

7 8 0.31450-01 0.10000-01 0.0 0.0 0.4510-02 -0.2909E 01 -0.3293E 02

8 9 0.31450-01 0.10000-01 0.0 0.0 0.9860-02 -0.2910E 01 -0.2907E 01

9 10 0.31450-01 0.10000-01 0.0 0.0 0.1660-02 -0.2907E 01 -0.3287E 02

***** BOUNDARY NODE DATA *****

NODB TEMPB J2 HEAT FLOW 1.0225D 04 -1.1563E 01

SYSTEM TOTAL -1.0225E 04 -1.1563E 01

***** EXTERNAL CONNECTION DATA *****

NODS NODSB AREAS HSURE POWER RSURE TRANS HEAT FLOW AVG RATE

12 2001 5.616D 01 1.0000D 06 0.0 0.0 5.6156D 07 -1.0225E 04 -1.1563E 01

TRUMP OUTPUT DATA

* MISSLE PROBLEM

ONE DIMENSIONAL

DATA DECK 1

PRINTOUT	CYCLE	TCD	FAST	TOO SLOW	KWIT	DELTMX	t2	1.00000E 00	TVARY	NUTS
9	105	6	0	0	0	1.00000E 00				
TOTAL TIME	TIME STEP	-1.07468E 01	-1.1536E 04	TEMP FLOW	TEMP FROM FLUX	FLUX RATE	E 03	-1.13916E 01	-8.37232E 00	
1.01237E 03	1.07468E 01	1.07468E 01	1.07468E 01	1.07468E 01	1.07468E 01	1.07468E 01				
Avg TEMP	HEAT CAPACITY	1.35139D 00	1.35139D 00	HEAT CONTENT	GEN RATE	HEAT GEN		0.0	TEMP FROM GEN	
9.59246E 01	1.35139D 00	1.35139D 00	1.35139D 00	1.35139D 00	1.35139D 00	1.35139D 00			0.0	
NODE	TEMP	DT	0.0718D 02	0.0718D 02	0.0718D 02	0.0718D 02	0.0718D 02	0.0718D 02	0.0718D 02	CURE AT 280 F
1	0.0718D 02	0.0718D 02	0.0718D 02	0.0718D 02	0.0718D 02	0.0718D 02	0.0718D 02	0.0718D 02	0.0718D 02	
2	0.0718D 02	0.0718D 02	0.0718D 02	0.0718D 02	0.0718D 02	0.0718D 02	0.0718D 02	0.0718D 02	0.0718D 02	
3	0.0718D 02	0.0718D 02	0.0718D 02	0.0718D 02	0.0718D 02	0.0718D 02	0.0718D 02	0.0718D 02	0.0718D 02	
4	0.0718D 02	0.0718D 02	0.0718D 02	0.0718D 02	0.0718D 02	0.0718D 02	0.0718D 02	0.0718D 02	0.0718D 02	
5	0.0718D 02	0.0718D 02	0.0718D 02	0.0718D 02	0.0718D 02	0.0718D 02	0.0718D 02	0.0718D 02	0.0718D 02	
6	0.0718D 02	0.0718D 02	0.0718D 02	0.0718D 02	0.0718D 02	0.0718D 02	0.0718D 02	0.0718D 02	0.0718D 02	
7	0.0718D 02	0.0718D 02	0.0718D 02	0.0718D 02	0.0718D 02	0.0718D 02	0.0718D 02	0.0718D 02	0.0718D 02	
8	0.0718D 02	0.0718D 02	0.0718D 02	0.0718D 02	0.0718D 02	0.0718D 02	0.0718D 02	0.0718D 02	0.0718D 02	
9	0.0718D 02	0.0718D 02	0.0718D 02	0.0718D 02	0.0718D 02	0.0718D 02	0.0718D 02	0.0718D 02	0.0718D 02	
10	0.0718D 02	0.0718D 02	0.0718D 02	0.0718D 02	0.0718D 02	0.0718D 02	0.0718D 02	0.0718D 02	0.0718D 02	
11	0.0718D 02	0.0718D 02	0.0718D 02	0.0718D 02	0.0718D 02	0.0718D 02	0.0718D 02	0.0718D 02	0.0718D 02	
12	0.0718D 02	0.0718D 02	0.0718D 02	0.0718D 02	0.0718D 02	0.0718D 02	0.0718D 02	0.0718D 02	0.0718D 02	
MATERIAL DATA										
NAME	MATL	TOT CAP	0.0718E 00	1.0718E 02	TOT HEAT	Avg TEMP	0.0718E 01	0.0718E 01	0.0718E 01	TMELT
SOLID	1	1.0718E 00	1.0718E 02	1.0718E 02	1.0718E 02	1.0718E 02	0.0718E 01	0.0718E 01	0.0718E 01	HMELT
SSBL	2	1.0718E 00	1.0718E 02	1.0718E 02	1.0718E 02	1.0718E 02	0.0718E 01	0.0718E 01	0.0718E 01	
Node Data										
Node	Matl	Ntype	Radius	VOLUME	MASS	CAPACITY	CONDUCTIVITY	ZIP	SLIM	
1	1	1	0.0718E 001	0.0718E 001	0.0718E 001	0.0718E 001	0.0718E 001	0.0718E 001	0.0718E 001	
2	1	1	0.0718E 001	0.0718E 001	0.0718E 001	0.0718E 001	0.0718E 001	0.0718E 001	0.0718E 001	
3	1	1	0.0718E 001	0.0718E 001	0.0718E 001	0.0718E 001	0.0718E 001	0.0718E 001	0.0718E 001	
4	1	1	0.0718E 001	0.0718E 001	0.0718E 001	0.0718E 001	0.0718E 001	0.0718E 001	0.0718E 001	
5	1	1	0.0718E 001	0.0718E 001	0.0718E 001	0.0718E 001	0.0718E 001	0.0718E 001	0.0718E 001	
6	1	1	0.0718E 001	0.0718E 001	0.0718E 001	0.0718E 001	0.0718E 001	0.0718E 001	0.0718E 001	
7	1	1	0.0718E 001	0.0718E 001	0.0718E 001	0.0718E 001	0.0718E 001	0.0718E 001	0.0718E 001	
8	1	1	0.0718E 001	0.0718E 001	0.0718E 001	0.0718E 001	0.0718E 001	0.0718E 001	0.0718E 001	
9	1	1	0.0718E 001	0.0718E 001	0.0718E 001	0.0718E 001	0.0718E 001	0.0718E 001	0.0718E 001	
10	1	1	0.0718E 001	0.0718E 001	0.0718E 001	0.0718E 001	0.0718E 001	0.0718E 001	0.0718E 001	
11	1	1	0.0718E 001	0.0718E 001	0.0718E 001	0.0718E 001	0.0718E 001	0.0718E 001	0.0718E 001	
12	1	1	0.0718E 001	0.0718E 001	0.0718E 001	0.0718E 001	0.0718E 001	0.0718E 001	0.0718E 001	
INTERNAL CONNECTION DATA										
Node1	Node2	Area	HINT	RINT	TRAN	HEAT FLOW	AVG RATE			
1	2	0.1257E 001	0.1000E 13	0.0	0.6386D 05	-0.3383E 05	-0.3342E 05			
2	3	0.6283D 001	0.1000E 13	0.0	0.6386D 05	-0.3383E 05	-0.3342E 05			
3	4	0.6283D 002	0.1000E 13	0.0	0.6386D 05	-0.3383E 05	-0.3342E 05			
4	5	0.6283D 002	0.1000E 13	0.0	0.6386D 05	-0.3383E 05	-0.3342E 05			
5	6	0.6283D 002	0.1000E 13	0.0	0.6386D 05	-0.3383E 05	-0.3342E 05			
6	7	0.6283D 002	0.1000E 13	0.0	0.6386D 05	-0.3383E 05	-0.3342E 05			
7	8	0.6283D 002	0.1000E 13	0.0	0.6386D 05	-0.3383E 05	-0.3342E 05			
8	9	0.6283D 002	0.1000E 13	0.0	0.6386D 05	-0.3383E 05	-0.3342E 05			
9	10	0.6283D 002	0.1000E 13	0.0	0.6386D 05	-0.3383E 05	-0.3342E 05			
10	11	0.6283D 002	0.1000E 13	0.0	0.6386D 05	-0.3383E 05	-0.3342E 05			
11	12	0.6283D 002	0.1000E 13	0.0	0.6386D 05	-0.3383E 05	-0.3342E 05			
12	1	0.6283D 002	0.1000E 13	0.0	0.6386D 05	-0.3383E 05	-0.3342E 05			
BOUNDARY NODE DATA										
Node1	Node2	TempB	Heat Flow	Avg Rate						
2001	2001	1.2380E 02	-1.1533D 04	-1.392E 01						
System Total		-1.1533E 04	-1.1392E 01							
External Connection Data										
Nodes Nodsb Areas										
12	2001	5.6156D 01	1.0000E 06	0.0	RSURE	TRANS	HEAT FLOW	Avg Rate		

DATA DECK 1

* 4ISLE PROBLEM ONE DIMENSIONAL

PRINTOUT	CYCLE	TOO FAST	TOO SLOW	KW/H	DELTA X	SMALL	T-VARY	NUTS
10	120	0	0	1.06000E-12	1.00000E-00	0	0.0000E-00	
TOTAL TIME	1.34137E-03	-HEAT FLOW	TEMP FROM FLUX	FLUX RATE	TEMP RATE			
1.18976E-03	-1.25268E-04	-9.22865E-03	-1.05239E-01	-7.75573E-00				
Avg TEMP	1.1142BE-02	HEAT CAPACITY	HEAT CONTENT	GEN RATE	HEAT GEN			
1.114250E-02	1.25739D-00	1.51250E-02	0.0	0.0	0.0			
NODE	TEMP	DT	DDT	GE N RATE	H 1.587E-06	F 1.987E-35	CURE AT 280 F	
1	0.7912D-02	0.8219D-02	0.6128E-01	0.0	0.2095E-05	0.1542E-05		
2	0.7912D-02	0.8219D-02	0.6128E-01	0.0	0.2095E-05	0.1542E-05		
3	0.8003D-03	0.8399D-03	0.6215E-01	0.0	0.2144E-05	0.1573E-05		
4	0.8003D-03	0.8399D-03	0.6215E-01	0.0	0.2144E-05	0.1573E-05		
5	0.8064D-03	0.8464D-03	0.6274E-01	0.0	0.2172E-05	0.1601E-05		
6	0.8064D-03	0.8464D-03	0.6274E-01	0.0	0.2172E-05	0.1601E-05		
7	0.8150D-03	0.8549D-03	0.6333E-01	0.0	0.2201E-05	0.1629E-05		
8	0.8150D-03	0.8549D-03	0.6333E-01	0.0	0.2201E-05	0.1629E-05		
9	0.8207D-03	0.8603D-03	0.6392E-01	0.0	0.2229E-05	0.1657E-05		
10	0.8207D-03	0.8603D-03	0.6392E-01	0.0	0.2229E-05	0.1657E-05		
11	0.8250D-03	0.8658D-03	0.6451E-01	0.0	0.2258E-05	0.1685E-05		
12	0.8250D-03	0.8658D-03	0.6451E-01	0.0	0.2258E-05	0.1685E-05		
MATERIAL DATA	NAME	TOT CAP	TOT HEAT	Avg Temp	TMELT	HMET		
SAND	1	0.07359E-00	1.7114E-02	1.9114E-02	0.0	0.0		
STEEL	2	2.8356E-03	3.9193E-01	1.0130E-02	0.0	0.0		
AIR	3	1.4244E-03	1.8363E-01	1.9892E-02	0.0	0.0		
NODE DATA	NAME	RADUS	VOLUME	MASS	CAPACITY	CONDUCTIVITY	ZIP	SLIM
1	1	0.02000E-06	0.01702E-06	0.1599E-06	0.1470E-03	0.1050E-02	0.1910E-02	0.1910E-02
2	1	0.02000E-06	0.01702E-06	0.1599E-06	0.1470E-03	0.1050E-02	0.1910E-02	0.1910E-02
3	1	0.02000E-06	0.01702E-06	0.1599E-06	0.1470E-03	0.1050E-02	0.1910E-02	0.1910E-02
4	1	0.02000E-06	0.01702E-06	0.1599E-06	0.1470E-03	0.1050E-02	0.1910E-02	0.1910E-02
5	1	0.02000E-06	0.01702E-06	0.1599E-06	0.1470E-03	0.1050E-02	0.1910E-02	0.1910E-02
6	1	0.02000E-06	0.01702E-06	0.1599E-06	0.1470E-03	0.1050E-02	0.1910E-02	0.1910E-02
7	1	0.02000E-06	0.01702E-06	0.1599E-06	0.1470E-03	0.1050E-02	0.1910E-02	0.1910E-02
8	1	0.02000E-06	0.01702E-06	0.1599E-06	0.1470E-03	0.1050E-02	0.1910E-02	0.1910E-02
9	1	0.02000E-06	0.01702E-06	0.1599E-06	0.1470E-03	0.1050E-02	0.1910E-02	0.1910E-02
10	1	0.02000E-06	0.01702E-06	0.1599E-06	0.1470E-03	0.1050E-02	0.1910E-02	0.1910E-02
11	1	0.02000E-06	0.01702E-06	0.1599E-06	0.1470E-03	0.1050E-02	0.1910E-02	0.1910E-02
12	1	0.02000E-06	0.01702E-06	0.1599E-06	0.1470E-03	0.1050E-02	0.1910E-02	0.1910E-02
INTERNAL CONNECTION DATA	NO01	NO02	AREA	HINT	RINT	TRAN	HEAT FLOW	Avg RATE
1	1	0.1237E-01	0.1000E-13	0.0	0.0	0.696E-05	-1.162E-05	-0.1874E-02
2	1	0.0429E-02	0.1000E-13	0.0	0.0	0.1998E-05	-0.2229E-05	-0.374E-02
3	4	0.345E-02	0.1000E-13	0.0	0.0	0.589E-05	-0.7498E-05	-0.572E-02
4	5	0.67E-02	0.1000E-13	0.0	0.0	0.686E-05	-0.7819E-05	-0.572E-02
5	6	0.3142E-02	0.1000E-13	0.0	0.0	0.2495E-05	-0.1028E-05	-0.864E-02
6	7	0.3613D-02	0.1000E-13	0.0	0.0	0.1962E-05	-0.1035E-05	-0.864E-02
7	8	0.3771D-02	0.1000E-13	0.0	0.0	0.1630E-05	-0.1456E-05	-0.137E-02
8	9	0.4398E-02	0.1000E-13	0.0	0.0	0.9760E-05	-0.936E-05	-0.844E-02
9	10	0.5027E-02	0.1000E-13	0.0	0.0	0.1667E-05	-0.1040E-05	-0.1028E-01
10	11	0.5616D-02	0.1000E-13	0.0	0.0	0.2850E-05	-0.1050E-05	-0.894E-03
11	12	0.5616D-02	0.1000E-13	0.0	0.0	0.2850E-05	-0.1050E-05	-0.894E-03
BOUNDARY NODE DATA	NO0B	TEMPB	02	-1.1657E-04	Avg RATE			
2001	1.7929E-02	-1.2522E-04	-1.0519E-01					
SATEN TOTAL	-1.2522E-04	-1.0519E-01						
EXTERNAL CONNECTION DATA								
NO0S	NO0SB	AREAS	HSURE	POWER	RSURE	TRANS	HEAT FLOW	Avg RATE
12	2001	5.6156D-01	1.0300D-06	0.0	0.0	5.6150D-07	-1.2527E-04	-1.359E-01
WILL REPEAT CYCLE	130	DTMAX	3.720E-00	DPRE = 2.860E-00	DELT = 1.860E-03	SUMTH = 7.762D-01	SUMTH = 1.321E-03	

TRUMP OUTPUT DATA

* MISSLE PROBLEM ONE DIMENSIONAL

DATA DECK 1

```

***** PRINTOUT CYCLE TOO FAST TOO SLOW KWT DELTMAX SMALL TVALY NUTS
11 135 6 TIME STEP 0 1.0000E 12 1.0000E 00 1.0000E 00
TOTAL TIME 2.96298E 00 -1.1206E 04 TEMP FLOW FLUX RATE TEMP RATE
1.3361E 03 -8.25591E 03 -8.38547E 00 -6.1776E 00
AVG TEMP HEAT CAPACITY HEAT CONTENT GEN RATE HEAT GEN TEMP FROM GEN
1.1839E 02 1.35739D 00 1.6071E 02 0.0 0.0 0.0
***** NODE TEMP DT DDT GEN RATE H CURE AT 280 F
1 0.1085D 03 0.1825D 00 0.3808D 01 0.0 -0.665E -06
2 0.1085D 03 0.1825D 00 0.3807D 01 0.0 -0.200E -06
3 0.1097D 03 0.163D 00 0.3673D 01 0.0 -0.200E -06
4 0.1120D 03 0.163D 00 0.3354D 01 0.0 -0.158E -06
5 0.1152D 03 0.163D 00 0.2758D 01 0.0 -0.158E -06
6 0.1192D 03 0.163D 00 0.1671D 01 0.0 -0.132E -06
7 0.1224D 03 0.163D 00 0.1043D 01 0.0 -0.134E -06
8 0.1269D 03 0.163D 00 -0.1464D 01 0.0 -0.134E -06
9 0.1265D 03 0.163D 00 -0.1464D 01 0.0 -0.134E -06
10 0.1278D 03 0.163D 00 -0.1273D 00 0.0 -0.121E -0.3
11 0.1284D 03 0.163D 00 -0.1273D 00 0.0 -0.121E -0.3
12 0.1288D 03 0.163D 00 -0.1272D 00 0.0 -0.121E -0.3
***** MATERIAL DATA
NAME MATL TOT CAP AVG TEMP TMELT HMELT
SAND 1.07352E 00 1.1057E 02 1.1057E 02 0.0 0.0
STEEL 2.12336E 01 1.4246E 03 1.4246E 03 0.0 0.0
AIR 3.12328E 01 1.4246E 03 1.4246E 03 0.0 0.0
***** NODE DATA
NODE MATL NTYPE RADIUS VOLUME MASS CONDUCTIVITY ZIP SLIM
1 1 4 0.1000E -02 0.1252E -06 0.6336D -06 0.1247D -06 0.2700D -03 0.1914D -05
2 1 4 0.6192E -01 0.3109E -01 0.1977D -01 0.2700D -03 0.1913D -02
3 1 4 0.2150E -01 0.0914E -01 0.1624D -01 0.2700D -03 0.1914D -02
4 1 4 0.2150E -01 0.0914E -01 0.2273D -00 0.2700D -03 0.1914D -02
5 1 4 0.3502E -01 0.2821E -01 0.2292D -00 0.2700D -03 0.1914D -02
6 1 4 0.4537E -01 0.3524E -01 0.2661E -00 0.2700D -03 0.1914D -02
7 1 4 0.5875E -01 0.4242E -01 0.2842D -00 0.2700D -03 0.1914D -02
8 2 4 0.5875E -01 0.4242E -01 0.2842D -00 0.2700D -03 0.1914D -02
9 2 4 0.6502E -01 0.4718E -01 0.4242D -00 0.2700D -03 0.1914D -02
10 3 4 0.6502E -01 0.4718E -01 0.4242D -00 0.2700D -03 0.1914D -02
11 3 4 0.8469E -01 0.4939E -02 0.2555D -02 0.2250D -04 0.2150D -02
12 3 4 0.8938E -01 0.4939E -02 0.275D -02 0.2200D -03 0.2386D -02
***** INTERNAL CONNECTION DATA
NODE1 NODE2 AREA HINT RINT HEAT FLOW AVG RATE
1 2 0.1257D -01 0.1000E 13 0.0 0.6786D -05
2 3 0.6283D 01 0.1000E 13 0.0 0.6786D -05
3 4 0.1255D 02 0.1000E 13 0.0 0.6786D -05
4 5 0.1885D 02 0.1000E 13 0.0 0.6786D -05
5 6 0.2514D 02 0.1000E 13 0.0 0.6786D -05
6 7 0.3142D 02 0.1000E 13 0.0 0.6786D -05
7 8 0.3710D 02 0.1000E 13 0.0 0.6786D -05
8 9 0.4329D 02 0.1000E 13 0.0 0.6786D -05
9 10 0.5020D 02 0.1000E 13 0.0 0.6786D -05
10 11 0.5616D 02 0.1000E 13 0.0 0.6786D -05
11 12 0.5616D 02 0.1000E 13 0.0 0.6786D -05
***** BOUNDARY NODE DATA
NODE TEMP HEAT FLOW AVG RATE
2001 1.2832E 02 -1.1207E 04 -8.3856E 00
SYSTEM TOTAL -1.1207E 04 -8.3856E 00
EXTERNAL CONNECTION DATA
NODS NODSB AREAS HSURE POWER RSURE TRANS HEAT FLOW AVG RATE
12 2001 5.6160 01 1.0000 0.6 0.0 5.6160 07 -1.206E 04 -8.3855E 00
*****
```

TRUMP OUTPUT DATA

* MISSLE PROBLEM ONE DIMENSIONAL

```

DATA DECK 1

PRINTOUT CYCLE TOO FAST TOO SLOW KWHIT DELTHX SMAWT TIVARY NUTS 4
12 150 0 1.00000E 12 1.00000E 00 1.00000E 00
TOTAL TIME TIME STEP HEAT FLOW TEMP FROM FLUX FLUX RATE TEMP RATE
1.39691E 03 4.16738E 00 3.74844E 03 2.75152E 03 2.68338E 00 1.97688E 00
AVG TEMP HEAT CAPACITY HEAT CONTENT GEN RATE HEAT GEN TEMP FROM GEN
1.18103E 02 1.35739D 00 1.63011E 02 0.0 0.0 0.0
*****
```

NODE	TEMP	DT	DOT	GEN RATE	H	CURE AT -65 F
1	0.1200 03	0.1420 03	0.51400-01	0.0	0.1454E 04	-0.4205E-06
2	0.1293 03	0.1420 03	0.51400-01	0.0	0.1636E 01	-0.3208E-06
3	0.1392 03	0.1420 03	0.51400-01	0.0	0.1802E 01	0.0
4	0.1490 03	0.1420 03	0.51400-01	0.0	0.1967E 01	-0.3208E-06
5	0.1587 03	0.1420 03	0.51400-01	0.0	0.2124E 01	0.0
6	0.1684 03	0.1420 03	0.51400-01	0.0	0.2279E 01	-0.3208E-06
7	0.1780 03	0.1420 03	0.51400-01	0.0	0.2435E 01	0.0
8	0.1876 03	0.1420 03	0.51400-01	0.0	0.2590E 01	-0.3208E-06
9	0.1971 03	0.1420 03	0.51400-01	0.0	0.2745E 01	0.0
10	0.2066 03	0.1420 03	0.51400-01	0.0	0.2899E 01	-0.3208E-06
11	0.2160 03	0.1420 03	0.51400-01	0.0	0.3054E 01	0.0
12	0.2253 03	0.1420 03	0.51400-01	0.0	0.3209E 01	-0.3208E-06

***** MATERIAL DATA *****

NAME	MATL	TOT CAP	TOT HEAT	Avg TEMP	MELT
SAND	1	1.0732E 00	1.2625E 02	1.1702E 02	0.0
STEEL	2	2.8224E-03	3.2892E 01	1.2092E 01	0.0
AlTiC	3	1.4421E-03	1.5813E 01	1.2092E 01	0.0

***** NODE DATA *****

NODE	MATL	NTYPE	RADIUS	VOLUME	MASS	CONDUCTIVITY	CONDUCTIVITY	ZIP	SIM
1	3	1000E-22	0.257E-04	0.6836D-06	0.1299D-06	0.2700D-03	0.686D-05	0.114D-01	
2	3	5000E-01	0.325E-01	0.1709D-00	0.9741D-01	0.2700D-03	0.501D-02	0.913D-02	
3	3	10000E-01	0.395E-01	0.8545D-00	0.1622D-00	0.2700D-03	0.882D-02	0.1914D-02	
4	3	30000E-01	0.457E-01	0.1966D-00	0.2227D-00	0.2700D-03	0.188D-01	0.1914D-02	
5	3	100000E-01	0.529E-01	0.2297E-00	0.1538D-01	0.2700D-03	0.168D-01	0.1914D-02	
6	3	300000E-01	0.592E-01	0.2333E-00	0.1378D-01	0.2700D-03	0.154D-01	0.1914D-02	
7	3	1000000E-01	0.655E-01	0.238E-00	0.2590D-01	0.2700D-03	0.144D-01	0.1914D-02	
8	3	3000000E-01	0.718E-01	0.244E-00	0.1781D-02	0.2700D-03	0.134D-01	0.1914D-02	
9	3	10000000E-01	0.782E-01	0.249E-00	0.2055D-02	0.2700D-03	0.124D-01	0.1914D-02	
10	3	30000000E-01	0.845E-01	0.255E-00	0.1750D-02	0.2700D-03	0.114D-01	0.1914D-02	
11	3	100000000E-01	0.909E-01	0.260E-00	0.2055D-02	0.2700D-03	0.104D-01	0.1914D-02	
12	3	300000000E-01	0.973E-01	0.265E-00	0.1750D-02	0.2700D-03	0.94D-01	0.1914D-02	

***** INTERNAL CONNECTION DATA *****

NOOL	NOOD	AREA	HINT	RINT	TRAN	HEAT FLOW	AVG RATE
1	2	0.457D-01	0.0000E 13	0.0000E 13	0.6786D-15	0.0000E 00	0.0000E 00
2	3	0.6283D-01	0.0000E 13	0.0000E 13	0.6786D-15	0.0000E 00	0.0000E 00
3	4	0.457D-01	0.0000E 13	0.0000E 13	0.6786D-15	0.0000E 00	0.0000E 00
4	5	0.6283D-01	0.0000E 13	0.0000E 13	0.6786D-15	0.0000E 00	0.0000E 00
5	6	0.457D-01	0.0000E 13	0.0000E 13	0.6786D-15	0.0000E 00	0.0000E 00
6	7	0.6283D-01	0.0000E 13	0.0000E 13	0.6786D-15	0.0000E 00	0.0000E 00
7	8	0.457D-01	0.0000E 13	0.0000E 13	0.6786D-15	0.0000E 00	0.0000E 00
8	9	0.6283D-01	0.0000E 13	0.0000E 13	0.6786D-15	0.0000E 00	0.0000E 00
9	10	0.457D-01	0.0000E 13	0.0000E 13	0.6786D-15	0.0000E 00	0.0000E 00
10	11	0.6283D-01	0.0000E 13	0.0000E 13	0.6786D-15	0.0000E 00	0.0000E 00
11	12	0.457D-01	0.0000E 13	0.0000E 13	0.6786D-15	0.0000E 00	0.0000E 00

***** BOUNDARY NODE DATA *****

NOOD	TEMPB	HEAT FLOW	AVG RATE
2001	1.1382E 02	3.7483E 03	2.6833E 00

***** SYSTEM TOTAL *****

SYSTEM TOTAL	3.7483E 03	2.6833E 00
--------------	------------	------------

***** EXTERNAL CONNECTION DATA *****

NOOSB	NOOD	AREAS	HSURE	POWER	R.SURE	TRANS	HEAT FLOW	AVG RATE
12	2001	5.6156D 01	1.0320D 06	0.0	0.0	5.156D 07	3.7484E 03	2.6834E 00

TRUMP OUTPUT DATA

* MISSLE PROBLEM ONE DIMENSIONAL

DATA DECK 1

PRINTOUT	CYCLE	T00 FAST	T00 SLOW	KWIT	DELTMX	SMALL	TVARY
13	161	0	0	1.30000E 12	1.00000E 03	1.00000E 00	NUTS 2
TOTAL TIME	TIME STEP	HEAT FLOW	TEMP FROM FLUX	FLUX RATE	TEMP RATE		
1.44030E 03	1.37476E 00	3.93701E 03	2.0044E 03	2.73404E 00	2.0419E 03		
Avg TEMP	HEAT CAPACITY	TEMP GEN	GEN RATE	HEAT GEN	TEMP FROM GEN		
1.16574E 02	1.35739E 00	1.8236E 02	0.0	0.0	0.0		

NODE	TEMP	DT	GE N RATE	H	14795E-04	F	CURE AT 28J F
1	0.1390 03	0.52200E-01	0.13170E-01	0.16703E-06	-0.7515E-07	0.0	0.0
2	0.1390 03	0.52200E-01	0.13170E-01	0.16703E-06	-0.7515E-07	0.0	0.0
3	0.11460 03	0.42440E-01	0.11780E-01	0.18310E-06	-0.7515E-07	0.0	0.0
4	0.11590 03	0.42440E-01	0.11780E-01	0.18310E-06	-0.7515E-07	0.0	0.0
5	0.11720 03	0.42440E-01	0.11780E-01	0.18310E-06	-0.7515E-07	0.0	0.0
6	0.11760 03	0.42440E-01	0.11780E-01	0.18310E-06	-0.7515E-07	0.0	0.0
7	0.11780 03	0.42440E-01	0.11780E-01	0.18310E-06	-0.7515E-07	0.0	0.0
8	0.11800 03	0.42440E-01	0.11780E-01	0.18310E-06	-0.7515E-07	0.0	0.0
9	0.11820 03	0.42440E-01	0.11780E-01	0.18310E-06	-0.7515E-07	0.0	0.0
10	0.11840 03	0.42440E-01	0.11780E-01	0.18310E-06	-0.7515E-07	0.0	0.0
11	0.11860 03	0.42440E-01	0.11780E-01	0.18310E-06	-0.7515E-07	0.0	0.0
12	0.11880 03	0.42440E-01	0.11780E-01	0.18310E-06	-0.7515E-07	0.0	0.0

MATERIAL DATA									
NAME	MATL	TOT CAP	TOT HEAT	Avg TEMP	THELT	HHELT			
SAND	1	1.03539E 03	1.26380E 02	1.1696E 02	0.0	0.0			
STEL	2	1.03556E 03	1.26380E 02	1.1569E 02	0.0	0.0			
ARM	3	1.03424E 03	1.26380E 02	1.0855E 02	0.0	0.0			

NODE DATA									
NODE	MATL	NTYPE	RADIUS	VOLUME	MASS	CONDUCTIVITY	SL1W		
1	1	1	0.10000E-02	0.1254E-04	0.6336E-06	0.1295E-06	0.1865E-05		
2	1	1	0.50100E-02	0.3124E-04	0.3192E-06	0.3444E-06	0.3050E-05		
3	1	1	0.15000E-02	0.9374E-04	0.9592E-06	0.9946E-06	0.9500E-05		
4	1	1	0.25000E-02	0.1562E-04	0.1596E-06	0.1749E-06	0.1744E-05		
5	1	1	0.35000E-02	0.2291E-04	0.2296E-06	0.2363E-06	0.2350E-05		
6	1	1	0.45000E-02	0.3019E-04	0.3019E-06	0.3472E-06	0.3450E-05		
7	1	1	0.55000E-02	0.3747E-04	0.3747E-06	0.3722E-06	0.3700E-05		
8	1	1	0.65000E-02	0.4475E-04	0.4475E-06	0.4475E-06	0.4450E-05		
9	1	1	0.75000E-02	0.5203E-04	0.5203E-06	0.5203E-06	0.5160E-05		
10	1	1	0.85000E-02	0.5931E-04	0.5931E-06	0.5931E-06	0.5120E-05		
11	1	1	0.95000E-02	0.6659E-04	0.6659E-06	0.6659E-06	0.5080E-05		
12	1	1	0.10500E-02	0.7387E-04	0.7387E-06	0.7387E-06	0.5040E-05		

INTERNAL CONNECTION DATA									
NGD1	NGD2	AREA	HINT	RINT	TRAN	HEAT FLOW	AVG RATE		
1	2	0.128570E-01	0.10000E 13	0.0	0.6784E-05	-0.6784E-07	-0.3050E-04		
2	3	0.128570E-01	0.10000E 13	0.0	0.1698E-02	-0.4255E-01	-0.9550E-03		
3	4	0.128570E-01	0.10000E 13	0.0	0.3393E-02	-0.1750E-01	-0.1944E-03		
4	5	0.128570E-01	0.10000E 13	0.0	0.5089E-02	-0.3770E-01	-0.7530E-03		
5	6	0.128570E-01	0.10000E 13	0.0	0.6784E-02	-0.5769E-01	-0.6930E-03		
6	7	0.128570E-01	0.10000E 13	0.0	0.8479E-02	-0.7768E-01	-0.6910E-03		
7	8	0.128570E-01	0.10000E 13	0.0	0.10174E-02	-0.9767E-01	-0.6924E-03		
8	9	0.128570E-01	0.10000E 13	0.0	0.11863E-02	-0.11766E-01	-0.6934E-03		
9	10	0.128570E-01	0.10000E 13	0.0	0.13552E-02	-0.13755E-01	-0.6942E-03		
10	11	0.128570E-01	0.10000E 13	0.0	0.15241E-02	-0.15744E-01	-0.6950E-03		
11	12	0.128570E-01	0.10000E 13	0.0	0.16930E-02	-0.17733E-01	-0.6958E-03		

BOUNDARY NODE DATA									
NODE	TEMPB	HEAT FLOW	AVG RATE						
2001	1.0350E 02	3.939E 03	2.7339E 00						

SYSTEM TOTAL									
EXTERNAL CONNECTION DATA									
NODES	NOSES	AREAS	HSURE	POWER	RSURE	TRANS	HEAT FLOW	AVG RATE	
12	2001	5.6150 01	1.0000 06	0.0	0.0	5.6156 07	3.9370E 03	2.7340E 00	

INTERNAL CONNECTION DATA										
INTERNAL CONNECTION DATA										
TOTAL NUMBER OF ITERATIONS = 1102										
MAX KWT = 1.611, MAX CYC = 1.611, MAX UNTIM = 0.1400E 04, CMAX = 0.0000000000000000										
ENDED PROB. 1										
UNITED PROB. 1										

```

//WIR71687 JOB (1687,0860FT,NF12),'WIRZBURGER.A.' BOX W*,TIME=(4,00)
//JQBLIB DD UNIT=2321,DSNAME='S1734.KATZ'
//DISP=(OLD,PASS) *VOLUME='SER=CEL001'
//EXEC PGM=TRUNP,REGION=350K
//FT06F001 SYSDIN=SYSPRINT
//SPACE=(CYL,(6,1))
//FT05F021 DD

```

MISSI E PROBLEMI TWO DIMENSIONALI

BLOCK 1 CONTROLS, LIMITS, CONSTANTS
5 1 1.000 E 00 1.000E
2 3

114.0	BLOCK 2 ASLAND ASTEL AAIR	MATERIAL NAMES,	NUMBERS, 0.0544 0.2807 0.0000436	THERMAL PROPERTIES. 0.19 0.109 0.240	0.00027 0.0364 0.0000225
	1				
	2				
	3				

MISSLE PROBLEM TWO DIMENSIONAL
 INPUT UNIT = 5. OUTPUT UNIT = 6.
 CONTROLS, LIMITS, CONSTANTS
 DATA BLOCK 10

IPRINT	NUM	KDATA	KSPEC	MCYC	MSEC	NPUNCH	NODT	IRITE	SCALE	
20	0	30000	30000	0	0	0	0	0	0.1000E 01	
K2	KT	3	1.0E10	12	1.0000E 03	1.0000E 00	0.1AU	1.4400E 03	1.0000E 12	
K0	KSYM		SIGMA		TBASE			TMAX	1.0000E 12	
K2	KSYM	1	6.28319D 00	1.73000E-09	4.6600E 02			TMIN		
TONE	ALONE		8.0NE	0.0	0.0	GONE	GONE	RONE	PONE	
1.0400E 02	0.0								0.0	
DATA BLOCK 20	MATERIAL NAMES, NUMBERS, THE MATERIAL PROPERTIES.									
NAME	MATL	INDEX	KA	KB	LTABC	LTABK	DENSITY	CAPACITY	CONDUCTIVITY	THELT
SAND	1	1	0	0	0	0	5.400E-02	1.9000E-01	2.7000E-04	0.0
STYL	2	2	0	0	0	0	2.800E-02	1.9000E-01	2.6400E-04	0.0
AIR	3	3	0	0	0	0	4.6600E-01	2.6400E-01	2.2500E-05	0.0
DATA BLOCK 40	NODE NUMBERS, MATERIAL REFERENCES, TYPES, VOLUMES.									
1	1	1	0	0	0	0	0.000000E+00	0.000000E+00	0.000000E+00	0.000000E+00
2	2	2	0	0	0	0	0.000000E+00	0.000000E+00	0.000000E+00	0.000000E+00
3	3	3	0	0	0	0	0.000000E+00	0.000000E+00	0.000000E+00	0.000000E+00
4	4	4	0	0	0	0	0.000000E+00	0.000000E+00	0.000000E+00	0.000000E+00
5	5	5	0	0	0	0	0.000000E+00	0.000000E+00	0.000000E+00	0.000000E+00
6	6	6	0	0	0	0	0.000000E+00	0.000000E+00	0.000000E+00	0.000000E+00
7	7	7	0	0	0	0	0.000000E+00	0.000000E+00	0.000000E+00	0.000000E+00
8	8	8	0	0	0	0	0.000000E+00	0.000000E+00	0.000000E+00	0.000000E+00
9	9	9	0	0	0	0	0.000000E+00	0.000000E+00	0.000000E+00	0.000000E+00
10	10	10	0	0	0	0	0.000000E+00	0.000000E+00	0.000000E+00	0.000000E+00
11	11	11	0	0	0	0	0.000000E+00	0.000000E+00	0.000000E+00	0.000000E+00
12	12	12	0	0	0	0	0.000000E+00	0.000000E+00	0.000000E+00	0.000000E+00
13	13	13	0	0	0	0	0.000000E+00	0.000000E+00	0.000000E+00	0.000000E+00
14	14	14	0	0	0	0	0.000000E+00	0.000000E+00	0.000000E+00	0.000000E+00
15	15	15	0	0	0	0	0.000000E+00	0.000000E+00	0.000000E+00	0.000000E+00
16	16	16	0	0	0	0	0.000000E+00	0.000000E+00	0.000000E+00	0.000000E+00
17	17	17	0	0	0	0	0.000000E+00	0.000000E+00	0.000000E+00	0.000000E+00
18	18	18	0	0	0	0	0.000000E+00	0.000000E+00	0.000000E+00	0.000000E+00
19	19	19	0	0	0	0	0.000000E+00	0.000000E+00	0.000000E+00	0.000000E+00
20	20	20	0	0	0	0	0.000000E+00	0.000000E+00	0.000000E+00	0.000000E+00
21	21	21	0	0	0	0	0.000000E+00	0.000000E+00	0.000000E+00	0.000000E+00
22	22	22	0	0	0	0	0.000000E+00	0.000000E+00	0.000000E+00	0.000000E+00
23	23	23	0	0	0	0	0.000000E+00	0.000000E+00	0.000000E+00	0.000000E+00
24	24	24	0	0	0	0	0.000000E+00	0.000000E+00	0.000000E+00	0.000000E+00
25	25	25	0	0	0	0	0.000000E+00	0.000000E+00	0.000000E+00	0.000000E+00
26	26	26	0	0	0	0	0.000000E+00	0.000000E+00	0.000000E+00	0.000000E+00
27	27	27	0	0	0	0	0.000000E+00	0.000000E+00	0.000000E+00	0.000000E+00
28	28	28	0	0	0	0	0.000000E+00	0.000000E+00	0.000000E+00	0.000000E+00
29	29	29	0	0	0	0	0.000000E+00	0.000000E+00	0.000000E+00	0.000000E+00
30	30	30	0	0	0	0	0.000000E+00	0.000000E+00	0.000000E+00	0.000000E+00
31	31	31	0	0	0	0	0.000000E+00	0.000000E+00	0.000000E+00	0.000000E+00
32	32	32	0	0	0	0	0.000000E+00	0.000000E+00	0.000000E+00	0.000000E+00
33	33	33	0	0	0	0	0.000000E+00	0.000000E+00	0.000000E+00	0.000000E+00
34	34	34	0	0	0	0	0.000000E+00	0.000000E+00	0.000000E+00	0.000000E+00
35	35	35	0	0	0	0	0.000000E+00	0.000000E+00	0.000000E+00	0.000000E+00
36	36	36	0	0	0	0	0.000000E+00	0.000000E+00	0.000000E+00	0.000000E+00
37	37	37	0	0	0	0	0.000000E+00	0.000000E+00	0.000000E+00	0.000000E+00
38	38	38	0	0	0	0	0.000000E+00	0.000000E+00	0.000000E+00	0.000000E+00
39	39	39	0	0	0	0	0.000000E+00	0.000000E+00	0.000000E+00	0.000000E+00
40	40	40	0	0	0	0	0.000000E+00	0.000000E+00	0.000000E+00	0.000000E+00
41	41	41	0	0	0	0	0.000000E+00	0.000000E+00	0.000000E+00	0.000000E+00
42	42	42	0	0	0	0	0.000000E+00	0.000000E+00	0.000000E+00	0.000000E+00
43	43	43	0	0	0	0	0.000000E+00	0.000000E+00	0.000000E+00	0.000000E+00
44	44	44	0	0	0	0	0.000000E+00	0.000000E+00	0.000000E+00	0.000000E+00
45	45	45	0	0	0	0	0.000000E+00	0.000000E+00	0.000000E+00	0.000000E+00
46	46	46	0	0	0	0	0.000000E+00	0.000000E+00	0.000000E+00	0.000000E+00
47	47	47	0	0	0	0	0.000000E+00	0.000000E+00	0.000000E+00	0.000000E+00
48	48	48	0	0	0	0	0.000000E+00	0.000000E+00	0.000000E+00	0.000000E+00

INTERNAL THERMAL CONNECTION NODE NUMBERS.

DATA BLOCK 73

BOUNDARY TEMPERATURE VARIATION.

NODE	INDEX	LTABT	TEMPB	SLOPE	TIMLB
2001	1	12	8.400000E+01 7.900000E+01 7.100000E+01 6.400000E+01 8.400000E+01 1.200000E+02 1.460000E+02 1.540000E+02 1.510000E+02 9.900000E+01	-4.166666E-02 -5.833333E-02 -8.333333E-02 -5.833333E-02 -1.666666E-02 -3.083333E-01 2.386666E-01 6.666666E-02 -2.500000E-02 -1.666666E-01	1.200000E+02 2.400000E+02 3.600000E+02 4.800000E+02 6.000000E+02 7.200000E+02 8.400000E+02 9.600000E+02 1.080000E+03 1.200000E+03 1.320000E+03 1.440000E+03
2002	2	12	8.700000E+01 7.700000E+01 6.700000E+01 9.600000E+01 1.130000E+02 1.152000E+02 1.147000E+02 1.030000E+02	-4.166666E-02 -4.166666E-02 -5.000000E-02 -8.333333E-02 -1.466667E-01 -1.666666E-01 -1.583333E-01 -4.166666E-01	1.200000E+02 2.400000E+02 3.600000E+02 4.800000E+02 6.000000E+02 7.200000E+02 8.400000E+02 9.600000E+02 1.080000E+03 1.200000E+03 1.320000E+03 1.440000E+03
2003	3	12	9.100000E+01 8.300000E+01 7.900000E+01 8.400000E+01 9.800000E+01 1.060000E+02 1.180000E+02 1.210000E+02 1.030000E+02	-3.333333E-02 -3.333333E-02 -5.000000E-02 -9.166664E-02 -1.166666E-01 -6.666666E-02 -4.166666E-02 -2.500000E-02 -1.500000E-01	1.200000E+02 2.400000E+02 3.600000E+02 4.800000E+02 6.000000E+02 7.200000E+02 8.400000E+02 9.600000E+02 1.080000E+03 1.200000E+03 1.320000E+03 1.440000E+03
2004	4	12	9.600000E+01 9.000000E+01 8.100000E+01 7.400000E+01 1.000000E+02 1.110000E+02 1.210000E+02 1.300000E+02 1.090000E+02	-5.000000E-02 -4.166666E-02 -3.333333E-02 -7.499999E-02 -1.333333E-01 -9.166664E-02 -1.666666E-02 -7.499999E-02 -8.333333E-03 -1.750000E-01	1.200000E+02 2.400000E+02 3.600000E+02 4.800000E+02 6.000000E+02 7.200000E+02 8.400000E+02 9.600000E+02 1.080000E+03 1.200000E+03 1.320000E+03 1.440000E+03

===== DATA ENDED -10 ===== LAST CARD OF DATA DECK =====

TRUMP OUTPUT DATA

* MISSLE PROBLEM TWO DIMENSIONAL

DATA DECK 1

PRINTOUT	CYCLE	TG ₀	FAST	TOO SLOW	KWIT	DELTMX	SMALL	TVARY	NUTS
1	0	0	0	0	0	3.13978E-05	3.13977E-05	1.00300E 00	0
TOTAL TIME	TIME STEP	HEAT FLOW	TEMP FROM FLUX	FLUX RATE	TEMP RATE				
1.00000E-12	1.00000E-12	4.29983E-14	3.16773E-14	4.29984E-02	3.16773E-02				
Avg TEMP	HEAT CAPACITY	HEAT CONTENT	GEN RATE	HEAT GEN	TEMP FROM GEN				
1.14000E 02	1.35739E 00	1.5472E 02	0.0	0.0	0.0				
=====	=====	=====	=====	=====	=====	=====	=====	=====	=====
NODE	TEMP	DT	DDT	GE N RATE	F				
1	0.11400	0.3	0.0	0.0	H				
13	0.11400	0.3	0.0	0.0	0.0				
25	0.11400	0.3	0.0	0.0	0.0				
37	0.11400	0.3	0.0	0.0	0.0				
2	0.11400	0.3	0.0	0.0	0.0				
146	0.11400	0.3	0.0	0.0	0.0				
38	0.11400	0.3	0.0	0.0	0.0				
3	0.11400	0.3	0.0	0.0	0.0				
157	0.11400	0.3	0.0	0.0	0.0				
27	0.11400	0.3	0.0	0.0	0.0				
39	0.11400	0.3	0.0	0.0	0.0				
168	0.11400	0.3	0.0	0.0	0.0				
405	0.11400	0.3	0.0	0.0	0.0				
17	0.11400	0.3	0.0	0.0	0.0				
29	0.11400	0.3	0.0	0.0	0.0				
41	0.11400	0.3	0.0	0.0	0.0				
18	0.11400	0.3	0.0	0.0	0.0				
30	0.11400	0.3	0.0	0.0	0.0				
42	0.11400	0.3	0.0	0.0	0.0				
19	0.11400	0.3	0.0	0.0	0.0				
31	0.11400	0.3	0.0	0.0	0.0				
34	0.11400	0.3	0.0	0.0	0.0				
38	0.11400	0.3	0.0	0.0	0.0				
20	0.11400	0.3	0.0	0.0	0.0				
32	0.11400	0.3	0.0	0.0	0.0				
44	0.11400	0.3	0.0	0.0	0.0				
9	0.11400	0.3	0.0	0.0	0.0				
21	0.11400	0.3	0.0	0.0	0.0				
33	0.11400	0.3	0.0	0.0	0.0				
45	0.11400	0.3	0.0	0.0	0.0				
10	0.11400	0.3	0.0	0.0	0.0				
34	0.11400	0.3	0.0	0.0	0.0				
46	0.11400	0.3	0.0	0.0	0.0				
11	0.11400	0.3	0.0	0.0	0.0				
33	0.11400	0.3	0.0	0.0	0.0				
35	0.11400	0.3	0.0	0.0	0.0				
47	0.11400	0.3	0.0	0.0	0.0				
NODE	TEMP	DT	DDT	GE N RATE	F				
12	0.89000	0.2	-0.25000	0.2	H				
24	0.92000	0.2	-0.22000	0.2	0.7649E-23	0.6126E-13	0.0	0.0	0.0
36	0.95000	0.2	-0.19000	0.2	0.6732E-23	0.5314E-13	0.0	0.0	0.0
48	0.10200	0.3	-0.12000	0.2	0.5832E-24	0.4655E-13	0.0	0.0	0.0
=====	=====	=====	=====	=====	=====	=====	=====	=====	=====
MATERIAL DATA									
NAME	MATL	TOT CAP	AVG TEMP	TMELT	HMETL				
1	1.0359E 00	1.2238E 02	1.1400E 02	0.0	0.0				
2	2.8236E-01	3.2488E-01	1.1400E 02	0.0	0.0				
3	1.4446E-03	1.6444E-01	1.1400E 02	0.0	0.0				
=====	=====	=====	=====	=====	=====	=====	=====	=====	=====
CURE AT 280 F									

TRUMP OUTPUT DATA TWO DIMENSIONAL

DATA DECK 1

PRINTOUT	CYCLE	TOO FAST	TOO SLOW	KW/H	DELTIMX	SMALL	TVARY	NUTS
3	20	11	0	1.08086E 01	1.00000E 00	1.00000E 00	1.00000E 00	12
TOTAL TIME	TIME STEP	HEAT FLOW	TEMP FROM	FLUX	FLUX RATE	TEMP RATE		
2.48340E 01	4.86662E 00	2.52999E 03	1.86387E 03	1.01876E 02	7.50532E 01			
Avg TEMP	HEAT CAPACITY	HEAT CONTENT	GEN RATE	HEAT GEN	TEMP FROM GEN			
1.12415E 02	1.35739E 00	1.52952E 02	0.0	0.0	0.0			

CURE AT 280 F
H 377655-113 -0 H 377225-05 -0

MATERIAL DATA				TOT CAP	TOT HEAT	Avg Temp	T MELT	H MELT
NAME	WT L	1	2					
SAND	1	1-039E+00	1-215E+02			1-317E+02	0-3	0-0
STEEL	2	2-823E+00	3-094E+01			1-195E+02	0-0	0-0

TRUMP OUTPUT CAT A

INTRODUCING THE NEW DIMENSIONS GUIDE

DATA DECK 1

TRUMP OUTPUT DATA
* MISSLE PROBLEM TWO DIMENSIONAL

DATA DECK 1

PRINOUT	CYCLE	100 FAST	100 SLOW	KWIT	DELTHX	SMALL	TWAVY	NUTS
5	60	11	0	0	1.00000E 12	1.00000E 00	1.00000E 00	NUTS
TOTAL TIME	TIME STEP	HEAT FLOW	TEMP FROM FLUX	FLUX RATE	TEMP RATE			
6.11440E 02	2.49350E 00	3.96811E 03	2.92335E 03	6.48977E 00	4.78108E 00			
Avg TEMP	HEAT CAPACITY	HEAT CONTENT	GEN RATE	HEAT GEN	TEMP FROM GEN			
8.72991E 01	1.35739E 00	1.18498E 02	0.0	0.0	0.0			
NODE	TEMP	DT	DT	GE N RATE	H	CURE AT 280 F		
1	0.93650	02	0.61850	-0.2	0.3041E -05	F		
13	0.93650	02	0.61850	-0.2	0.3041E -05			
25	0.94550	02	0.61850	-0.2	0.6085E -05			
37	0.94490	02	0.61850	-0.2	0.6085E -05			
14	0.94490	02	0.61850	-0.2	0.6085E -05			
26	0.93650	02	0.61850	-0.2	0.6085E -05			
38	0.93650	02	0.61850	-0.2	0.6085E -05			
15	0.94440	02	0.61850	-0.2	0.6085E -05			
39	0.94440	02	0.61850	-0.2	0.6085E -05			
16	0.93650	02	0.61850	-0.2	0.6085E -05			
28	0.93650	02	0.61850	-0.2	0.6085E -05			
40	0.93650	02	0.61850	-0.2	0.6085E -05			
45	0.93650	02	0.61850	-0.2	0.6085E -05			
17	0.91280	02	0.61850	-0.2	0.6085E -05			
29	0.91280	02	0.61850	-0.2	0.6085E -05			
41	0.85690	02	0.61850	-0.2	0.6085E -05			
18	0.85690	02	0.61850	-0.2	0.6085E -05			
30	0.85690	02	0.61850	-0.2	0.6085E -05			
42	0.88240	02	0.61850	-0.2	0.6085E -05			
19	0.88240	02	0.61850	-0.2	0.6085E -05			
43	0.85460	02	0.61850	-0.2	0.6085E -05			
48	0.80430	02	0.61850	-0.2	0.6085E -05			
20	0.81020	02	0.61850	-0.2	0.6085E -05			
32	0.83580	02	0.61850	-0.2	0.6085E -05			
44	0.83580	02	0.61850	-0.2	0.6085E -05			
21	0.78310	02	0.61850	-0.2	0.6085E -05			
46	0.78310	02	0.61850	-0.2	0.6085E -05			
19	0.78310	02	0.61850	-0.2	0.6085E -05			
47	0.76770	02	0.61850	-0.2	0.6085E -05			
NODE	TEMP	DT	DT	GE N RATE	H	CURE AT 280 F		
12	0.65480	02	0.63780	0.0	0.13190E -24	F		
24	0.67740	02	0.31800	0.0	0.65930E -25			
36	0.73810	02	0.35000	0.0	0.72520E -25			
48	0.75660	02	0.28700	0.0	0.59340E -25			
MATERIAL DATA	NAME	MATL	TOT CAP	TOT HEAT	TWELT	HMETLT		
	NAME	1	1.07359E 00	9.51664E 01	3.0	0.0		
	SAND	2	2.82356E 01	2.23524E 01	0.0	0.0		
	STEEL	3	2.44246E -13	1.59248E 01	0.123E -23	0.128E 04		
	AIR							

TRUMP OUTPUT DATA

* MISSLE PROBLEM TWO DIMENSIONAL

PRINTOUT	CYCLE	TOT. FAST	TOD SLOW	KW/T	DELT MX	12	SMALL	TVARY	NUTS
6	80	11	0	1.0000E 00	1.0000E 00	1.0000E 00	1.0000E 00	1.0000E 00	00
TOTAL TIME	TIME STEP	5.98896E 00	-2.17842E 04	TEMP FROM FLCH	FLUX RATE				
7.17775E 02				-1.60488E 04	-3.03498E 01				
AVG TEMP	HEAT CAPACITY	HEAT CONTENT	HEAT GEN	GEN RATE	TEMP FROM GEN				
8.53896E 01	1.35739E 00	1.1590E 02	0.0	0.0	0.0				
NODE	TEMP	DT	DDT	GEN RATE					
13	92170.02	0.31090.00	-0.51750.01	0.0					
237	92370.02	-0.31090.00	-0.51750.01	0.0					
32	1470.02	0.31090.00	-0.51750.01	0.0					
38	1260.02	0.31090.00	-0.51750.01	0.0					
157	1260.02	0.31090.00	-0.51750.01	0.0					
39	1280.02	0.31090.00	-0.51750.01	0.0					
46	1280.02	0.31090.00	-0.51750.01	0.0					
179	1280.02	0.31090.00	-0.51750.01	0.0					
405	1280.02	0.31090.00	-0.51750.01	0.0					
179	1302.41	0.31090.00	-0.51750.01	0.0					
43	1302.41	0.31090.00	-0.51750.01	0.0					
8	1302.41	0.31090.00	-0.51750.01	0.0					
20	1302.41	0.31090.00	-0.51750.01	0.0					
32	1302.41	0.31090.00	-0.51750.01	0.0					
44	1302.41	0.31090.00	-0.51750.01	0.0					
123	1302.41	0.31090.00	-0.51750.01	0.0					
35	1302.41	0.31090.00	-0.51750.01	0.0					
47	1302.41	0.31090.00	-0.51750.01	0.0					
NODE	TEMP	DT	DDT	GEN RATE					
12	0.8333D 02	0.9969D 00	0.1660D 00	0.0					
24	0.8333D 02	0.4984D 00	0.8289D 01	0.0					
36	0.8333D 02	0.5483D 00	0.9246D 01	0.0					
48	0.8333D 02	0.4486D 00	0.7468D 01	0.0					
MATERIAL DATA	NAME	MATL	TOT CAP	Avg TEMP	THMELT				
SAND	1	1.07159E 00	9.24010E 01	8.60675E 01	0.0				
SEAL	2	1.83556E -01	2.33869E 01	8.28278E 01	0.0				
ARR	3	1.44446E -03	1.18769E -01	8.23378E 01	0.0				

TRUMP OUTPUT DATA

* MISSLE PROBLEM TWO DIMENSIONAL

```

PRINTOUT CYCLE TOO FAST TOO SLOW KWIT DELTMAX
7 100 11 0 0 1.00000E 12 SMALL TINY 1.00000E 00 NUTS
TOTAL TIME TIME STEP HEAT FLOW TEMP FROM FLUX FLUX RATE TEMP RATE
7.8895F 02 3.2434E 00 -2.0633E 04 -1.52009E 04 -2.6288E 01 -1.51668E 01
AVG TEMP HEAT CAPACITY HEAT CONTENT GEN RATE HEAT GEN TEMP FROM GEN
3.62263E 01 1.35790 00 1.17042E 02 0.0 0.0 0.0 0.0
NODE TEMP DT DDT GE N RATE CURE AT 280 F
13 0.87290 0.000 0.58870 -0.1 0.2834E -05 H 673E -06
25 0.87300 0.000 0.58870 -0.1 0.2834E -05 H 673E -06
37 0.87310 0.000 0.58870 -0.1 0.2834E -05 H 673E -06
52 0.87320 0.000 0.58870 -0.1 0.2834E -05 H 673E -06
74 0.87330 0.000 0.58870 -0.1 0.2834E -05 H 673E -06
96 0.87340 0.000 0.58870 -0.1 0.2834E -05 H 673E -06
118 0.87350 0.000 0.58870 -0.1 0.2834E -05 H 673E -06
140 0.87360 0.000 0.58870 -0.1 0.2834E -05 H 673E -06
162 0.87370 0.000 0.58870 -0.1 0.2834E -05 H 673E -06
184 0.87380 0.000 0.58870 -0.1 0.2834E -05 H 673E -06
206 0.87390 0.000 0.58870 -0.1 0.2834E -05 H 673E -06
228 0.87400 0.000 0.58870 -0.1 0.2834E -05 H 673E -06
250 0.87410 0.000 0.58870 -0.1 0.2834E -05 H 673E -06
272 0.87420 0.000 0.58870 -0.1 0.2834E -05 H 673E -06
294 0.87430 0.000 0.58870 -0.1 0.2834E -05 H 673E -06
316 0.87440 0.000 0.58870 -0.1 0.2834E -05 H 673E -06
338 0.87450 0.000 0.58870 -0.1 0.2834E -05 H 673E -06
360 0.87460 0.000 0.58870 -0.1 0.2834E -05 H 673E -06
382 0.87470 0.000 0.58870 -0.1 0.2834E -05 H 673E -06
404 0.87480 0.000 0.58870 -0.1 0.2834E -05 H 673E -06
426 0.87490 0.000 0.58870 -0.1 0.2834E -05 H 673E -06
448 0.87500 0.000 0.58870 -0.1 0.2834E -05 H 673E -06
470 0.87510 0.000 0.58870 -0.1 0.2834E -05 H 673E -06
492 0.87520 0.000 0.58870 -0.1 0.2834E -05 H 673E -06
514 0.87530 0.000 0.58870 -0.1 0.2834E -05 H 673E -06
536 0.87540 0.000 0.58870 -0.1 0.2834E -05 H 673E -06
558 0.87550 0.000 0.58870 -0.1 0.2834E -05 H 673E -06
580 0.87560 0.000 0.58870 -0.1 0.2834E -05 H 673E -06
602 0.87570 0.000 0.58870 -0.1 0.2834E -05 H 673E -06
624 0.87580 0.000 0.58870 -0.1 0.2834E -05 H 673E -06
646 0.87590 0.000 0.58870 -0.1 0.2834E -05 H 673E -06
668 0.87600 0.000 0.58870 -0.1 0.2834E -05 H 673E -06
690 0.87610 0.000 0.58870 -0.1 0.2834E -05 H 673E -06
712 0.87620 0.000 0.58870 -0.1 0.2834E -05 H 673E -06
734 0.87630 0.000 0.58870 -0.1 0.2834E -05 H 673E -06
756 0.87640 0.000 0.58870 -0.1 0.2834E -05 H 673E -06
778 0.87650 0.000 0.58870 -0.1 0.2834E -05 H 673E -06
800 0.87660 0.000 0.58870 -0.1 0.2834E -05 H 673E -06
822 0.87670 0.000 0.58870 -0.1 0.2834E -05 H 673E -06
844 0.87680 0.000 0.58870 -0.1 0.2834E -05 H 673E -06
866 0.87690 0.000 0.58870 -0.1 0.2834E -05 H 673E -06
888 0.87700 0.000 0.58870 -0.1 0.2834E -05 H 673E -06
910 0.87710 0.000 0.58870 -0.1 0.2834E -05 H 673E -06
932 0.87720 0.000 0.58870 -0.1 0.2834E -05 H 673E -06
954 0.87730 0.000 0.58870 -0.1 0.2834E -05 H 673E -06
976 0.87740 0.000 0.58870 -0.1 0.2834E -05 H 673E -06
998 0.87750 0.000 0.58870 -0.1 0.2834E -05 H 673E -06

```

TRUMP OUTPUT DATA

* MISSLE PROBLEM TWO DIMENSIONAL

PRINTOUT	CYCLE	TOO FAST	TOO SLOW	KWIT	DEPTHMX	SMALL	TIVARY	NUTS
8	120	11	0	0	1.00000E 12	1,20000E 03	1.00000E 00	NUTS
TOTAL TIME	TIME STEP	HEAT FLOW		TEMP FROM FLUX	FLUX RATE			
8.5164E 02	4.3884E 00	-2.30600E 04		-1.69885E 04	-2.0771E 01			
Avg TEMP	HEAT CAPACITY	HEAT CONTENT		GEN RATE	TEMP GEN			
8.88412E 01	1.35719D 00	1.20594E 02		0.0	0.0			

NODE	TEMP	DDT	GE N RATE	H	F	CURE AT 280 F
1	1.3	0.0000000000000000	0.0000000000000000	0.0000000000000000	0.0000000000000000	0.0000000000000000
2	2.5	0.0000000000000000	0.0000000000000000	0.0000000000000000	0.0000000000000000	0.0000000000000000
3	3.7	0.0000000000000000	0.0000000000000000	0.0000000000000000	0.0000000000000000	0.0000000000000000
4	14	0.0000000000000000	0.0000000000000000	0.0000000000000000	0.0000000000000000	0.0000000000000000
5	26	0.0000000000000000	0.0000000000000000	0.0000000000000000	0.0000000000000000	0.0000000000000000
6	38	0.0000000000000000	0.0000000000000000	0.0000000000000000	0.0000000000000000	0.0000000000000000
7	50	0.0000000000000000	0.0000000000000000	0.0000000000000000	0.0000000000000000	0.0000000000000000
8	38	0.0000000000000000	0.0000000000000000	0.0000000000000000	0.0000000000000000	0.0000000000000000
9	157	0.0000000000000000	0.0000000000000000	0.0000000000000000	0.0000000000000000	0.0000000000000000
10	39	0.0000000000000000	0.0000000000000000	0.0000000000000000	0.0000000000000000	0.0000000000000000
11	168	0.0000000000000000	0.0000000000000000	0.0000000000000000	0.0000000000000000	0.0000000000000000
12	280	0.0000000000000000	0.0000000000000000	0.0000000000000000	0.0000000000000000	0.0000000000000000
13	405	0.0000000000000000	0.0000000000000000	0.0000000000000000	0.0000000000000000	0.0000000000000000
14	291	0.0000000000000000	0.0000000000000000	0.0000000000000000	0.0000000000000000	0.0000000000000000
15	347	0.0000000000000000	0.0000000000000000	0.0000000000000000	0.0000000000000000	0.0000000000000000
16	180	0.0000000000000000	0.0000000000000000	0.0000000000000000	0.0000000000000000	0.0000000000000000
17	19	0.0000000000000000	0.0000000000000000	0.0000000000000000	0.0000000000000000	0.0000000000000000
18	347	0.0000000000000000	0.0000000000000000	0.0000000000000000	0.0000000000000000	0.0000000000000000
19	343	0.0000000000000000	0.0000000000000000	0.0000000000000000	0.0000000000000000	0.0000000000000000
20	388	0.0000000000000000	0.0000000000000000	0.0000000000000000	0.0000000000000000	0.0000000000000000
21	449	0.0000000000000000	0.0000000000000000	0.0000000000000000	0.0000000000000000	0.0000000000000000
22	335	0.0000000000000000	0.0000000000000000	0.0000000000000000	0.0000000000000000	0.0000000000000000
23	450	0.0000000000000000	0.0000000000000000	0.0000000000000000	0.0000000000000000	0.0000000000000000
24	340	0.0000000000000000	0.0000000000000000	0.0000000000000000	0.0000000000000000	0.0000000000000000
25	341	0.0000000000000000	0.0000000000000000	0.0000000000000000	0.0000000000000000	0.0000000000000000
26	340	0.0000000000000000	0.0000000000000000	0.0000000000000000	0.0000000000000000	0.0000000000000000
27	341	0.0000000000000000	0.0000000000000000	0.0000000000000000	0.0000000000000000	0.0000000000000000
28	345	0.0000000000000000	0.0000000000000000	0.0000000000000000	0.0000000000000000	0.0000000000000000
29	47	0.0000000000000000	0.0000000000000000	0.0000000000000000	0.0000000000000000	0.0000000000000000
30	470	0.0000000000000000	0.0000000000000000	0.0000000000000000	0.0000000000000000	0.0000000000000000
31	402	0.0000000000000000	0.0000000000000000	0.0000000000000000	0.0000000000000000	0.0000000000000000
32	347	0.0000000000000000	0.0000000000000000	0.0000000000000000	0.0000000000000000	0.0000000000000000
33	348	0.0000000000000000	0.0000000000000000	0.0000000000000000	0.0000000000000000	0.0000000000000000
34	348	0.0000000000000000	0.0000000000000000	0.0000000000000000	0.0000000000000000	0.0000000000000000
35	348	0.0000000000000000	0.0000000000000000	0.0000000000000000	0.0000000000000000	0.0000000000000000
36	348	0.0000000000000000	0.0000000000000000	0.0000000000000000	0.0000000000000000	0.0000000000000000
37	347	0.0000000000000000	0.0000000000000000	0.0000000000000000	0.0000000000000000	0.0000000000000000
38	347	0.0000000000000000	0.0000000000000000	0.0000000000000000	0.0000000000000000	0.0000000000000000
39	348	0.0000000000000000	0.0000000000000000	0.0000000000000000	0.0000000000000000	0.0000000000000000
40	348	0.0000000000000000	0.0000000000000000	0.0000000000000000	0.0000000000000000	0.0000000000000000
41	348	0.0000000000000000	0.0000000000000000	0.0000000000000000	0.0000000000000000	0.0000000000000000
42	348	0.0000000000000000	0.0000000000000000	0.0000000000000000	0.0000000000000000	0.0000000000000000
43	348	0.0000000000000000	0.0000000000000000	0.0000000000000000	0.0000000000000000	0.0000000000000000
44	348	0.0000000000000000	0.0000000000000000	0.0000000000000000	0.0000000000000000	0.0000000000000000
45	348	0.0000000000000000	0.0000000000000000	0.0000000000000000	0.0000000000000000	0.0000000000000000
46	348	0.0000000000000000	0.0000000000000000	0.0000000000000000	0.0000000000000000	0.0000000000000000
47	348	0.0000000000000000	0.0000000000000000	0.0000000000000000	0.0000000000000000	0.0000000000000000
48	348	0.0000000000000000	0.0000000000000000	0.0000000000000000	0.0000000000000000	0.0000000000000000

MATERIAL DATA

NAME	MATL	TOT CAP	Avg Temp	Tmelt
1	SAND	1.77352E 03	9.453373E 01	0.28845E -23
2	STFL	2.82325E 03	9.17339E 01	0.50022E -23
3	AIR	1.44246E 03	9.33724E 01	0.46521E -23

TRUMP OUTPUT DATA

* MISSLE PROBLEM TWO DIMENSIONAL

```
=====
PRINTOUT      CYCLE    TOO FAST   TOO SLOW   KWIT      DELTMAX    SMALL
9          140        TIME STEP   HEAT FLOW   TEMP FROM FLUX   FLUX RATE
9.47229E 02   4.8000E 00   -2.3410E 04   -1.7246E 04   -2.4150E 01   -1.8278E 01
=====
AVG TEMP     HEAT CAPACITY   HEAT CONTENT   GEN RATE   HEAT GEN   TEMP FROM GEN
9.43739E 01   1.35739D 00   1.28102E 02   0.0         0.0         0.0
=====
```

```
=====
NODE      TEMP      DT      DDT      GE N RATE
0.8785D 02   0.8785D 02   -0.3074D-01   -0.6404D-02   0.2853E-05
13      0.8785D 02   -0.3074D-01   -0.6404D-02   0.2853E-05
25      0.8785D 02   -0.3074D-01   -0.6404D-02   0.2853E-05
37      0.8785D 02   -0.3074D-01   -0.6404D-02   0.2853E-05
52      0.8785D 02   -0.3074D-01   -0.6404D-02   0.2853E-05
14      0.8763D 02   -0.3074D-01   -0.6404D-02   0.2853E-05
26      0.8763D 02   -0.3074D-01   -0.6404D-02   0.2853E-05
38      0.8763D 02   -0.3074D-01   -0.6404D-02   0.2853E-05
15      0.8790D 02   -0.3074D-01   -0.6404D-02   0.2853E-05
27      0.8790D 02   -0.3074D-01   -0.6404D-02   0.2853E-05
41      0.8790D 02   -0.3074D-01   -0.6404D-02   0.2853E-05
16      0.8768D 02   -0.3074D-01   -0.6404D-02   0.2853E-05
28      0.8768D 02   -0.3074D-01   -0.6404D-02   0.2853E-05
39      0.8768D 02   -0.3074D-01   -0.6404D-02   0.2853E-05
40      0.8768D 02   -0.3074D-01   -0.6404D-02   0.2853E-05
17      0.87835D 02   -0.3074D-01   -0.6404D-02   0.2853E-05
29      0.87835D 02   -0.3074D-01   -0.6404D-02   0.2853E-05
41      0.87835D 02   -0.3074D-01   -0.6404D-02   0.2853E-05
18      0.8824D 02   -0.3074D-01   -0.6404D-02   0.2853E-05
30      0.8824D 02   -0.3074D-01   -0.6404D-02   0.2853E-05
42      0.8824D 02   -0.3074D-01   -0.6404D-02   0.2853E-05
19      0.8824D 02   -0.3074D-01   -0.6404D-02   0.2853E-05
31      0.8824D 02   -0.3074D-01   -0.6404D-02   0.2853E-05
43      0.8824D 02   -0.3074D-01   -0.6404D-02   0.2853E-05
20      0.8824D 02   -0.3074D-01   -0.6404D-02   0.2853E-05
32      0.8824D 02   -0.3074D-01   -0.6404D-02   0.2853E-05
44      0.8824D 02   -0.3074D-01   -0.6404D-02   0.2853E-05
21      0.8824D 02   -0.3074D-01   -0.6404D-02   0.2853E-05
33      0.8824D 02   -0.3074D-01   -0.6404D-02   0.2853E-05
45      0.8824D 02   -0.3074D-01   -0.6404D-02   0.2853E-05
22      0.8824D 02   -0.3074D-01   -0.6404D-02   0.2853E-05
34      0.8824D 02   -0.3074D-01   -0.6404D-02   0.2853E-05
46      0.8824D 02   -0.3074D-01   -0.6404D-02   0.2853E-05
23      0.8824D 02   -0.3074D-01   -0.6404D-02   0.2853E-05
35      0.8824D 02   -0.3074D-01   -0.6404D-02   0.2853E-05
47      0.8824D 02   -0.3074D-01   -0.6404D-02   0.2853E-05
24      0.8824D 02   -0.3074D-01   -0.6404D-02   0.2853E-05
36      0.8824D 02   -0.3074D-01   -0.6404D-02   0.2853E-05
48      0.8824D 02   -0.3074D-01   -0.6404D-02   0.2853E-05
=====
MATERIAL DATA
NAME  MATEL   TOT CAP   TOT HEAT   AVG TEMP   TRELAT   HHELT
SAND  1.07359E 00   9.9596E 01   9.22694E 01   0.0         0.0
STEEL 2.82356E-03   2.83471E 01   1.0395E 02   0.0         0.0
AIR   1.44246E-03   1.58701E 01   1.0022E 02   0.0         0.0
=====
```

DATA DECK 1

TRUMP OUTPUT DATA

* MISSILE PROBLEM TWO DIMENSIONAL

PRINTOUT	CYCLE	T0J	FAST	TOO SLOW	KWIT	DELT MX	SMALL	TVARY	NUTS
10	160	0	0	0	0	1.00000E 12	1.00000E 00	1.00000E 00	3
	TOTAL TIME	TIME STEP	-HEAT FLOW	TEMP FROM FLUX	FLUX RATE				
1.06258E 03	6.0103E 00	-2.4940E 04	-1.8373E 04	-2.3471E 01	-1.7291E 01				
	Avg TEMP	HEAT CAPACITY	HEAT CONTENT	GEN RATE	HEAT GEN	TEMP FROM GEN			
1.02454F 02	1.35739D 00	1.39670E 02	0.0	0.0	0.0	0.0			

DATA DECK 1

NODE	TEMP	D _T	GEN RATE	CURE AT 280 F
1	90200	0.2	0.0	0.0
2	92000	0.0	0.0	0.0
3	92000	0.0	0.0	0.0
4	92000	0.0	0.0	0.0
5	92000	0.0	0.0	0.0
6	92000	0.0	0.0	0.0
7	92000	0.0	0.0	0.0
8	92000	0.0	0.0	0.0
9	92000	0.0	0.0	0.0
10	92000	0.0	0.0	0.0
11	92000	0.0	0.0	0.0
12	92000	0.0	0.0	0.0
13	92000	0.0	0.0	0.0
14	92000	0.0	0.0	0.0
15	92000	0.0	0.0	0.0
16	92000	0.0	0.0	0.0
17	92000	0.0	0.0	0.0
18	92000	0.0	0.0	0.0
19	92000	0.0	0.0	0.0
20	92000	0.0	0.0	0.0
21	92000	0.0	0.0	0.0
22	92000	0.0	0.0	0.0
23	92000	0.0	0.0	0.0
24	92000	0.0	0.0	0.0
25	92000	0.0	0.0	0.0
26	92000	0.0	0.0	0.0
27	92000	0.0	0.0	0.0
28	92000	0.0	0.0	0.0
29	92000	0.0	0.0	0.0
30	92000	0.0	0.0	0.0
31	92000	0.0	0.0	0.0
32	92000	0.0	0.0	0.0
33	92000	0.0	0.0	0.0
34	92000	0.0	0.0	0.0
35	92000	0.0	0.0	0.0
36	92000	0.0	0.0	0.0
37	92000	0.0	0.0	0.0
38	92000	0.0	0.0	0.0
39	92000	0.0	0.0	0.0
40	92000	0.0	0.0	0.0
41	92000	0.0	0.0	0.0
42	92000	0.0	0.0	0.0
43	92000	0.0	0.0	0.0
44	92000	0.0	0.0	0.0
45	92000	0.0	0.0	0.0
46	92000	0.0	0.0	0.0
47	92000	0.0	0.0	0.0
48	92000	0.0	0.0	0.0

MATERIAL DATA

NAME	MATL	TOT CAP	TOT HEAT	Avg TEMP	MELT	H MELT
1	1.07559E 00	1.07231E 02	1.00285E 02	0.0	0.0	0.0
2	1.08256E -01	3.14424E -03	1.01060E 02	0.0	0.0	0.0
3	1.01130E 03	1.74116E -01	1.20708E 02	0.0	0.0	0.0
4	1.01000E 03	3.55300E 03	1.00000E 00	0.0	0.0	0.0

TRUMP OUTPUT DATA VISSLE PROBLEM TWO DIMENSIONAL

TRUMP OUTPUT DATA

* MISSILE PROBLEM TWO DIMENSIONAL

DATA DECK 1

```

PRINTOUT CYCLE TOO FAST TOO SLOW KWIT DELTMX SMALL TVARY 1.3CCCCC C C NUTS
12 200 0 0 0 1.00000E 12 0.00000E 03 1.3CCCCC C C NUTS
TOTAL TIME TIME STEP HEAT FLOW TEMP FROM FLUX RATE TEMP RATE
1.30776E 03 6.30006E 00 -2.75009E 04 -2.02602E 04 -2.10289E 51 -1.54922E 01
AUG TEMP HEAT CAPACITY HEAT CONTENT GEN RATE TEMP FROM GEN
1.7887E 02 1.35739E 00 1.6008E 02 0.0 0.0 0.0
=====
```

```

NONE TEMP DT DDT GE N RATE H 2440E-05 CURE AT 280 F
0.10590 03 0.34700 00 0.57840-01 0.0 0.0
13 0.10590 03 0.34710 00 0.57840-01 0.0 0.0
125 0.10590 03 0.34700 00 0.57840-01 0.0 0.0
37 0.10777 03 0.34700 00 0.57840-01 0.0 0.0
14 0.10590 03 0.34700 00 0.57840-01 0.0 0.0
26 0.10654 03 0.34700 00 0.57840-01 0.0 0.0
38 0.10590 03 0.34700 00 0.57840-01 0.0 0.0
33 0.10590 03 0.34700 00 0.57840-01 0.0 0.0
15 0.10654 03 0.34700 00 0.57840-01 0.0 0.0
39 0.10590 03 0.34700 00 0.57840-01 0.0 0.0
16 0.10654 03 0.34700 00 0.57840-01 0.0 0.0
28 0.10590 03 0.34700 00 0.57840-01 0.0 0.0
40 0.10654 03 0.34700 00 0.57840-01 0.0 0.0
17 0.10590 03 0.34700 00 0.57840-01 0.0 0.0
29 0.10590 03 0.34700 00 0.57840-01 0.0 0.0
41 0.10590 03 0.34700 00 0.57840-01 0.0 0.0
6 0.10590 03 0.34700 00 0.57840-01 0.0 0.0
18 0.10590 03 0.34700 00 0.57840-01 0.0 0.0
30 0.10590 03 0.34700 00 0.57840-01 0.0 0.0
42 0.10590 03 0.34700 00 0.57840-01 0.0 0.0
19 0.10590 03 0.34700 00 0.57840-01 0.0 0.0
31 0.10590 03 0.34700 00 0.57840-01 0.0 0.0
43 0.10590 03 0.34700 00 0.57840-01 0.0 0.0
22 0.10590 03 0.34700 00 0.57840-01 0.0 0.0
44 0.10590 03 0.34700 00 0.57840-01 0.0 0.0
21 0.10590 03 0.34700 00 0.57840-01 0.0 0.0
35 0.10590 03 0.34700 00 0.57840-01 0.0 0.0
10 0.10590 03 0.34700 00 0.57840-01 0.0 0.0
22 0.10590 03 0.34700 00 0.57840-01 0.0 0.0
34 0.10590 03 0.34700 00 0.57840-01 0.0 0.0
46 0.10590 03 0.34700 00 0.57840-01 0.0 0.0
11 0.10590 03 0.34700 00 0.57840-01 0.0 0.0
23 0.10590 03 0.34700 00 0.57840-01 0.0 0.0
37 0.10590 03 0.34700 00 0.57840-01 0.0 0.0
47 0.10590 03 0.34700 00 0.57840-01 0.0 0.0
NONE TEMP DT DDT GE N RATE H 2440E-05 CURE AT 280 F
12 0.13200 03 -0.10000 01 -0.1667D 00 0.0 0.0
24 0.14750 03 -0.25000 01 -0.1667D 00 0.0 0.0
36 0.12070 03 -0.15000 01 -0.2500D 01 0.0 0.0
48 0.13010 03 -0.50000 01 -0.8334D 02 0.0 0.0
=====
```

```

MATERIAL DATA
NAME MATT TOT CAP AVG TEMP TMELT H MELT
SAND 1.37559E 00 1.24674E 02 0.0 0.0 0.0
STEEL 2.82366E-01 3.51579E 01 1.24517E 02 0.0 0.0
AIR 3.1.44226E-03 1.86460E-01 1.29265E 02 0.0 0.0
=====
```

TELEGRAM OUTLINE DATA

TRUMP OUTPUT DATA

DATA DECK 1

TRAINING OUTPUT RATE

TRUMP OUTPUT DATA

DATA DECK 1

TRUMP OUTPUT CAT A

* MISSLE PROBLEM TWO DIMENSIONAL

PRINTOUT	CYCLE	TOO FAST	TOO SLOW	KWIT	DELTMX	SMALL	TWARY	NUTS
15	249	0	0	1.0	1.0000E 12	1.0000E 00	1.0000E 00	1.0000E 00
	TOTAL TIME	TIME STEP	HEAT FLOW	TEMP FROM FLUX	FLUX RATE			
1.42000E 03	2.21753E 00	1.04904E 04	7.72941E 03	7.28502E 00	5.36695E 00			
	Avg TEMP	HEAT CONTENT	GEN RATE	HEAT GEN	TEMP FROM GEN			
1.16772E 02	1.35729E 00	1.85056E 02	0.0	0.0	0.0			
	Node	Temp	DdT	GE N RATE				
1	0.1500	0.3	0.1333	0.0				
25	0.1500	0.3	0.1333	0.0				
37	0.1500	0.3	0.1333	0.0				
14	0.1450	0.3	0.1317	0.0				
38	0.1450	0.3	0.1317	0.0				
15	0.1450	0.3	0.1317	0.0				
27	0.1450	0.3	0.1317	0.0				
39	0.1450	0.3	0.1317	0.0				
123	0.1450	0.3	0.1317	0.0				
17	0.1450	0.3	0.1317	0.0				
29	0.1450	0.3	0.1317	0.0				
41	0.1450	0.3	0.1317	0.0				
18	0.1450	0.3	0.1317	0.0				
37	0.1450	0.3	0.1317	0.0				
42	0.1450	0.3	0.1317	0.0				
19	0.1450	0.3	0.1317	0.0				
31	0.1450	0.3	0.1317	0.0				
43	0.1450	0.3	0.1317	0.0				
23	0.1450	0.3	0.1317	0.0				
35	0.1450	0.3	0.1317	0.0				
47	0.1450	0.3	0.1317	0.0				
Node	Temp	DdT	GE N RATE					
12	0.9000	0.2	0.59120	0.0				
24	0.9030	0.2	0.81310	0.0				
36	0.9030	0.2	0.33260	0.0				
48	0.9090	0.3	0.38810	0.0				

CURE AT 280 F

NAME	MATL	TOT CAP	TOT HEAT	Avg TEMP	TMELT	HMELT
SAND	1	1.37359E 00	1.3526E 02	1.1588E 02	0.0	0.0
STEL	2	2.0356E -03	3.5792E -01	1.0890E 02	0.0	0.0
AIR	3	1.4266E -03	1.5792E -01	0.0	0.0	0.0

MATERIAL DATA

APPENDIX D

Experimental Data

The data presented in this appendix were obtained from the thermocouples on the rocket motor storage container system located at China Lake, California. The thermocouple output was read out on a Honeywell Electronik 25, 24 channel recorder which had been calibrated at 50, 100 and 150°F. The data was taken on two consecutive, typical summer days (August 1 and 2, 1972) at China Lake. Each thermocouple was read once every 24 minutes. The first set of data presents the storage container temperature at four locations plus three different ways of averaging this data. It also presents the ambient temperature and the approximate time of day. The second set of data presents the surface temperature of the rocket motor and three ways to average this data. It also presents the temperature at the center of the rocket motor and the approximate time of day. Figure 32 shows the location of the thermocouples used to collect this temperature data.

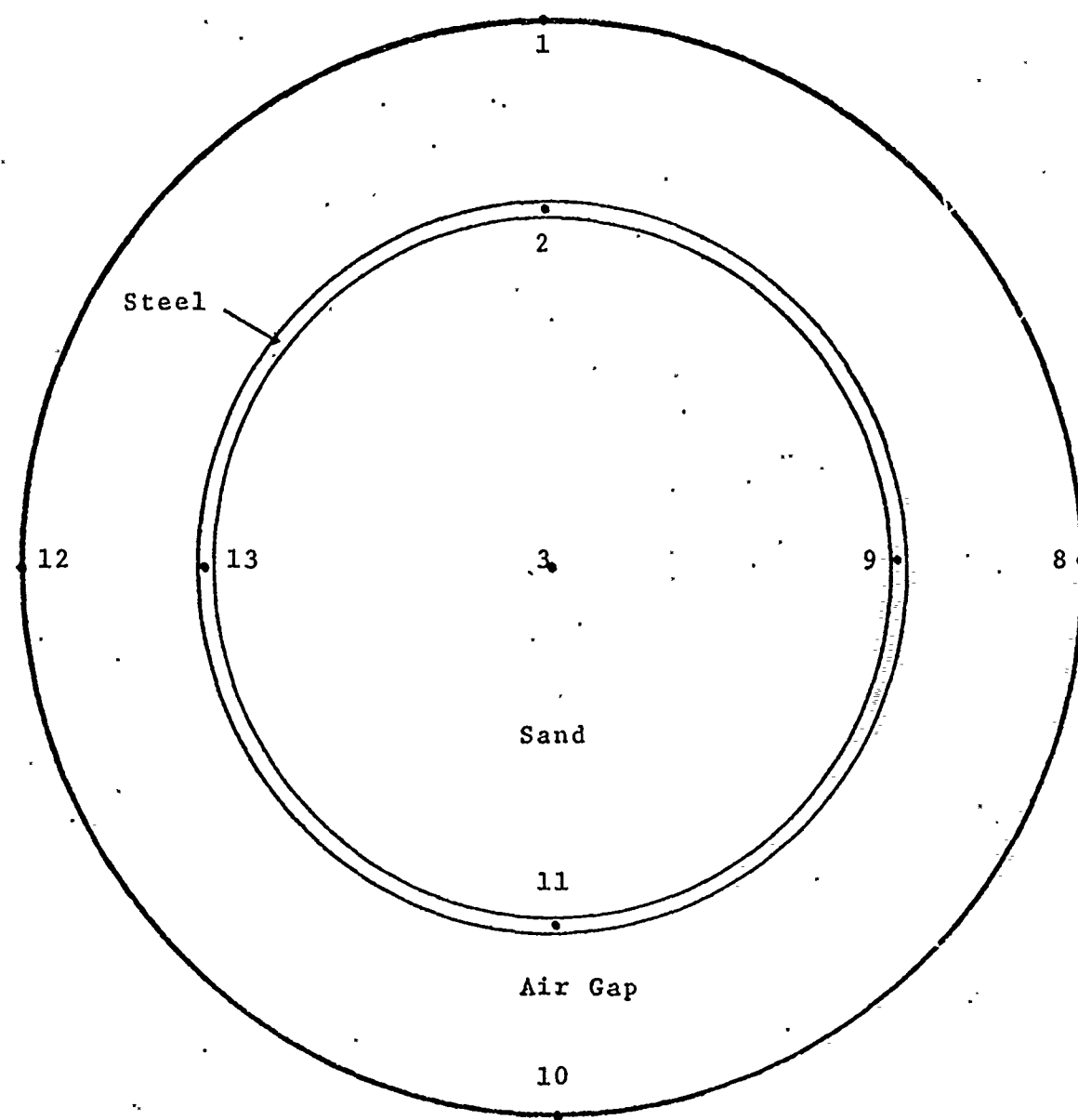


Figure 32: Thermocouple Locations for Experimental Data.

Series 1

Time (Approximate)	Ambient (°F)	#1 (°F)	#8 (°F)	#10 (°F)	#12 (°F)	Avg. #1 & #10 (°F)	#8 & #12 (°F)	Avg. all 4 "Bulk"
0536 Aug. 1, 1972	76	69	72	79	80	74	76	75
0600	77	68	72	79	80	73.5	76	74.75
0624	80	73	75	81	82	77	78.5	77.75
0648	80	81	79	87	85	84	82	83
0712	83	90	82	90	89	90	85.5	87.75
0736	85	98	87	93	92	95.5	89.5	92.5
0800	87	105	90	94	94	99.5	92	95.75
	89	110	93	96	97	103	95	99
	91	116	96	98	99	107	97.5	102.25
	92	121	100	101	102	111	101	106
	94	129	103	102	105	115.5	104	109.75
1000	96	133	107	105	108	119	107.5	113.25
	97	139	110	107	110	123	110	116.5
	100	143	113	107	112	125	112.5	118.75
	101	147	117	109	115	128	116	122
	103	150	119	109	116	129.5	117.5	123.5
	104	153	124	110	119	131.5	121.5	126.5
	106	156	128	112	122	134	125	129.5
	106	157	131	113	124	135	127.5	131.25
	106	154	133	114	125	134	129	131.5
	107	157	138	115	127	136	132.5	134.25
	108	154	143	117	129	135.5	136	135.75
	109	153	142	118	129	135.5	135.5	135.5
	110	148	142	119	129	133.5	135.5	134.5
	110	143	141	118	128	130.5	134.5	132.5
	109	142	143	119	128	130.5	135.5	133
1400	107	137	143	119	128	128	135.5	131.75
	108	134	139	117	127	125.5	133	129.25
	108	130	139	117	127	123.5	133	128.25
	106	126	138	116	126	121	122	126.5
	104	123	136	115	125	119	130.5	124.75

Time (Approximate)	Ambient (°F)	#1 (°F)	#8 (°F)	#10 (°F)	#12 (°F)	Avg. #1 & #10 (°F)	#10 (°F)	Avg. #8 & #12 (°F)	Avg. all 4 "Bulk
Aug. 1, 1972									
1800	103	118	131	113	123	115.5	127	121.25	
	101	113	127	111	120	112	123.5	117.75	
	99	107	121	108	117	107.5	119	113.25	
	96	101	106	103	111	102	108.5	105.25	
	95	91	93	98	104	94.5	98.5	96.5	
2000	93	88	91	95	101	91.5	96	93.75	
	91	86	89	94	99	90	94	92	
	90	85	88	92	97	88.5	92.5	90.5	
	89	84	87	91	96	87.5	91.5	89.5	
	87	83	85	89	94	86	89.5	87.75	
2200	87	81	84	88	93	84.5	88.5	86.5	
	85	80	83	87	91	83.5	87	85.25	
	86	79	82	86	91	82.5	86.5	84.5	
	86	79	82	87	90	83	86	84.5	
	84	79	82	86	89	82.5	85.5	84	
0000 2 Aug.	82	77	80	85	88	81	84	82.5	
	81	74	78	84	86	79	82	80.5	
	81	72	76	83	85	77.5	80.5	79	
	81	72	77	83	85	77.5	81	79.25	
	79	72	75	81	83	76.5	79	77.75	
0200	79	72	75	80	83	76	79	77.5	
	79	72	74	80	82	76	78	77	
	78	72	74	79	82	75.5	78	76.75	
	77	71	73	79	81	75	77	76	
	75	70	72	78	80	74	76	75	
0400	73	67	69	77	78	72	73.5	72.75	
	72	66	69	75	77	70.5	73	71.75	
	73	65	68	75	76	70	72	71	
	69	64	67	73	75	68.5	71	69.75	
	69	63	66	72	74	67.5	70	68.75	
0600	68	63	66	71	73	67	69.5	68.25	
	71	65	67	75	76	70	71.5	70.75	
	77	74	71	80	79	77	75	76	
	79	84	77	84	84	84	80.5	82.25	

Time (Approximate) Aug. 2, 1972	Ambient (°F)	#1 (°F)	#8 (°F)	#10 (°F)	#12 (°F)	Avg. #1 & #10 Avg. (°F)	#12 Avg. #8 & #12 Avg. "bulk"
0800	80	93	81	89	87	91	84
	83	101	85	92	91	96.5	88
	85	108	89	93	93	100.5	91
	86	114	93	96	97	105	95
	88	121	96	98	100	109.5	98
	89	126	98	98	101	112	99.5
1000	91	130	101	100	103	115	102
	94	137	106	102	106	119.5	106
	96	143	109	104	109	123.5	109
	100	146	113	106	111	126	112
	100	149	117	107	114	128	115.5
1200	101	151	121	108	117	129.5	119
	103	150	127	110	119	130	123
	104	156	129	110	121	133	125
	104	154	133	111	122	132.5	127.5
	105	155	137	112	125	133.5	131
	105	156	141	114	126	135	133.5
	107	149	143	114	127	131.5	127
	107	149	146	115	128	132	131.5
	106	151	152	118	131	134.5	141.5
	107	144	152	120	132	132	142
1600	108	139	152	119	131	129	141.5
	107	136	147	120	130	128	138.5
	107	136	147	121	130	128.5	137
	106	151	152	118	131	135	133.5
	107	144	152	120	132	132	141.5
	105	131	147	121	130	128	138.5
	103	124	144	120	128	122	136
	103	117	134	117	124	117	129
	100	111	119	113	121	112	120
	98	105	118	108	117	106.5	117.5
	95	99	103	103	109	101	106
	93	91	93	97	103	94	98
2000	91	87	90	94	100	90.5	95
	90	85	88	93	98	89	93
	88	83	86	91	96	87	91
							89

Time (Approximate) Aug. 2, 1972

	Ambient (°F)	#1 (°F)	#2 (°F)	#3 (°F)	#8 (°F)	#10 (°F)	#12 (°F)	Avg. #1 (°F)	#10 Avg. (°F)	#12 Avg. (°F)	"Bulk"
2200	87	81	85	90	94	94	94	85.5	89.5	89.5	87.5
	85	80	83	88	93	93	84	84	88	88	86
	84	78	81	87	91	91	82.5	82.5	86	86	84.25
	82	75	78	86	89	89	80.5	80.5	83.5	83.5	82
	85	74	79	85	88	88	79.5	79.5	83.5	83.5	81.5
	83	76	78	85	87	87	80.5	80.5	82.5	82.5	81.5
	81	74	77	84	86	86	79	79	81.5	81.5	80.25
0000 3 Aug.	78	71	75	83	84	84	77	77	79.5	79.5	78.25
	81	69	74	81	84	84	75	75	79	79	77
	79	70	73	81	83	83	75.5	75.5	78	78	76.75
	79	72	74	80	83	83	76	76	78.5	78.5	77.25
	78	71	73	79	82	82	75	75	77.5	77.5	76.25
0200	77	70	72	78	81	81	74	74	76.5	76.5	75.25
	73	69	71	77	79	79	73	73	75	75	74
	72	65	69	76	78	78	70.5	70.5	73.5	73.5	72
	70	64	68	74	77	77	69	69	72.5	72.5	70.75
	67	63	66	73	75	75	68	68	70.5	70.5	69.25
	67	61	65	71	74	74	66	66	69.5	69.5	67.75
0400	66	60	64	70	73	73	65	65	68.5	68.5	66.75
	65	60	63	70	72	72	65	65	67.5	67.5	66.25
	65	58	61	69	71	71	63.5	63.5	66	66	64.75

FIRST DAY'S TEMPERATURE RANGES				SECOND DAY'S TEMPERATURE RANGES			
HIGH	110	157	143	119	129	136	136
LOW	69	64	67	73	75	68.5	71
AVG	89.5	110.5	105	96	102	102.25	103.5
HIGH	108	156	152	121	132	135	142
LOW	65	58	61	69	71	63.5	66
AVG	86.5	107	106.5	95	101.5	99.25	104

Series 2

Time (Approximate) Aug. 1, 1972	#3 (°F)	#2 (°F)	#9 (°F)	#11 (°F)	#13 (°F)	Avg. (°F)	#2 & #11 Avg. (°F)	#9 & #13 Avg. (°F)	#11 4 (°F)
0536	97	83	84	85	85	84.5	84.5	84.5	84.25
0600	96	82	83	85	84	83.5	83.5	83.5	83.5
0624	95	82	83	84	85	83	84	84	83.5
0648	94	85	84	86	89	85.5	86.5	86.5	86
0712	94	88	86	88	93	88	89.5	88.5	88.75
0736	93	91	88	90	96	90.5	92	91.5	91.25
0800	92	95	90	91	99	93	94.5	93.75	93.75
	91	98	92	93	102	95.5	97	96.25	
	91	101	94	95	104	98	99	98.5	
	91	105	96	97	107	101	101.5	101.5	
	91	108	98	98	109	103	103.5	103.5	
	91	112	101	100	112	106	106.5	106.5	
	91	115	103	102	113	108.5	108	108	108.25
	92	118	105	103	115	110.5	110	110	110.25
	94	120	108	105	117	112.5	112.5	112.5	
1000	94	122	110	106	118	114	114	114	
	95	125	111	108	119	116.5	115	115	115.75
	96	126	114	109	120	117.5	117	117	117.25
	98	128	117	111	121	119.5	119	119	119.25
	100	130	119	112	122	121	120.5	120.5	120.75
	101	130	120	113	122	121.5	121	121	121.25
	102	131	122	114	122	122.5	122	122	122.25
	103	131	123	115	121	123.			122.5
	105	131	124	117	121	124	122.5	122.5	123.25
	107	129	125	117	121	123	123	123	123
	108	129	125	118	120	123.5	122.5	122.5	
	109	127	125	117	119	122	122	122	
	111	126	125	117	119	121.5	122	122	121.75
	112	125	125	118	118	121.5	121.5	121.5	121.5
	113	124	125	118	117	121	121	121	
	114	123	124	117	116	120	120	120	
1400									
1600									

Time (Approximate)	#3 Aug. 1, 1972	#2 (°F)	#9 (°F)	#11 (°F)	#13 (°F)	Avg.#2 & #11 (°F)	#13 (°F)	Avg.all 4 (°F)
1800	115	121	123	117	115	119	119	119
	115	119	121	115	113	117	117	117
	116	117	119	114	112	115.5	115.5	115.5
	117	115	116	112	111	113.5	113.5	113.5
	117	111	111	109	108	110	109.5	109.5
2000	117	107	107	106	106	106.5	106.5	106.5
	117	105	105	104	104	104.5	104.5	104.5
	116	103	103	103	102	103	102.5	102.5
	116	101	101	101	101	101	101	101
	115	100	100	100	100	100	100	100
2200	114	98	98	98	98	98	98	98
	113	97	97	97	97	97	97	97
	112	95	95	96	95	95.5	95	95.25
	111	94	95	95	95	94.5	95	94.75
	110	93	94	94	94	93.5	94	93.75
0000 2 Aug.	109	92	93	93	93	92.5	93	92.75
	107	91	91	92	92	91.5	91.5	91.5
	106	89	90	91	90	90	90	90
	105	88	89	90	89	89	89	89
	104	87	88	89	89	88	88.5	88.25
0200	103	87	87	88	88	87.5	87.5	87.5
	102	86	86	87	87	86.5	86.5	86.5
	101	85	86	87	86	86	86	86
	100	84	85	86	85	85	85	85
	99	83	84	85	85	84	84.5	84.25
0400	97	82	83	84	83	83	83	83
	96	81	82	83	82	82	82	82
	95	80	80	82	81	81	80.5	80.25
	94	79	80	81	80	80	80	80
	93	78	79	80	79	79	79	79
0600	92	77	78	79	78	78	78	78
	91	76	77	79	78	77.5	78.5	78.5
	90	79	78	80	84	79.5	81	80.25
	89	82	82	82	88	82	84	83

Time(Approximate) Aug. 2, 1972	#3 (°F)	#2 (°F)	#9 (°F)	#11 (°F)	#13 (°F)	Avg.#2 & #11 (°F)	Avg.#9 & #13 (°F)	Avg.all 4 (°F)
0800	88	87	82	85	92	86	87	86.5
	87	90	85	87	96	88.5	90.5	89.5
	86	95	87	89	99	92.5	93	92.5
	86	98	90	91	102	94.5	96	95.25
	86	102	92	93	105	97.5	98.5	98
1000	86	106	95	95	107	100.5	101	100.75
	87	108	97	95	108	102	102.5	102.25
	87	111	99	98	110	104.5	104.5	104.5
	88	115	102	100	113	107.5	107.5	107.5
	89	118	104	101	114	109.5	109	109.25
1200,	90	120	107	103	115	111.5	111	111.25
	91	122	109	105	116	113.5	112.5	113
	92	123	111	107	117	115	114	114.5
	94	125	114	108	117	116.5	115.5	116
	95	127	116	109	118	118	117	117.5
	97	127	118	110	118	118.5	118	118.25
1400	98	128	120	111	119	119.5	119.5	119.5
	100	128	121	112	118	120	119.5	119.75
	102	128	122	113	118	120.5	120	120.25
	103	129	125	115	118	122	121.5	121.75
	105	129	126	116	118	122.5	122	122.25
1600	106	128	127	116	118	122	122.5	122.25
	107	127	127	117	117	122	122	122
	109	126	127	118	117	122	122	122
	110	126	128	119	117	122.5	122.5	122.25
	111	124	127	118	116	121	121.5	121.25
	112	122	125	117	115	119.5	120	119.75
1800	114	120	123	117	113	118.5	118	118.25
	114	117	120	114	112	115.5	116	115.75
	115	114	116	112	110	113	113	113
	116	110	110	108	107	109	108.5	108.75
2000	116	107	107	106	105	106.5	106	106.25
	116	104	104	103	103	103.5	103.5	103.5
	115	102	102	102	101	102	101.5	101.75

Time (Approximate)	#3	#2	#9	#11	#13	#9 & #11	Avg.all 4
Aug. 2, 1972	(°F)	(°F)	(°F)	(°F)	(°F)	(°F)	(°F)
2200	114	98	99	99	98	98.5	98.5
	113	96	97	97	96	96.5	96.5
	112	95	95	96	95	95.5	95.25
	111	93	94	94	93	93.5	93.5
	110	92	93	93	93	92.5	92.75
	109	91	91	92	91	91.5	91.25
0000 3 Aug.	108	89	90	91	90	90	90
	106	88	89	90	89	89	89
	105	87	88	89	88	88	88
	104	86	87	88	87	87	87
	103	85	86	87	87	86.5	86.25
	101	85	86	86	86	85.5	85.5
	100	84	84	85	85	84.5	84.5
	99	82	83	84	83	83	83
	98	81	82	83	82	82	82
	97	80	80	81	81	80.5	80.5
0400	95	78	79	80	79	79	79
0424	94	77	78	79	78	78	78
0448	93	76	77	77	77	77	77
0512	92	75	76	77	76	76	76

FIRST DAY'S TEMPERATURE RANGES

	FIRST DAY'S TEMPERATURE RANGES			SECOND DAY'S TEMPERATURE RANGES			
HIGH	117	131	125	118	122	124	123.25
LOW	91	79	80	81	80	80	80
Avg	104	105	102.5	99.5	101	102	101.63
	SECOND DAY'S TEMPERATURE RANGES						
HIGH	116	129	128	119	119	122.5	122.5
LOW	86	75	76	77	76	76	76
Avg	101	102	102	98	97.5	99.25	99.25

APPENDIX E

Uncertainty Analysis

An uncertainty analysis was carried out on both the analytical solution and on a one dimensional TRUMP model of the rocket motor storage container system. In both models, the volumetric heat capacity of the sand (ρc), the conductivity of the sand (k), and the emissivity of the surfaces were each varied by ten percent to determine the sensitivity of the system temperature response to each variation. Although other factors may also be varied, it was theorized that these three had the greatest effect on the heat transfer of the system. These factors were also known with the least accuracy; the maximum uncertainty of each was estimated to be plus or minus ten percent (odds 20 to 1).

In the analytical solution, varying the volumetric heat capacity changed parameter a , varying the emissivity changed parameter β , and varying the conductivity changed both parameters a and β . The effects on each parameter from each variation are given in Table V.

Change in Property	Change in Parameters
Volumetric Heat Capacity + 10%	$a + .12$
Volumetric Heat Capacity - 10%	$a - .12$
Emissivity + 10%	$\beta + .49$
Emissivity - 10%	$\beta - .37$
Conductivity + 10%	$a - .11, \beta - .22$
Conductivity - 10%	$a + .13, \beta + .35$

Each factor was varied holding the other factors constant.

The changes in temperature and time delay were computed from the difference between these new values and those previously obtained from the analytical solution. To obtain uncertainty bounds on the analytical curve, the second power equation [Ref. 16] was used, namely

$$\omega_T = \sqrt{\omega_C^2 + \omega_k^2 + \omega_\epsilon^2}$$

where

ω_T = resulting uncertainty in the calculated temperature due to uncertainties in temperature caused by

ω_C = estimated uncertainty in volumetric heat capacity

ω_k = estimated uncertainty in conductivity

ω_ϵ = estimated uncertainty in emissivity

An identical calculation was carried out to calculate the uncertainty in time delay. The results of these calculations are shown in Figures 12 and 13 for the surface and center of the rocket motor respectively. The uncertainty in temperature varied with time with a maximum variation of $\pm 2.75^\circ\text{F}$ at the center of the motor and a maximum variation of $\pm 1.85^\circ\text{F}$ at the surface of the rocket motor. The time delay varied by ± 31 minutes at the center of the motor and ± 11 minutes at the surface. The actual experimental data was also plotted on these Figures for comparison.

The experimental data also had an uncertainty bound. Three primary factors made up this uncertainty bound; the accuracy of the thermocouple wire ($\pm 1.5^\circ\text{F}$), the readability of the recorder ($\pm 1^\circ\text{F}$), and the variation in temperature

caused by inaccuracy in the placement of the thermocouples ($\pm 1^{\circ}\text{F}$, estimated). The overall uncertainty in the experimental data was also calculated from the second power equation as

$$\omega_T = \sqrt{\omega_{\text{WIRE}}^2 + \omega_{\text{READ}}^2 + \omega_{\text{PLACE}}^2} \approx 2^{\circ}\text{F}$$

These uncertainty bounds are also shown in Figures 12 and 13.

A procedure, similar to that used to find the uncertainties of the analytical solution, was used to analyze the resulting uncertainty in the TRUMP numerical calculation. The results of these calculations are shown in Figures 14 and 15. The uncertainty in temperature varied with time with a maximum variation of $\pm 2.95^{\circ}\text{F}$ at the center of the rocket motor and a maximum variation of $\pm 1.95^{\circ}\text{F}$ at the surface of the motor. The time delay varied from ± 20 minutes at the center of the motor to ± 9 minutes at the surface of the motor.

On the basis of the propagation of uncertainty analysis, it was determined that the solutions were most sensitive, in order of importance, to changes in the volumetric heat capacity, emissivity, and the conductivity.

LIST OF REFERENCES

1. Arpacı, V. S., Conduction Heat Transfer, p. 324-328, Addison-Wesley, 1966.
2. Lawrence Radiation Laboratory Report No. UCRL-14754, Rev. II, TRUMP: A Computer Program for Transient and Steady-State Temperature Distributions in Multi-dimensional Systems, by A. L. Edwards, 1 July 1969.
3. Erbayrum, C., A Computer Program for Solving Transient Heat Conduction Problems, M.S. Thesis, Naval Postgraduate School, Monterey, California, 1971.
4. Meyer, J. F., MacKenzie, D. K., and Wirzburger, A. H., Thermal Mapping of Surface Temperatures Using Cholesteric Liquid Crystals, laboratory study done at Naval Postgraduate School, Monterey, California, 9 June 1972.
5. Crawford, L. and Lemlich, R., "Natural Convection in Horizontal Concentric Cylindrical Annuli," Industrial and Engineering Chemistry Fundamentals, Vol. 1, No. 4, p. 260-264, November 1962.
6. Baumeister, T., Marks Standard Handbook for Mechanical Engineers, 7th Edition, p. 4-11, 4-95, 4-111, McGraw-Hill, 1967.
7. Liu, C. Y., Mueller, W. K., and Landis, F., Natural Convection Heat Transfer in Long Horizontal Cylindrical Annuli, paper presented at 1961 International Heat Transfer Conference, Boulder, Colorado, 28 August - 1 September 1961.
8. Fergason, J. L., Taylor, T. R., and Harsch, T. B., "Liquid Crystals and their Applications," Electro-Technology, p. 41-50, January 1970.
9. Fergason, J. L., "Liquid Crystals," Scientific American, V. 211, p. 77-85, August 1964.
10. Naval Air Development Center Report No. NADC-MA-6922, Development of a Reusable Strippable Film as a Carrier for Liquid Crystals for Use in NDT, by E. Th. Vadala, p. 1-3, 22 May 1969.
11. Hoehn, R. and Binkert, B., Cholesteric Liquid Crystals: A New Visual Aid to Study Flap Circulation, paper presented at Annual Meeting of the American Society of Plastic and Reconstructive Surgeons, Los Angeles, California, 3 October 1970.

12. Mock, J. A., "Liquid Crystals Track Flaws in a Colorful Way," Materials Engineering, p. 66-67, February 1969.
13. McLachlan, N. W., Bessel Functions for Engineers, 2nd Ed., p. 135-136, Oxford University Press, 1961.
14. Hottel, H. C., and Sarofim, A. F., Radiative Transfer, p. 31-39, McGraw-Hill, 1967.
15. Chapman, A. J., Heat Transfer, 2nd Ed., p. 450-455, Macmillan Co., 1967.
16. Kline, S. J., and McClintock, F. A., "Describing Uncertainties in Single-Sample Experiments," Mechanical Engineering, p. 3-8, January 1953.